

Master Thesis

Evaluation and Comparison of Natural Gas and Supercritical CO₂ Correlation Models for Thermodynamic Applications

Written by:

Nicholas Matev, BSc
0835307

Advisor:

Univ.-Prof. Dipl.-Ing. Dr.mont. Herbert Hofstätter
Dipl.-Ing. Dr.mont. Rudolf Fruhwirth

Leoben, 09.06.2016

EIDESSTATTLICHE ERKLÄRUNG

Ich erkläre an Eides statt, dass ich die vorliegende Diplomarbeit selbständig verfasst, andere als die angegebenen Quellen und Hilfsmittel nicht benutzt und die den benutzten Quellen wörtlich und inhaltlich entnommenen Stellen als solche erkenntlich gemacht habe.

AFFIDAVIT

I hereby declare that the content of this work is my own composition and has not been submitted previously for any higher degree. All extracts have been distinguished using quoted references and all information sources have been acknowledged.

Kurzfassung

Das Verständnis speziell thermodynamischer aber auch anderer Eigenschaften von Erdgas und mitgeförderten Produkten wie zum Beispiel Sauer gas, Stickstoff und Kohlendioxid ist von entscheidender Bedeutung für einen sicheren und effizienten Betrieb von Anlagen in der Erdölindustrie. Das gleiche gilt für überkritisches Kohlendioxid welches in verschiedenen Bereichen der Erdölindustrie zur Anwendung kommt. Beispiele hierfür sind CO₂-Abscheidung und -Speicherung, CO₂-Injektion in der tertiären Ölgewinnung oder der Verwendung von CO₂ als Wärmeübertragungsflüssigkeit in geothermischen Energierückgewinnungssysteme.

Genauere Kenntnisse von Fluideigenschaften sind unabdingbare Voraussetzungen für eine erfolgreiche Anwendung von zum Beispiel Zustandsgleichungen zur Modellierung von thermo- und hydrodynamischen Zuständen bei Ein- und Mehrphasenströmung im Untergrund. Bohrlochmodelle und Simulatoren für Anwendungen in der Erdgasproduktion und Geothermie basieren auf Fluid- und Wärmeübertragungsmodellen. Diese sind wiederum von Parametern wie Dichte, Viskosität, Wärmekapazität und Wärmeleitfähigkeit, pseudokritischen Eigenschaften und Z-Faktoren abhängig. Korrelationen für die Bestimmung der genannten Eigenschaften kommen – da deterministische Modelle entweder äußerst komplex bzw. überhaupt nicht verfügbar sind – üblicherweise in Forschung und Industrie zur Anwendung.

In dieser Arbeit werden derartige Korrelationen für Erdgas und überkritisches CO₂ zusammengefasst, analysiert und letztendlich hinsichtlich deren Anwendbarkeit bewertet. Die verschiedenen Korrelationsmodelle werden dabei evaluiert und miteinander verglichen. Korrelationen, welche in der Regel abhängig von Temperatur, Druck, Dichte und spezifischem Gewicht sind, wurden dazu programmiert. Eine Bewertung und Überprüfung bezüglich der Genauigkeit und des Gültigkeitsbereichs der verschiedenen Modelle ist dadurch einerseits genauer und andererseits nachvollziehbar. Darüber hinaus kann direkt auf die programmierten Modelle zugegriffen werden und eine weitere Implementierung in andere Anwendungen ist möglich.

Die Korrelationsergebnisse werden graphisch aufbereitet und mit Daten des National Institute of Standards and Technology (NIST) verglichen. Diese NIST Daten werden für diese Studie als Referenzdaten verwendet und zusätzlich mit experimentellen, aus der Literatur entnommenen Daten, überprüft. Evaluierungsstudien der pseudokritischen Parameter, der Erdgas Viskosität und der CO₂-Viskosität sind aus der Literatur erhältlich und die Ergebnisse dieser Studien formen in zusammengefasster Weise einen Teil dieser Arbeit. Abschließend wird eine Reihung nach Genauigkeit und Anwendbarkeit aller evaluierten Korrelationsmodelle erstellt und die Abweichungen der Korrelationsergebnisse in Relation zu den NIST Daten wird dargestellt.

Abstract

Understanding the thermodynamic characteristics but also the fluid behaviour of natural gas and associated components such as sour gas, nitrogen and CO₂ is crucial for the safe and efficient planning and operation of facilities throughout the petroleum industry. The same applies to supercritical carbon dioxide when considering petroleum engineering related applications such as carbon capture and storage, CO₂ injection in enhanced oil recovery operations or the use of CO₂ as a heat transmission fluid in geothermal energy recovery systems.

Fluid properties such as gas density along with viscosity are required parameters for many gas-flow equations including wellbore pressure drop calculations for single and two phase flow, calculations in connection with deliverability testing of gas wells and calculations predicting the gas-liquid flow regime in pipes. Wellbore models and simulators for both natural gas production and geothermal energy recovery systems are based on fluid and heat transfer models. These in turn depend on parameters such as density, viscosity, heat capacity and thermal conductivity, pseudo critical properties and Z-factors. Correlations for determining the mentioned properties find widespread use in industry and research applications as deterministic models are either very complex or not available at all.

In this thesis such correlations for natural gas and supercritical CO₂ are summarized, analysed and finally evaluated in regard to their applicability. The different correlation models are thereby evaluated and compared against each other. Correlations, which are usually dependent on temperature, pressure, density and specific gravity have been programmed. This allows a detailed assessment and verification in terms of accuracy and applicable range of the different correlations. Furthermore the programmed models are readily available and can be accessed directly or be implemented into further applications. The correlation results are plotted and compared with data from National Institute of Standards and Technology (NIST). The NIST data is used as a reference database for this study and additionally checked against experimental data obtained from literature.

Evaluation studies on pseudocritical properties, natural gas viscosity and CO₂ viscosity are available from the literature and the main findings of those studies are provided in a summarized form and are a part of this work. Finally, a ranking according to accuracy and applicability of all evaluated correlation models is presented and the deviations of the individual correlation results in relation to the NIST data are listed.

List of Tables

Table 3-1: Coefficients for the DAK correlation.	13
Table 3-2: Coefficients for Equations (3-18) and (3-19).	17
Table 3-3: Accuracy of calculating Z-factor for sour gases with gas gravity correlations 18	18
Table 3-4: Properties of sour gas data used by Elsharkawy and Elkamel.	18
Table 3-5: Associated-gas data base	20
Table 3-6: Gas condensate data base	21
Table 3-7: Coefficients for Equations (3-51) and (3-52).	24
Table 3-8: Coefficients for Equations (3-51) and (3-52).	25
Table 3-9: Coefficients for equations (3-57) and (3-58).	26
Table 3-10: Data ranges for the Wichert and Aziz method.	27
Table 3-11: Coefficients for Equation (3-82).	33
Table 3-12: Coefficients determined by Chen and Ruth.	38
Table 3-13: Coefficients by Londono et al.	39
Table 3-14: Coefficients by Londono et al.	39
Table 3-15. Coefficients for the Londono et al polynomial model.	40
Table 3-16: Coefficients for Equation (3-131).	40
Table 3-17: Coefficients for Equations proposed by Galliéro et al.	44
Table 3-18: Optimized molecular parameters of some n-alkanes.	44
Table 3-19: Molecular parameters of some petroleum compounds of interest.	45
Table 3-20: Coefficients for the Equations proposed by Sanaei et al.	46
Table 3-21: Ranges of different gas properties	46
Table 3-22: Coefficients for the correlation of the thermal conductivity.	51
Table 3-23: Coefficients for the specific isobaric heat capacity departure calculation.	53
Table 3-24: Coefficients for the calculation of the isobaric heat capacity.	53
Table 3-25: Parameters for the correlation.	54
Table 4-1: Coefficients for Equations (4-30) to (4-33) to predict viscosity of carbon dioxide. 63	63
Table 4-2: Coefficients for Equation (4-34).	64
Table 4-3: Coefficients for Equations (4-37) to (4-40) to predict thermal conductivity of CO ₂ 67	67
Table 4-4: Correlation coefficients.	67
Table 4-5: Coefficients used for the calculation of the thermal conductivity.	68

Table 4-6: Coefficients for Equation (4-44).	69
Table 4-7: Twelve commonly used EOSs.	70
Table 4-8: Coefficients for Equation (4-45).	72
Table 4-9: Coefficients for Equation (4-46).	73
Table 4-10: Coefficients for Equations (4-48) to (4-51).	74
Table 4-11: Value for b_{ij} coefficients in Equation (4-47) for pressures < 3000 Psia.	74
Table 4-12: Value for b_{ij} coefficients in Equation (4-47) for pressures > 3000 psia.	75
Table 5-1: Relative errors of several gas z-factor correlations based on gas specific gravity. The Sutton (2007) correlations include the Wichert-Aziz correlation for hydrogen sulphide and carbon dioxide.	77
Table 5-2: Average relative errors (ARE) Average absolute relative errors (AARE) of gas Z-factor correlations compared with gases with non-hydrocarbon components.	78
Table 5-3: Accuracy of correlations using compositional data and gas gravity correlations.	78
Table 5-4: Relative errors of the gas viscosity correlations evaluated by McCain et al.	83
Table 5-5: Summary of AAREs for five different models and the proposed correlation versus validation data as presented by Heidaryan et al. *The Bahadori and Vuthaluru correlation is only valid in a range from 260K to 450K as well as a pressure range between 10 MPa and 70 MPa. The presented AARE for that model was calculated as an average of the individual AAREs values within that range.	90
Table 5-6: Pseudocritical properties correlations for unknown compositions – gas gravity correlations. AREs and AAREs according to McCain et al.	104
Table 5-7: Comparison of pseudocritical properties gas gravity correlations for mixtures with a non-hydrocarbon content greater than 5% including the Wichert and Aziz correction. AREs and AAREs according to McCain et al.	104
Table 5-8: Comparison of pseudocritical properties for correlations based on compositional data. AREs and AAREs according to Elsharkawy and Elkamel.	105
Table 5-9: Comparison of dynamic viscosity correlations for gas mixtures. AREs and AAREs according to McCain et al. *from Chen and Ruth (1993)	105
Table 5-10: Correlation for the calculation of the natural gas mixture thermal conductivity. AREs and AAREs in reference to NIST data	105
Table 5-11: Correlation for the calculation of the natural gas mixture heat capacity. AREs and AAREs in reference to NIST data.	106
Table 5-12: Comparison of supercritical CO ₂ viscosity correlations. AREs and AAREs in reference to NIST data.	106

Table 5-13: Comparison of supercritical CO ₂ thermal conductivity correlations. AREs and AAREs in reference to NIST data.....	106
Table 5-14: Comparison of supercritical CO ₂ density correlations. AREs and AAREs in reference to NIST data.....	107

List of Figures

Figure 2-1: Phase diagram of a dry gas system.....	5
Figure 2-2: Phase diagram of a wet gas system.....	6
Figure 2-3: Retrograde condensation.	6
Figure 2-4: Phase diagram of a condensate gas system.	6
Figure 2-5: Phase diagram of an oil and associated gas system.	7
Figure 2-6: The law of corresponding states applied to methane and nitrogen.	8
Figure 3-1: Standing and Katz z-factor chart.	11
Figure 3-2: Errors of different z-factor methods evaluated by Sutton (2007).	12
Figure 3-3: Pseudocritical properties correlations for natural gases	15
Figure 3-4: Carr-Kobayashi-Burrows's Correction Method for non-hydrocarbon components.	28
Figure 3-5: Viscosity of gas at 1 atmosphere vs. molecular weight	31
Figure 3-6: Viscosity ratio vs. pseudoreduced temperature.	32
Figure 3-7: Thermal conductivity of natural and hydrocarbon gases at one atmosphere (14,696 psia).	48
Figure 3-8: Thermal conductivity ratio for gases.	48
Figure 3-9: Thermal conductivity of miscellaneous gases at one atmosphere.	48
Figure 4-1: Phase diagram of carbon dioxide.	56
Figure 4-2: Viscosity of carbon dioxide.	57
Figure 4-3: The thermal conductivity of CO ₂ along isobars.	64
Figure 4-4: Thermal conductivity of carbon dioxide near the critical point.	64
Figure 4-5: The extent of the thermal conductivity correlation and its estimated uncertainty. [75].....	66
Figure 4-6: The thermal conductivity of CO ₂ in the critical region as a function of density at different pressures. The solid curves represent the mathematical model developed by Vesovic et al. to describe the thermal conductivity changes around the critical point while the data points are experimental results.	66
Figure 4-7: Variation curve for the density of supercritical CO ₂ with reduced pressures when the reduced temperature is 1.03.	71
Figure 4-8: Variation curves for the relative errors of CO ₂ density of various EOSs at a reduced temperature of 1.03.	72

Figure 5-1: Comparisons of relative errors in gas z-factor correlations using data split by gas specific gravity.....	79
Figure 5-2: Error in calculated z factor from DAK for CH ₄ /H ₂ S mixture.	79
Figure 5-3: Error in the calculated z-factor from DAK for CH ₄ /CO ₂ mixture.	80
Figure 5-4: Error in the calculated z-factor from DAK for varying levels of N ₂	80
Figure 5-5: Pseudocritical temperature correlations as a function of the specific gas gravity.	81
Figure 5-6: Pseudocritical pressure correlations as a function of the specific gas gravity.	81
Figure 5-7: Pseudocritical temperature correlations including the correction by Wichert and Aziz (1972) as a function of the specific gas gravity for a hypothetical gas mixture containing 10% H ₂ S, 10% CO ₂ and 5% N ₂	82
Figure 5-8: Pseudocritical pressure correlations including the correction by Wichert and Aziz (1972) as a function of the specific gas gravity for a hypothetical gas mixture containing 10% H ₂ S, 10% CO ₂ and 5% N ₂	82
Figure 5-9: Comparisons of relative errors in gas viscosity correlations as a function of temperature.	84
Figure 5-10: Comparisons of the LGE and Londono et al. gas viscosity correlations as a function of temperature.	84
Figure 5-11: The LGE and Gurbanov and Dadash-Zade gas viscosity correlations as a function of temperature.	85
Figure 5-12: Comparison of the correlation results with methane data obtained from the NIST WebBook. The Jarrahan and Heidaryan correlation results are displayed in green for selected isobars. The yellow dotted line represents the range as recommended by the authors.	86
Figure 5-13: Comparison of the correlation results with data from Pátek et al for xCH ₄ = 0.4994 and xCO ₂ = 0.5006. The Jarrahan and Heidaryan correlation results are displayed in green for 1, 4 and 7MPa.	86
Figure 5-14: The average relative error (ARE) and absolute relative error (AARE) as a function of temperature for the thermal conductivity correlation developed by Jarrahan and Heidaryan (2014).....	87
Figure 5-15: The average relative error (ARE) and absolute relative error (AARE) as a function of pressure for the thermal conductivity correlation developed by Jarrahan and Heidaryan (2014).	87
Figure 5-16: Comparison of the correlation results with NIST data. The Ouyang (2011) isobaric heat capacity correlation results are displayed in green for selected isobars. The yellow dotted line represents the range as recommended by the author.	88

Figure 5-17: The average relative error (ARE) and absolute relative error (AARE) as a function of pressure for the isobaric heat capacity correlation developed by Moshfeghian (2011).....	89
Figure 5-18: The average relative error (ARE) and absolute relative error (AARE) as a function of temperature for the isobaric heat capacity correlation developed by Moshfeghian (2011).	89
Figure 5-19: Experimental data from Stephan and Lucas (1979) plotted against the NIST reference data.	91
Figure 5-20: Comparison of the correlation results with NIST data. The Bahadori and Vuthaluru (2009) viscosity correlation results are displayed in green for selected isobars. The yellow dotted line represents the range as recommended by the authors.....	92
Figure 5-21: The average relative error (ARE) and absolute relative error (AARE) as a function of pressure.....	92
Figure 5-22: Comparison of the correlation results with NIST data. The Heidaryan et al. (2010) viscosity correlation results are displayed in green for selected isobars. The yellow dotted line represents the range as recommended by the authors.....	93
Figure 5-23: The average relative error (ARE) and absolute relative error (AARE) as a function of pressure.....	93
Figure 5-24: Experimental data from Le Neindre et al. (1973) plotted against the NIST reference data.	94
Figure 5-25: Comparison of the correlation results with NIST data. The Bahadori and Vuthaluru (2009) thermal conductivity correlation results are displayed in green for selected isobars. The yellow dotted line represents the range as recommended by the authors.	95
Figure 5-26: The average relative error (ARE) and absolute relative error (AARE) as a function of pressure for the thermal conductivity correlation developed by Bahadori and Vuthaluru (2009).	96
Figure 5-27 Comparison of the correlation results with NIST data. The Ouyang (2012) thermal conductivity correlation results are displayed in green for selected isobars. The yellow dotted line represents the range as recommended by the authors.....	96
Figure 5-28: The average relative error (ARE) and absolute relative error (AARE) as a function of pressure.....	97
Figure 5-29: Comparison of the correlation results with NIST data. The Jarrahan and Heidaryan (2012) thermal conductivity correlation results are displayed in green for selected isobars. The yellow dotted line represents the range as recommended by the authors.	97
Figure 5-30 The average relative error (ARE) and absolute relative error (AARE) as a function of pressure.....	98

Figure 5-31: Comparison of the correlation results with NIST data. The Amooey (2013) thermal conductivity correlation results are displayed in green for selected isobars. The yellow dotted line represents the range as recommended by the authors.....	98
Figure 5-32: The average relative error (ARE) and absolute relative error (AARE) as a function of pressure.....	99
Figure 5-33: Experimental data from Le Neindre et al. (1973) plotted against the NIST reference data.....	100
Figure 5-34: Comparison of the correlation results with NIST data. The Wang et al. (2015) density correlation results are displayed in green for selected isobars. The yellow dotted line represents the range as recommended by the authors.	101
Figure 5-35: The average relative error (ARE) and absolute relative error (AARE) as a function of pressure.....	101
Figure 5-36: Comparison of the correlation results with NIST data. The Bahadori et al (2009) density correlation results are displayed in green for selected isobars. The yellow dotted line represents the range as recommended by the authors.	102
Figure 5-37: The average relative error (ARE) and absolute relative error (AARE) as a function of pressure.....	102
Figure 5-38: Comparison of the correlation results with NIST data. The Ouyang (2011) density correlation results are displayed in green for selected isobars. The yellow dotted line represents the range as recommended by the authors.	103
Figure 5-39: The average relative error (ARE) and absolute relative error (AARE) as a function of pressure.....	103

Abbreviations

AAD	Average absolute deviation, %
AAE	Average absolute error, %
AARE	Average absolute relative error, %
ARE	Average relative error, %
C7+	heptane plus fraction
CCE	Constant composition expansion
CS	Corresponding states
DAK	Dranchuk and Abou-Kassem correlation
EOS	Equation of state
GERG	European gas research group
HPHT	High pressure and high temperature
NIST	National Institute of Standards and Technology
NS	Nishiumi-Saito correlation
R	Coefficient of correlation
SBV	Stewart, Burkhardt, and Voo correlation
SC-CO ₂	Supercritical CO ₂
SD	Standard deviation, %
SW-EOS	Spann and Wagner equation of state
TRAPP	Transport property prediction method

Table of content

	Page
1 INTRODUCTION.....	1
2 GENERAL.....	4
2.1.1 Ideal gas law.....	4
2.1.2 Apparent molecular weight (M_a).....	4
2.1.3 Specific gas gravity (γ_g).....	5
2.1.4 Characterization of different types of gas.....	5
2.1.5 Statistical parameters.....	7
2.1.6 Corresponding states theory.....	8
3 NATURAL GAS MIXTURES.....	9
3.1 National Institute of Standards and Technology (NIST) database.....	9
3.2 Density.....	9
3.3 Z-factor.....	10
3.3.1 Dranchuk and Abou-Kassem (1975) Z-factor correlation.....	12
3.3.2 Z-factor calculation at high density and high pressure (HPHT).....	13
3.4 Pseudo critical properties correlations.....	14
3.4.1 Correlations for unknown compositions based on gas gravity.....	15
3.4.1.1 Standing (1981).....	15
3.4.1.2 Sutton (1985).....	16
3.4.1.3 Piper et al. (1993).....	16
3.4.1.4 Elsharkawy et al. (2000).....	17
3.4.1.5 Elsharkawy and Elkamel (2000).....	18
3.4.1.6 Londono et al. (2002).....	19
3.4.1.7 Sutton (2007).....	19
3.4.2 Correlations for known compositions based on mixing rules.....	21
3.4.2.1 Kay (1936).....	21
3.4.2.2 Stewart, Burkhardt and Voo (SBV) (1959).....	21
3.4.2.3 Sutton (SSBV) (1985).....	22
3.4.2.4 Corredor et al. (1992).....	23
3.4.2.5 Piper et al. (1993).....	24
3.4.2.6 Elsharkawy et al. (2000).....	25
3.4.3 Adjustment methods for accompanying non-hydrocarbons.....	26
3.4.3.1 Wichert and Aziz (1972).....	26

3.4.3.2	Carr, Kobayashi, and Burrows (1954)	27
3.4.4	Correlation of pseudocritical properties for the heptane plus fraction	28
3.5	Dynamic viscosity of natural gas mixtures	29
3.5.1	Carr-Kobayashi-Burrows (1954).....	30
3.5.2	Jossi et al. (1962)	33
3.5.3	Lohrenz et al. (1964).....	34
3.5.4	Dean and Stiel (1965).....	35
3.5.5	Lee-Gonzalez-Eakin (1966)	36
3.5.6	Lucas (1981).....	36
3.5.7	Gurbanov and Dadash-Zade (1986)	38
3.5.8	Londono et al. (2005).....	38
3.5.9	Sutton (2007).....	41
3.5.10	Viswanathan (2007)	41
3.5.11	Elsharkawy (2006)	42
3.5.12	Galliéro et al. (2009)	43
3.5.13	Sanaei et al. (2015).....	45
3.6	Thermal conductivity of natural gas mixtures	46
3.6.1	Gas processors suppliers association engineering data book	47
3.6.2	Pedersen et al. (1989)	49
3.6.3	Jarrahan and Heidaryan (2014).....	49
3.7	Heat capacity of natural gas mixtures	51
3.7.1	Abou-Kassem and Dranchuk (1982)	52
3.7.2	Moshfeghian (2011).....	53
3.7.3	Lateef and Omeke (2011)	54
4	SUPERCRITICAL CARBON DIOXIDE.....	56
4.1	National Institute of Standards and Technology (NIST) web database.....	56
4.2	Supercritical CO ₂ dynamic viscosity.....	57
4.2.1	Lucas Method (1980).....	58
4.2.2	Zabaloy et al. (2005) - Lenard Jones fluid model	60
4.2.3	Bahadori and Vuthaluru (2009)	62
4.2.4	Heidaryan et al. (2010)	63
4.3	Supercritical CO ₂ thermal conductivity.....	64
4.3.1	Vesovic (1990).....	65
4.3.2	Bahadori and Vuthaluru (2009).....	66
4.3.3	Ouyang (2012).....	67
4.3.4	Jarrahan and Heidaryan (2012).....	68
4.3.5	Amooey (2013)	68

4.4	Supercritical CO ₂ density	69
4.4.1	Prediction of supercritical CO ₂ properties through EOS	69
4.4.2	Wang et al. (2015)	70
4.4.3	Haghighbakhsh et al. (2013).....	72
4.4.4	Bahadori et al. (2009)	73
4.4.5	Ouyang (2011).....	74
4.5	Supercritical CO ₂ heat capacity	75
5	EVALUATION AND COMPARISON	76
5.1	Natural gas correlation models	76
5.1.1	Pseudocritical properties correlations.....	76
5.1.2	Dynamic viscosity of natural gas mixtures.....	82
5.1.3	Thermal conductivity of natural gas mixtures	85
5.1.4	Heat capacity of natural gas mixtures	87
5.2	CO ₂ correlation models.....	90
5.2.1	CO ₂ viscosity correlation models.....	90
5.2.2	CO ₂ thermal conductivity.....	94
5.2.3	CO ₂ density correlation models.....	99
5.3	Evaluation and comparison summary	104
6	CONCLUSION	108
7	NOMENCLATURE.....	110
8	REFERENCES.....	112

1 Introduction

Understanding the thermodynamic characteristics but also the fluid behaviour of natural gas and associated components such as sour gas, nitrogen and CO₂ is crucial for the safe and efficient planning and operation of facilities throughout the petroleum industry. The same applies to supercritical carbon dioxide when considering petroleum engineering related applications such as carbon capture and storage, CO₂ injection in enhanced oil recovery operations or the use of CO₂ as a heat transmission fluid in geothermal energy recovery systems.

Models and simulators can be employed as prediction and optimizing tools and provide the basis for developing and improving petroleum industry systems by calculating the system performance and proving economic feasibility. As Schwaiger (2016) [1] showed in his Master thesis, a functioning wellbore simulator depends on an accurate physical representation of different parameters, including elements such as reservoir properties, casing geometry and an entrained droplet model for predicting the gas-liquid flow regime. It is also essential to implement an accurate heat transfer model which in turn requires the modelling of several interlinked gas parameters including the density, viscosity, heat capacity, thermal conductivity and PVT properties for thermodynamic computations.

In addition, gas density along with viscosity are required parameters for many gas-flow equations including wellbore pressure drop calculations for single and two phase flow, calculations in connection with deliverability testing of gas wells and calculations predicting the gas-liquid flow regime in pipes. Gas pressure gradient calculations need the density as an input while the formation volume factor (FVF) and flow calculation using Darcy's law require the corresponding PVT properties and therefore the Z-factor is required. Knowledge of the gas density is also essential for some casing design scenarios and well control situations i.e. gas kicks.

Understanding the behaviour of carbon dioxide properties, especially in the supercritical state, is equally important. CO₂ is not only employed for petroleum engineering related applications but is one of the most common substances used in supercritical applications across different industries including the pharmaceutical and food industry. In recent years carbon capture and sequestration, also known as CCS has become increasingly popular and major CCS projects are in operation or planned in many countries.[2] Further applications for supercritical fluids are found in enhanced oil recovery (EOR) and sequestration in deep saline aquifers. [3] EOR which uses gases such as natural gas, nitrogen, or carbon dioxide injection accounts for nearly 60 percent of EOR production in the United States. [4]

Carbon capture and storage is one of the effective ways to remove significant volumes of combustion emissions in an effort to reduce the global warming effect which geological researchers believe to be due to increased concentrations of atmospheric greenhouse gases, especially CO₂. Carbon dioxide may be stored in geological formations through different mechanisms. It can be injected into an oil reservoir for enhanced oil recovery, stored in

depleted oil and gas reservoirs, injected to replace methane in deep coal beds (ECBM), injected into deep saline aquifers, and stored in salt caverns. [5] Understanding the phase behaviour properties of carbon dioxide, especially in the supercritical state is a prerequisite for safe and efficient operations. Due to the special thermodynamic characteristics of carbon dioxide an alteration of the operating conditions may lead to rapid change in pressure, temperature and phase behaviour. Parameters such as density, viscosity, solubility, thermal conductivity, enthalpy and entropy have to be known for accurately predicting wellbore and pipeline hydraulics and ensuring a safe and effective system design.[2] Apart from factors such as flow rate, pipeline material roughness, amount and type of bends in pipe and diameter, many other design parameters for the carbon capture and storage process depend on the viscosity and thermal conductivity of CO₂. [6] By operating a pipeline at pressures above the critical pressure, temperature variations will lead to the formation of gaseous CO₂ and the problems encountered with two-phase flow. [7]

CO₂ is also widely used in supercritical fluid extraction because it is non-flammable, noncorrosive and inexpensive. For example to calculate the solubility parameter, which is a rough measure of the ability of a solvent to dissolve a solute, the supercritical CO₂ density is required. [8] The thermo-physical properties of CO₂ also make it attractive as a heat transmission fluid. A study by Pruess and Azaroual (2006) [9] suggest that CO₂ is roughly comparable and perhaps somewhat superior to water in its ability to mine heat from an EGS (enhanced geothermal system) reservoir. CO₂ appears to offer advantages for wellbore hydraulics such as a lower viscosity that would yield larger flow velocities for a given pressure gradient. Furthermore the large expansivity would generate greater density differences between the cold CO₂ in the injection well and the hot CO₂ in the production well, and would provide buoyancy force which in return would reduce the power consumption of the fluid circulation system. In addition CO₂ could reduce or eliminate scaling problems as it is much less effective as a solvent for rock minerals. The lower mass heat capacity of CO₂ would be partially compensated by the greater flow capacity due to lower viscosity. [9] The chair of petroleum and geothermal energy recovery (Montanuniversität Leoben) plans on developing a closed geothermal wellbore system that employs CO₂ as a heat transfer fluid. Such a system would of course also benefit from the above-mentioned advantages of CO₂ as heat transfer fluid.

Wellbore models and simulators for both natural gas production and geothermal energy recovery systems are based on fluid and heat transfer models. These in turn depend on parameters such as density, viscosity, heat capacity and thermal conductivity, pseudo critical properties and Z-factors. Correlations for determining the above- mentioned properties find widespread use in industry and research applications as deterministic models are either very complex or not available at all. It is for that reason necessary to find suitable fluid correlations which accurately represent the properties.

In general the prediction of properties may be based on theoretical formulations like equations of state (EOS), on correlations of experimental values, or on a combination of both. Completely empirical correlations can be very useful as long as they are employed within the range of

conditions for which they were developed. [10, p. 1.2] An estimation method such as a correlation would be ideally be able to: provide reliable physical and thermodynamic properties for pure substances as well as for mixtures at any temperature, pressure, and composition, indicate the phase (solid, liquid, or gas), require a minimum of input data, indicate the probable error and minimize computation time. [10, p. 1.4]

As mentioned above deterministic models are not always suitable or available for engineering applications. Despite the availability of fast computers, simple equations are necessary for some engineering fields such as Computational Fluid Dynamic (CFD) where a large number of differential equations should be solved simultaneously. [11] Furthermore, for engineering applications which might only require approximate estimates a simple estimation method requiring less input data is often preferred over a more complex, possibly more accurate model. It is also important to note that greater complexity does not necessarily enhance accuracy. [3, p. 1.4]

Based on the need for reliable and simple to use correlation models the objectives of this study are to:

- provide an overview of the available natural gas and supercritical CO₂ correlations models for pseudocritical gas properties, density, viscosity, thermal conductivity and heat capacity,
- evaluate the proposed methods according to applicability, accuracy and range,
- compare the various correlations against each other and reference data,
- present a ranking according to accuracy and applicability for the evaluated correlation and list the deviations of the individual correlation results in relation to reference data.

Chapter 2 of this thesis outlines some basic concepts and methods while Chapter 3 and Chapter 4 consist of a literature review and provide an overview of the available property correlation models by describing and summarizing the individual methods. The findings and results of this study, which include a ranking of all the evaluated correlation models, their respective performance in terms of accuracy, evaluations from the literature, and recommendations where applicable, are presented in Chapter 5. Finally a conclusion is given in Chapter 6.

2 General

Concepts that are useful to understanding the following chapters are briefly explained in the next sections below.

2.1.1 Ideal gas law

For an ideal gas the volume of the individual molecules is neglected and it is assumed that these molecules have no attractive or repulsive forces. All the collisions between the molecules are perfectly elastic. Based on this kinetic gas theory the ideal gas law is expressed by the Equation of state providing a relationship between the pressure, p , volume, V , and temperature, T , for a given quantity of moles of gas, n : [12]

$$pV = nRT \quad (2-1)$$

2.1.2 Apparent molecular weight (M_a)

One of the main properties of interest to engineering applications is the apparent molecular weight M_a . It is mathematically defined by the following equation. [12, p. 137]

$$M_a = \sum_{i=1} \gamma_i M_i \quad (2-2)$$

M_a is the apparent molecular weight of the gas mixture where γ_i represents the mole fraction of the i th component in a gas mixture.

The mole fraction of a particular component, i , is given by the number of moles of that component, n_i , divided by the total number of moles, n :

$$\gamma_i = \frac{n_i}{n} = \frac{n_i}{\sum_i n_i} \quad (2-3)$$

The weight and volume fraction of a particular component can be calculated by:

$$w_i = \frac{m_i}{m} = \frac{m_i}{\sum_i m_i} \text{ and } v_i = \frac{V_i}{V} = \frac{V_i}{\sum_i V_i} \quad (2-4)$$

The conversion from mole fraction to weight fraction is accomplished by following steps

$$n = \frac{m}{M} ; \gamma_i = \frac{n_i}{n} = \frac{n_i}{1} = n_i ; m_i = n_i M_i = \gamma_i M_i \quad (2-5)$$

$$w_i = \frac{m_i}{m} = \frac{m_i}{\sum_i m_i} = \frac{\gamma_i M_i}{\sum_i \gamma_i M_i} = \frac{\gamma_i M_i}{M_a} \quad (2-6)$$

and similarly

$$\gamma_i = \frac{w_i/M_i}{\sum_i w_i/M_i} \quad (2-7)$$

2.1.3 Specific gas gravity (γ_g)

The specific gravity is defined as the ratio of the gas density to that of air. The densities of air and gas are measured or expressed at the same temperature and pressure. Normally, the standard pressure, p_{sc} , and standard temperature, T_{sc} , are used to define the gas specific gravity. [12]

$$\gamma_g = \frac{\text{gas density @ 14,7 psi and 60}^\circ\text{F}}{\text{air density @ 14,7 psi and 60}^\circ\text{F}} = \frac{\rho_g}{\rho_{air}} \quad (2-8)$$

The specific gas gravity can then be expressed as

$$\gamma_g = \frac{\frac{p_{sc}M_a}{RT_{sc}}}{\frac{p_{sc}M_{air}}{RT_{sc}}} \quad \text{or} \quad \gamma_g = \frac{M_a}{M_{air}} = \frac{M_a}{28,96} \quad (2-9)$$

assuming that the behaviour of the gas mixtures is described by the ideal gas equation.

2.1.4 Characterization of different types of gas

A natural gas may be characterized according to the phases present at reservoir or surface conditions. Natural gases are classified as dry, wet, associated or condensate gas depending on whether a liquid hydrocarbon phase coexists during any stage of the production. [13] It can be helpful and even necessary to distinguish between the different gas types when applying pseudocritical gas correlations.

The first distinction can be made between dry and wet gas. A dry gas does not form a liquid phase during the entire production process and the points representing the surface and reservoir condition lie out outside the two phase region (Figure 2-1). In contrast a wet gas is classified as a gas that will form a liquid phase at the surface without retrograde condensation in the reservoir. The point which represents the surface conditions is located within the vapour liquid domain (Figure 2-2). [13]

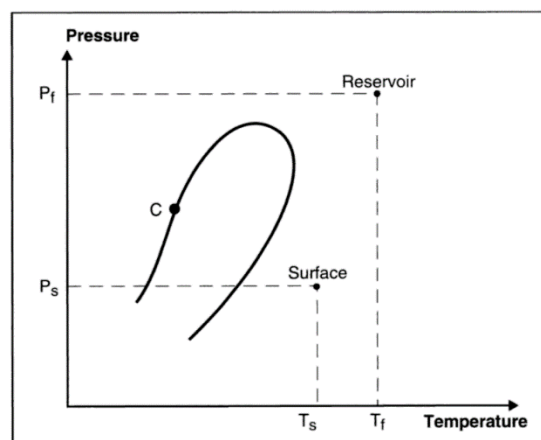


Figure 2-1: Phase diagram of a dry gas system. [13]

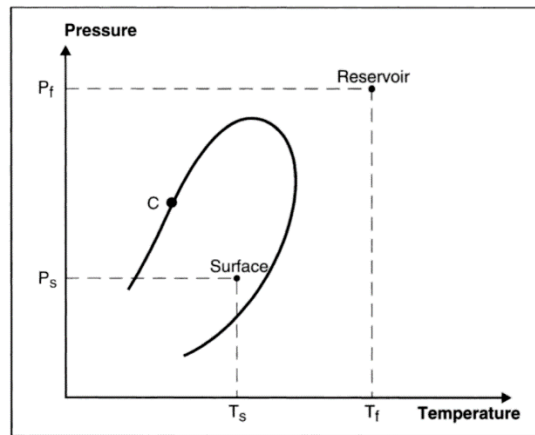


Figure 2-2: Phase diagram of a wet gas system. [13]

Condensate gas forms a liquid phase in the reservoir by retrograde condensation (described by Figure 2-3 and Figure 2-4). The decompression of the gas during production leads to the formation of a liquid phase by retrograde condensation. The condensed phase is enriched with heavy components and this leads to a change in composition over time. [13]

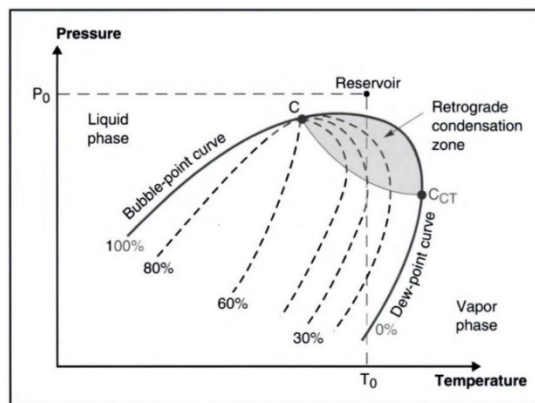


Figure 2-3: Retrograde condensation. [13]

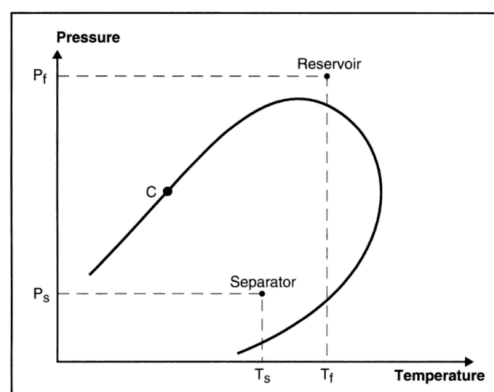


Figure 2-4: Phase diagram of a condensate gas system. [13]

Associated gas is gas that coexists in the reservoir with a liquid oil phase. It may be produced as solution gas in oil or in the form of a gas cap lying above the oil reservoir (Figure 2-5). [13] Associated gas which is liberated from oil is typically rich in ethane through pentane while gas

condensates contains significant amounts of heptane-plus. [14] This difference in composition is of special interest when selecting the appropriate gas correlations.

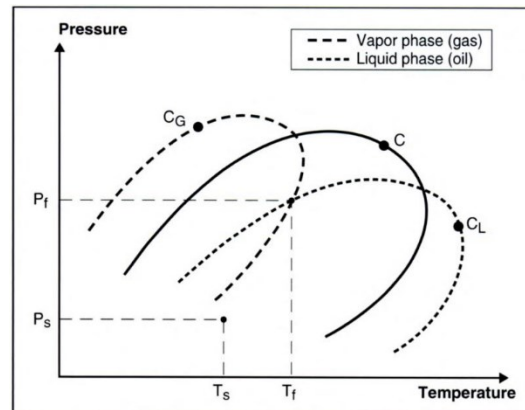


Figure 2-5: Phase diagram of an oil and associated gas system. [13]

2.1.5 Statistical parameters

Statistical parameters such as the average relative error (ARE), the average absolute relative error (AARE) and the correlation coefficient R^2 are commonly used throughout the literature to evaluate the performance of various correlation methods.

The ARE defined in Equation (2-10) is the arithmetic average of the relative error and a measure of the bias of the correlation. A value of zero would mean a random deviation of the measured values around the correlation. If laboratory-measured values of a property are truly random, a small value of the ARE will therefore indicate that the estimated values are as accurate, or possibly more accurate, than laboratory measurements. [15]

$$ARE = \frac{100}{n} \sum_{i=1}^n \frac{y_{expected} - y_{calculated}}{y_{expected}} \quad (2-10)$$

AARE is an indication of the precision of the correlation as well as the accuracy of the data. It is defined as the arithmetic average of the absolute values of the relative errors as shown in Equation (2-11). While a small value of AARE suggests a good correlation based on good data a large value of AARE could be an indication of a poor quality correlation (inadequate functional form). Conversely, several different correlation, all with large values of AARE would most likely indicate poor quality data. [15]

$$AARE = \frac{100}{n} \sum_{i=1}^n \left| \frac{y_{expected} - y_{calculated}}{y_{expected}} \right| \quad (2-11)$$

The correlation coefficient R^2 defined in Equation (2-12) is a measure of the precision of the fit of the data. A value of zero indicates that there is no correlation between the data and model while a value of one would mean that the data is perfectly correlated. A combined small value of the AARE, and a R^2 value close to one would denote a good correlation based on good data. [16]

$$R^2 = 1 - \frac{\sum_{i=1}^n (y_{\text{expected}} - y_{\text{calculated}})^2}{\sum_{i=1}^n (y_{\text{mean}} - y_{\text{calculated}})^2} \quad (2-12)$$

Where y_{mean} is the mean value, y_{expected} is the actual or expected value and $y_{\text{calculated}}$ is the forecast or calculated value.

2.1.6 Corresponding states theory

Amongst a variety of molecular theories that can be useful for data correlation the law of corresponding states, also known as the corresponding-states principle, is especially helpful. The theory of corresponding states asserts “that if pressure, volume, and temperature are divided by the corresponding critical properties, the function relating reduced pressure to reduced volume and reduced temperature becomes the same for all substances.” [10, p. 1.4] This circumstance is shown in Figure 2-6 where the reduced density and volume of methane and nitrogen for saturated liquid and saturated vapour result in almost identical curves.

The reduced properties are expressed as a fraction of the respective critical properties:

$$T_r = \frac{T}{T_c}; \quad p_r = \frac{p}{p_c}; \quad V_r = \frac{V}{V_c} \quad (2-13)$$

The corresponding states theory plays an important part in the z-factor estimation and has been applied to estimation methods such as viscosity correlations where the viscosity of interest can be obtained by expressing it as a ratio of high-pressure to low pressure gas viscosity at the critical temperature. [10, p. 1.4]

If the gases have similar molecular characteristics the law of corresponding states is more accurate. This is the case for natural gases which are generally composed of molecules of the same class of organic compounds. [17, p. 110]

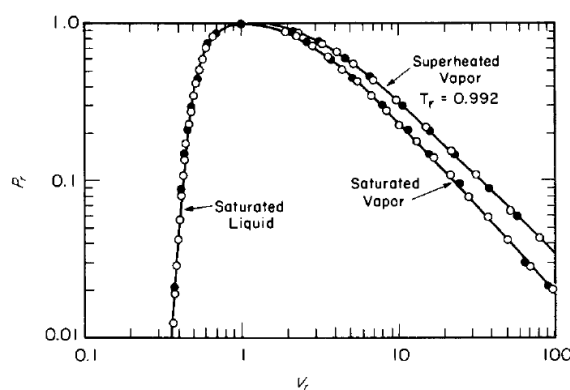


Figure 2-6: The law of corresponding states applied to methane and nitrogen. Methane:○; Nitrogen:●. [10, p. 1.5]

3 Natural gas mixtures

3.1 National Institute of Standards and Technology (NIST) database.

The NIST WebBook provides thermochemical, thermophysical, and ion energetics data compiled by NIST under the Standard Reference Data Program. NIST is an agency of the U.S. Department of Commerce and states that:

“[NIST] uses its best efforts to deliver a high quality copy of the Database and to verify that the data contained therein have been selected on the basis of sound scientific judgment”

Several thermo-physical properties such as density, viscosity, thermal conductivity, enthalpy and surface tension are available for numerous pure fluids over a wide temperature and pressure range. Amongst others, the data base includes fluids of especial interest to the petroleum industry such as water, carbon dioxide, hydrogen sulphide, and all kinds of naturally occurring gases.

Pure hydrocarbon fluid data form ethane to decane and other miscellaneous gases such carbon dioxide, hydrogen sulphide, nitrogen or noble gases can be easily accessed through the NIST website data site listed in Reference [15]. Once the desired Temperature, pressure or density range has been set the data may be displayed and easily downloaded in a tabulated text file format.

The database consists of experimental and or empirical data. Reference is made to the underlying models and additional information such as the correlation uncertainties are provided.

For this study is the data provided by NIST is used as a reference to compare both the natural gas and carbon dioxide correlation model results.

The extended fee based NIST Reference Fluid Thermodynamic and Transport Properties Database (REFPROP) in the latest version 9.1 includes additional features such as mixture model for natural gas fluids based on the GERG-2008 (GERG is the European Gas Research Group) equation and the AGA-8 natural gas mixture models. [55] This equation is based on an excess Helmholtz energy approach using pure fluid equations of state and a mixture model that specifies the excess contribution.

3.2 Density

Based on the ideal gas equation of state, the compressibility factor EOS is given as:

$$pV = ZnRT \quad (3-1)$$

The density ρ is defined as the mass of gas per unit volume, while the number of moles, n , can be expressed as the ratio of mass to molar mass M_w :

$$n = \frac{m}{M_w}; \quad V = \frac{m}{\rho} \quad (3-2)$$

Combining the above equations the density of real gas is related to the compressibility factor by:

$$\rho = \frac{pM_w}{ZRT} \quad (3-3)$$

Instead of using the z-factor EOS an equation of state such as the van der Waals or Peng – Robinson EOS can be also used to calculate the density of real gases.

Three of the most commonly used EOS in the petroleum industry are the Soave-Redlich-Kwong (SRK-EOS), Peng-Robinson (PR-EOS) and, Patel-Teja (PT-EOS). Comparing these EOS to models based on the calculation of pseudocritical properties and the Z-factor Elsharkawy [18] showed the density of a natural gas may be calculated just as accurately with the compressibility factor equation of state. Estimating the density via z-factor EOS has the advantage of eliminating computational work involved in EOS calculations. For example the characterization of the plus fraction, and estimation of the binary interaction parameter which are necessary for EOS calculations are not required. [18]

3.3 Z-factor

The z-factor can be defined as the ratio of the volume actually occupied by a gas to the volume the gas would occupy if it behaved like an ideal gas at the same given temperatures and pressures. The Z-factor is also known as the compressibility factor or gas deviation factor. [17]

$$Z = \frac{V_{actual}}{V_{ideal}} \quad (3-4)$$

Inserting this correction factor into the ideal gas equation results in the compressibility equation of state which is one of the most commonly used in the petroleum industry. [17]

$$pV = ZnRT \quad (3-5)$$

$$pV_M = ZRT \quad (3-6)$$

The density ρ is connected to the compressibility factor by the equation:

$$\rho = \frac{M}{V} = \frac{pM}{ZRT} \quad (3-7)$$

For an ideal gas the compressibility factor is 1 whereas for a natural gas it varies with pressure. As the pressure of an ideal gas tends towards zero its behaviour approaches that of an ideal gas and therefore the Z-factor also tends towards 1. The z-factor goes through minimum as the pressure rises but increases again for higher pressures (Figure 3-1). [13]

If no experimental data is available the z-factor can be estimated by empirical correlations. The Standing and Katz (1942) (SK) gas z-factor chart has become a standard in the industry since

its publication in 1942. Since then various different, very accurate approaches have been developed to represent the chart digitally. Methods published by Hall and Yarborough (1973, 1974) (HY), Dranchuk et al. (1974) (DPR), and Dranchuk and Abou-Kassem (1975) (DAK) are the most common in the engineering community. All of them make use of some form of equation of state that has been fitted to a Z-factor chart. [14] [13, p. 87]

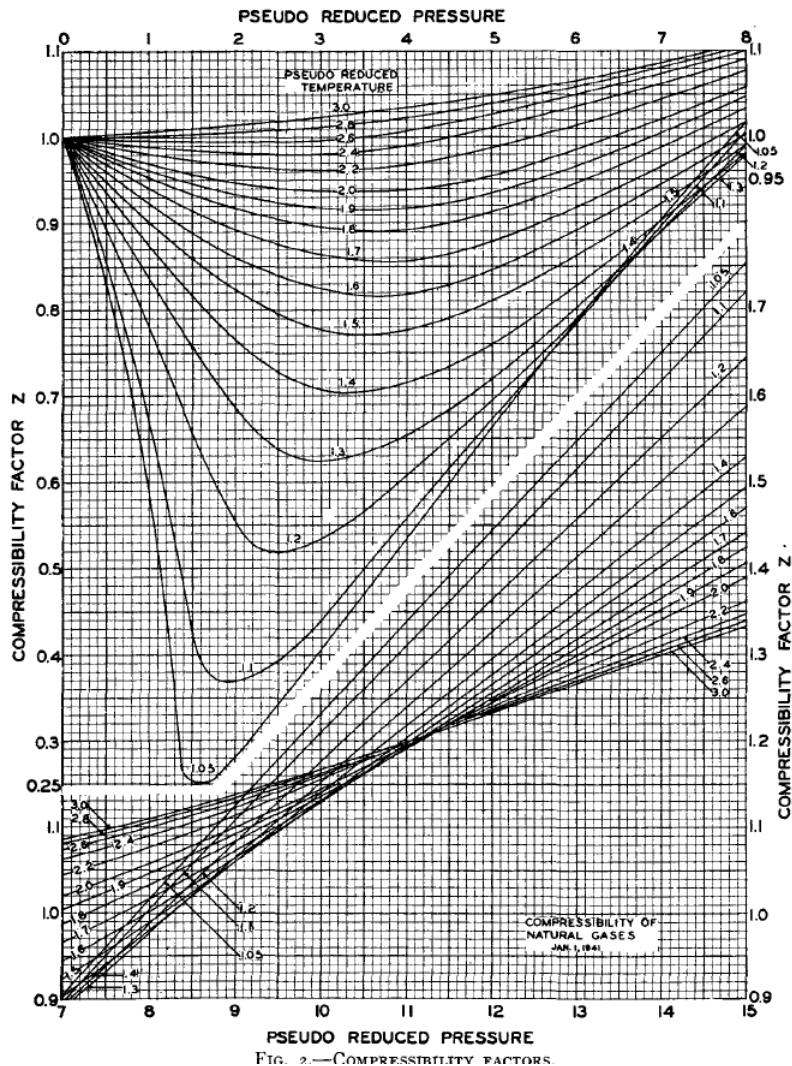


Figure 3-1: Standing and Katz z-factor chart. [19]

The z-factor chart is based on the principle of corresponding states which says that two substances at the same conditions referenced to their critical pressure and temperature will possess similar properties. [14] Therefore the definitions of the terms reduced temperature and reduced pressure were introduced and defined as

$$T_r = \frac{T}{T_c} \text{ and } p_r = \frac{p}{p_c} \quad (3-8)$$

In other words, all pure gases have the same Z-factor at the same reduced values. In a mathematical sense the SK chart relates these reduced properties to the Z-factor. [14] [17, p. 108] When dealing with gas mixtures the pseudocritical properties P_{pc} and T_{pc} are used. The use of estimation methods for these properties are discussed in the next chapters.

Takacs [20] compared eight correlations representing the Standing-Katz and found that the Hall and Yarborough (HY) [21] and the Dranchuk and Abou-Kassem (DAK) [22] equations give the most accurate representation for a wide range of temperatures and pressures. Both methods are valid for $1 \leq T_r \leq 3$ and $0.2 \leq p_r \leq 25$ to 30. [14]

In their evaluation of different pseudocritical and z-factor correlations McCain et al. [15] report that in a statistical sense there is no difference between the results from the HY and DAK equations. However the DAK method is recommended over the HY as the latter procedure does occasionally not converge. [15]

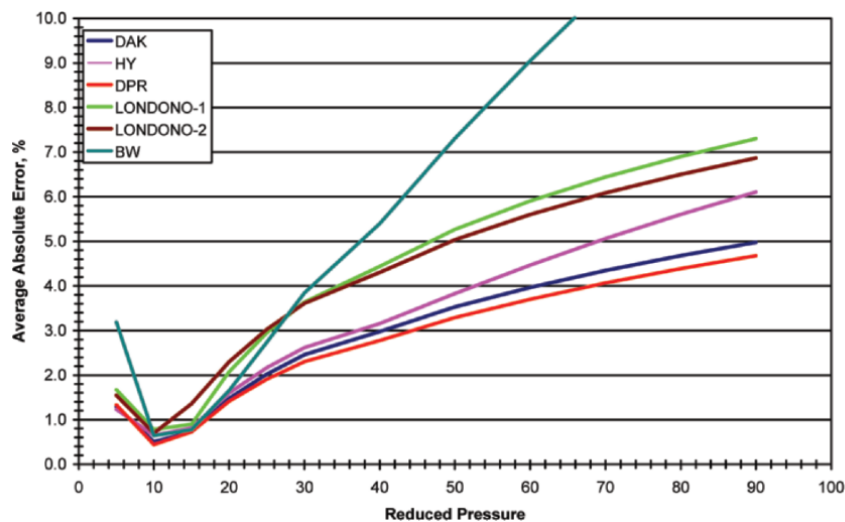


Figure 3-2: Errors of different z-factor methods evaluated by Sutton (2007). [14]

Sutton (2007) [14] recommends the DAK method over the slightly more accurate DPR method (Figure 3-2) as the DAK correlation “strikes a balance between low error and low standard deviation”. [14] Sutton also notes that the corrections proposed by Borges (1991) [23] must be made to obtain accurate z-factors at high pressures. Failure to do so will result in z factors that change exactly as pressure changes leading to constant densities formation volume factors. [14]

Based on the evaluations the DAK method is clearly one of the preferred z-factor correlations therefore discussed in the next subsection.

Apart from the mentioned z-factor correlations, specific empirical methods for calculating the compressibility factor of natural gases have been developed on the initiative of gas companies. In the United States the “AGA8” was developed by the Gas Research Institute while the “GERG” method was developed by a group of European gas companies. [13, p. 89]

3.3.1 Dranchuk and Abou-Kassem (1975) Z-factor correlation

The equation proposed by Dranchuk and Abou-Kassem is based on the generalized Starling equation that has been fitted to Katz z-factor correlation resulting in Equation (3-9). The DAK

equation is valid in a range of $1 \leq T_r \leq 3$ and $0.2 \leq p_r \leq 30$ and the corresponding coefficients are listed in Table 3-1. [22]

$$z = \left[A_1 + \frac{A_2}{T_{pr}} + \frac{A_3}{T_{pr}^3} + \frac{A_4}{T_{pr}^4} + \frac{A_5}{T_{pr}^5} \right] \rho_r + \left[A_6 + \frac{A_7}{T_{pr}} + \frac{A_8}{T_{pr}^2} \right] \rho_r^2 - A_9 \left[\frac{A_7}{T_{pr}} + \frac{A_8}{T_{pr}^2} \right] \rho_r^5 + A_{10} (1 + A_{11} \rho_r^2) \frac{\rho_r^2}{T_{pr}^3} e^{[-A_{11} \rho_r^2]} + 1 \quad (3-9)$$

The reduced density ρ_r is defined as:

$$\rho_r = \frac{0,27 p_{pr}}{Z T_{pr}} \quad (3-10)$$

Table 3-1: Coefficients for the DAK correlation. [22]

A_i		A_i	
A_1	0.3265	A_7	-0.7361
A_2	-1.0700	A_8	0.1844
A_3	-0.5339	A_9	0.1056
A_4	-0.05165	A_{10}	0.6134
A_5	-0.05165	A_{11}	0.7210
A_6	0.5475		

Dranchuk and Abou-Kassem (1975) provide a FORTAN program code (ZSTAR subroutine) to calculate the z-factor according to Equation (3-9). An improved FORTAN code is presented by Abou-Kassem et al (1990) [24]. To avoid inaccurate z-factor values within the range stated by Dranchuk and Abou-Kassem (1975) for high gas density calculations the modification introduced by Borges (1990) [23] has to be used. This corrections consists of setting a reduced density limit from 2.2 to a value of 3 or greater in the original ZSTAR code.

3.3.2 Z-factor calculation at high density and high pressure (HPHT)

Reservoirs with pressures from 10 000 psia to 30 000 psia and temperatures above 300°F are generally classified as high pressure and high temperature (HPHT) reservoirs. McCain et al. (2011) [15] report that densities calculated with the Piper et al.(see 3.4.1.3) and DAK (see 3.3.1) methods are in good agreement with NIST data [25] for methane at pressure and temperature ranges from 10 000 psia to 30 000 psia and 300°F to 400°F respectively. The authors also indicate that the above-mentioned methods may also be used, with reasonable confidence, for gases containing non-hydrocarbons at HPHT conditions. [15]

Rushing et al. [26] compared laboratory measurements correlations for a dry gas with varying CO₂ content. Several commonly used pseudocritical and z-factor correlations for four dry gas mixtures at pressures up to 20,000 psia and temperatures of 300°F and 400°F with carbon dioxide contents of 0, 5, 10, and 20mol% were tested against each other. Rushing et al. conclude that the HY z-factor correlation [21] in combination with the Sutton (2007) [14] and the Wichert and Aziz correction deliver the best results in many cases.

Interestingly McCain et al (2011) [15, p. 29] claim that z-factors calculated with the DAK and Piper et al. methods fit the Rushing et al. data within 1% for pressures from 3000 to 20 000 psia.

3.4 Pseudo critical properties correlations

For the purpose of obtaining critical properties for mixtures pseudocritical properties were introduced. These properties have no physical significance and were simply devised for the use in correlating different properties. [14] [17, p. 111]

The pseudocritical properties can most simply be found by applying Kay's equation [27], defining the pseudo reduced properties as the molal average critical temperature and pressure of the mixture components.

$$P_{pc} = \sum_i y_i P_{c_i} \text{ and } T_{pc} = \sum_i y_i T_{c_i} \quad (3-11)$$

However, it was found that this equation developed by Kay in 1936, is valid only for certain gas compositions and more accurate correlations incorporating different mixing rules were developed over the years. For example Kay's molar average rule does not provide satisfactory results for higher molar molecular weight gases and alternate methods were developed (e.g. Sutton 1985). [28]

Two classes of methods are available for the estimation of pseudocritical properties: Methods that correlate the pseudocritical properties with gas gravity and those which are based on gas composition and make use of various mixing rules.

If the gas composition is not available (i.e. no data from laboratory study available) the pseudocritical properties can be estimated by applying suitable correlations based on the specific gas gravity. Numerous correlations by different researchers are available for the estimation of pseudocritical properties based on specific gas gravity. [15] The gas specific gravity can easily be calculated for cases where composition is known and specific gas gravity correlations applied accordingly.

Furthermore natural gases can be classified into two relevant categories for the analysis of critical properties. Gas derived from associated gas which is liberated from oil is typically rich in ethane through pentane while gas condensates contains significant amounts of heptanes plus fractions. Additionally the gases may contain impurities such as hydrogen sulphide, carbon dioxide and nitrogen. Unacceptably high calculation errors may result if no distinction is made between the different kinds of gases. For associate and condensate gases Sutton lists specific hydrocarbon gas gravity ranges from 0,554 to 1,862 and 0,554 to 2,667 respectively and notes:

“The problem with using the correct gas pseudocritical-property model applies only to high-gas-gravity scenarios. For gases with a hydrocarbon-gas gravity less than 0.75

to 0.8, the differences in the pseudocritical-property relationships are too small to create significant errors in calculated Z factors.” [14]

3.4.1 Correlations for unknown compositions based on gas gravity

The use of mixing rules to estimate the pseudocritical properties requires knowledge of the gas composition which is not always available. As a result empirical correlations which only use the specific gas gravity as an input have been developed.

3.4.1.1 Standing (1981)

In 1948 Brown et al. [29] presented a graphical method for the approximation of the pseudocritical properties of gases shown in Figure 3-3 for cases when only the specific gas gravity is known.

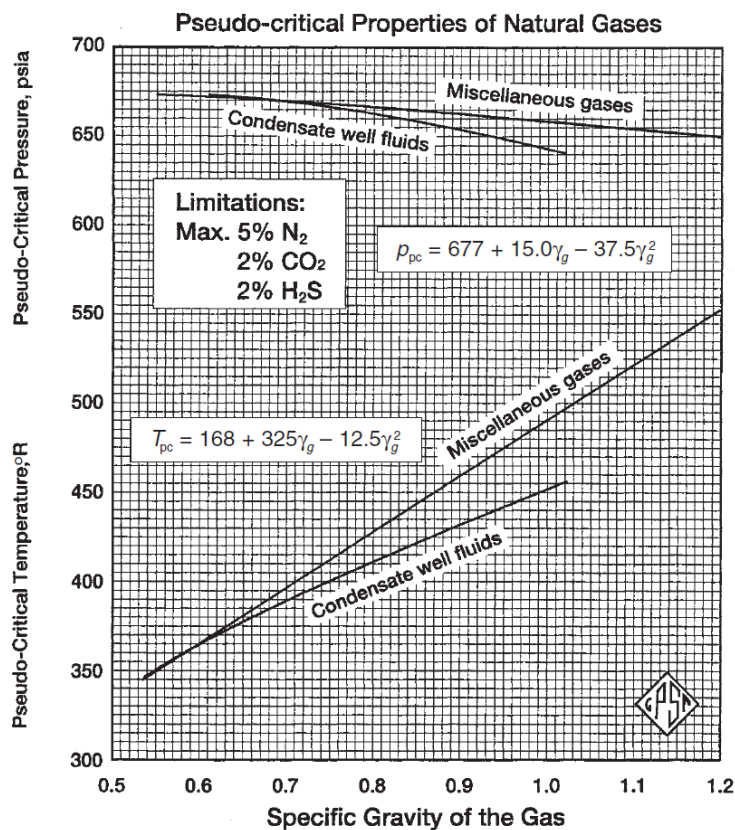


Figure 3-3: Pseudocritical properties correlations for natural gases [12, p. 146]

This graphical correlation was expressed in mathematical terms by Standing (1981) [30] resulting in Equations (3-12) and (3-13). [12]

$$p_{pc} = 677 + 15\gamma_g - 37,5\gamma_g^2 \quad (3-12)$$

$$T_{pc} = 168 + 325\gamma_g - 12,5\gamma_g^2 \quad (3-13)$$

For the condensate gas curves, Equations (3-14) and (3-15) are valid. The p_{pc} and T_{pc} are in psia and Rankine, respectively. Standing notes that there is no unique correlation of

pseudocritical properties and that the developed relationships only represent four out of an infinite number of relationships. [30]

$$p_{pc} = 706 + 51,7\gamma_{gHC} - 11,1\gamma_g^2 \quad (3-14)$$

$$T_{pc} = 187 + 330\gamma_g - 71,5\gamma_g^2 \quad (3-15)$$

Both relationships were derived from mixtures with negligible N₂, CO₂ and H₂S amounts. However, for gases that contain non-hydrocarbon components Standing recommends to use the Wichert and Aziz Correction (see 3.4.3.1). [30]

3.4.1.2 Sutton (1985)

Sutton found that Kay's molar average combination rules or comparable gravity relationships did not provide satisfactory results in calculating the z-factor for high molecular weight gases. Sutton investigated gases that derive their high molecular weight from a significant quantity of heptane plus (C7+) as opposed to gases for which relatively high concentrations of ethane and propane are responsible for a high molecular weight. [28]

The pseudocritical gas gravity relationship established by Sutton is based on 264 different gas samples. Nonlinear regression was used with the Dranchuk and Abou-Kassem equations providing pseudocritical properties which are 'tuned' to the equation and therefore the SK chart, ultimately resulting in more accurate z-factors. [28] As a result it was possible to obtain following pseudocritical properties correlations for hydrocarbon mixtures:

$$p_{pc} = 756,8 - 131,07\gamma_g - 3,6\gamma_g^2 \quad (3-16)$$

$$T_{pc} = 169,2 + 349,5\gamma_g - 74,0\gamma_g^2 \quad (3-17)$$

The p_{pc} and T_{pc} are in psia and Rankine, respectively. By using Equations (3-16) and (3-17) for the prediction of the pseudocritical properties and subsequently the z-factors Sutton [28] states the average absolute error can be reduced to 1,2% as compared errors as high as 15% percent when using Kay's rule to determine the pseudocritical properties.

3.4.1.3 Piper et al. (1993)

Piper et al. developed a pseudocritical gas gravity relationship taking the presence of acid gases into account. The objective of the proposed relationship is a more accurate representation of the z-factors when used in combination with the DAK-EOS for cases where the gas composition is unknown. Multiple regression techniques were used with 1482 pairs of the inferred Stewart Burkhardt and Voo (SBV) parameters J and K to establish a correlation based on the specific gas gravity. [31]

$$J = \alpha_0 + \sum_{i=1}^3 \alpha_i y_i \left(\frac{T_c}{p_c} \right)_i + \alpha_4 \gamma_g + \alpha_5 \gamma_g^2 \quad (3-18)$$

$$K = \beta_0 + \sum_{i=1}^3 \beta_i y_i \left(\frac{T_c}{\sqrt{p_c}} \right)_i + \beta_4 \gamma_g + \beta_5 \gamma_g^2 \quad (3-19)$$

where y_i describes y_{H_2S} , y_{CO_2} and y_{N_2} . T_{pc} and p_{pc} are calculated as:

$$T_{pc} = \frac{K^2}{J} \quad (3-20)$$

$$p_{pc} = \frac{T_{pc}^2}{J} \quad (3-21)$$

This method is simpler compared to e.g. Sutton's or Standing's technique as the effects of non-hydrocarbon and acid gases are directly accounted for. Piper et al. state that the proposed correlations may be used for any naturally occurring petroleum gas with acid gas contents as high as 50% and nitrogen content as high as 10%. Standing's and Sutton's correlation in combination with the Wichert and Aziz correction were evaluated and found to produce errors of 1.99 and 1.42 % respectively. However when assuming unknown amount of impurities, the aforementioned methods result in errors as high as 27%, while the Piper et al. method yield errors of 1,3 % with a maximum error of 7.3 %. High errors especially occurred for gases at high pressure and more than 5% acid gas content. It is therefore absolutely necessary to employ non-hydrocarbon adjustment methods to account for the presence of acid gas and nitrogen in cases where the Piper et al. correlation is not used. [31]

Table 3-2: Coefficients for Equations (3-18) and (3-19). [31]

i	α_i	β_i
0	1.1582E-1	3.8216E0
1	-4.5820E-1	-6.5340E-2
2	-9.0348E-1	-4.2113E-1
3	-6.6026E-1	-9.1249E-1
4	7.0729E-1	1.7438E1
5	-9.9397E-2	-3.2191E0

3.4.1.4 Elsharkawy et al. (2000)

Elsharkawy et al. presented new methods for calculating the gas compressibility factor by developing a new mixing rule and a new gas gravity correlation for cases where gas composition is unavailable. For the latter Elsharkawy et al. employed the DAK correlation to calculate the inferred pseudocritical values which were found to closely fit the Standing-Katz compressibility factor chart. Secondly the inferred values of J and K were calculated in order to later correlate them to the gas gravity. This procedure resulted in Equation (3-22) and (3-23). [32]

$$p_{pc} = 787,06 - 147,34\gamma_g - 7,916\gamma_g^2 \quad (3-22)$$

$$T_{pc} = 149,18 + 358,14\gamma_g - 66,976\gamma_g^2 \quad (3-23)$$

Comparing the newly established correlation against Sutton's (1985) and Standing's (1981) Elsharkawy et al. claim that it has smaller errors and standard deviations in the gas gravity ranges from 0.8 to 1.0 and 1.2 to 1.4. However, it is noted that the proposed correlation offers little improvement over Sutton's. [32] Elsharkawy et al. do not mention the use of any correction method for non-hydrocarbon components.

3.4.1.5 Elsharkawy and Elkamel (2000)

The method presented by Elsharkawy and Elkamel aims at estimating the pseudocritical properties from gas gravity specifically for sour gas when the composition is not available, without having to conduct a separate correction to account for the acid components. It was found that the pseudocritical pressure strongly correlates with the percentage of non-hydrocarbon gases while pseudocritical temperature while the pseudo critical temperature is dependent on total gas gravity. As a result the best correlation was attained by considering both the non-hydrocarbon gas gravity γ_2 And total gas gravity γ_g in Equation (3-24) and (3-25).[33]

$$P_c = 193,941 - 131,347\gamma_g + 217,144\frac{\gamma_1}{\gamma_g} + 1060,349\frac{\gamma_2}{\gamma_g} + 344,573\left(\frac{\gamma_1}{\gamma_g}\right)^2 - 60,591\left(\frac{\gamma_2}{\gamma_g}\right)^2 \quad (3-24)$$

$$T_c = 195,958 + 206,121\gamma_g + 25,855\frac{\gamma_1}{\gamma_g} - 6,421\frac{\gamma_2}{\gamma_g} + 9,022\left(\frac{\gamma_1}{\gamma_g}\right)^2 + 163,247\left(\frac{\gamma_2}{\gamma_g}\right)^2 \quad (3-25)$$

With γ_1 being the hydrocarbon specific gravity and γ_2 being the non-hydrocarbon specific gravity.

Elsharkawy and Elkamel also evaluated the developed correlation against Sutton's (1985), Sanding's and Elsharkawy's et al. methods (Table 3-3) employing the sour gas datasets (Table 3-4) used in their study. [33]

Table 3-3: Accuracy of calculating Z-factor for sour gases with gas gravity correlations [33]

Method	ARE	AAD	SD	R
Standing	-0.81	3.50	6.79	92.08
Sutton	-1.72	3.47	7.14	91.43
Elsharkawy et al	-2.25	3.48	7.30	91.23
Elsharkawy and Elkamel	-0.26	1.69	3.12	97.66

Table 3-4: Properties of sour gas data used by Elsharkawy and Elkamel. [33]

Property	Min.	Ave.	Max.
Pressure, psi	90	2900	12000
Reservoir temperature, F	40	190	327
Composition mole %			
Methane	17.27	74.14	97.40
Heptane plus	0	1.64	17.20
Mw C7+	98.0	127.0	253.0
γ C7+	0.72	0.77	0.85
Z-factor	0.402	0.900	1.775
Gas gravity (air=1)	0.566	0.811	1.895
Hydrogen sulfide	0	7.45	73.85
Carbon dioxide	0	4.04	67.16
Nitrogen	0	1.72	25.15

3.4.1.6 Londono et al. (2002)

After fitting the DAK-EOS and Nishiumi-Saito equation of state (NS-EOS) to three large data bases through regression analysis, Londono et al. developed two new models for pseudocritical property estimation based on these 'calibrated' EOS correlations. The databases consisted of data provided by Poettmann-Carpenter (1952) with 5960 data points, an additional pure component data base and combined pure component and mixture data with 8256 and 6032 data points respectively. An average absolute error of 3.06 percent is reported when using the correlation based on the 'calibrated' DAK equation. [34]

$$p_{pc} = 725,89 + 70,27\gamma_g - 9,05\gamma_g^2 \quad (3-26)$$

$$T_{pc} = 40,39 + 549,47\gamma_g - 94,01\gamma_g^2 \quad (3-27)$$

In a similar fashion, for the relationships (3-28) and (3-29) derived from the NS correlation an average absolute error of 2,55 percent was obtained. [34]

$$p_{pc} = 621,81 + 81,09\gamma_g - 56,51\gamma_g^2 \quad (3-28)$$

$$T_{pc} = 46,91 + 542,86\gamma_g - 93,14\gamma_g^2 \quad (3-29)$$

Londono et al. recommend further investigation of the explicit effects of non-hydrocarbon components such as water, nitrogen, carbon dioxide and water. Furthermore it is noted that the presented work may be extended to consider the behaviour of rich gas condensates. [34]

3.4.1.7 Sutton (2007)

Sutton established correlations by using a significant amount of new data added to the original database used by the same author in 1985. Separate relationships for associated and condensate gases were developed. While associated gases are typically rich in ethane through pentane and have a low heptane-plus component, it can be present in significant quantities. For such cases Sutton recommends the use of pseudocritical property correlations for gas condensates. [14]

The developed gas gravity relationships for associated gas are based on 967 gas compositions with a total of 4817 measurements points, summarized in Table 3-5. Equation and (3-30) and (3-31) were developed by applying a nonlinear regression routine that was established to infer pseudocritical properties for the updated hydrocarbon-gas data set: [14]

$$p_{pcHC} = 671,1 + 14\gamma_{gHC} - 34,3\gamma_{gHC}^2 \quad (3-30)$$

$$T_{pcHC} = 120,1 + 429\gamma_{gHC} - 62,9\gamma_{gHC}^2 \quad (3-31)$$

For the development of a gas condensate relationships, the updated data base contained 2264 compositions with 10117 measurements obtained from single-phase CCE experiments. The properties of these measurements are presented in Table 3-6. The highest hydrocarbon gas gravity in the database was 1,912 and pseudocritical properties were also correlated for oil in order to better define relationships for high gravity gases. Same as for associated gases these correlations represent relationships between pseudocritical properties and hydrocarbon gas gravity only. Modifications to pseudocritical properties to account for non-hydrocarbons have to be made separately. [14]

$$p_{pcHC} = 744 - 125,4\gamma_{gHC} - 5,9\gamma_{gHC}^2 \quad (3-32)$$

$$T_{pcHC} = 164,3 + 357,7\gamma_{gHC} - 67,7\gamma_{gHC}^2 \quad (3-33)$$

In addition to the gas gravity correlation Sutton developed new equations for adjusting pseudocritical properties for the effects of non-hydrocarbons. The coefficients and exponents of the original Wichert and Aziz Equation are modified in order to tune the new equation for optimal use with the proposed new relationships. [14]

$$\varepsilon = 107,6 \left[(y_{H_2S} + y_{CO_2}) - (y_{H_2S} + y_{CO_2})^{2,2} \right] + 5,9(\gamma_{H_2S}^{0,06} - \gamma_{H_2S}^{0,68}) \quad (3-34)$$

Despite a significant change to the coefficients and exponents, changes in the accuracy of the calculated Z factor are insignificant compared to the method proposed by Wichert and Aziz (1972). Therefore that original method is recommended by Sutton to adjust pseudocritical properties for the presence of H₂S and CO₂. [14]

Table 3-5: Associated-gas data base [14]

Property	Minimum	Maximum
Hydrogen sulfide [mol %]	0.0	10.0
Carbon dioxide [mol%]	0.0	55.8
Nitrogen [mol%]	0.0	21.7
Total gas gravity	0.554	1.862
Hydrocarbon-gas gravity	0.554	1.862
Pressure [psia]	12	10000
Temperature [°F]	32	460
Z-factor	0.105	2.328

Table 3-6: Gas condensate data base [14]

Property	Minimum	Maximum
Hydrogen sulfide [mol %]	0.0	90.0
Carbon dioxide [mol%]	0.0	89.9
Nitrogen [mol%]	0.0	33.3
Total gas gravity	0.554	2.667
Hydrocarbon-gas gravity	0.554	2.819
Pressure [psia]	12	17065
Temperature [°F]	0	460
Z-factor	0.129	2.795

3.4.2 Correlations for known compositions based on mixing rules

Mixing rules provide a suitable means to estimate the pseudocritical properties when the exact gas composition is known. Several different mixing rules have been developed and modified by various researchers. Among these, Kay, Stewart- Burkhardt-Voo (SBV) and SBV Modified by Sutton (SSBV) are commonly used in the Industry. Piper et al. and Corredor et al. proposed methods similar to the SBV but treated the non-hydrocarbons and C₇₊ in a different way. The SBV mixing rule is also the starting point for the method developed by Elsharkawy et al. [32]

3.4.2.1 Kay (1936)

By defining the pseudocritical properties as the molal average of the components and their critical properties, Kay's mixing rule [27] represents the simplest form of mixing rule, as can be seen in Equation (3-35). It can usually be applied to lean natural gases that contain no non-hydrocarbons. [35] For higher specific gravity gases ($\gamma_g > 0.75$) Sutton suggests the use of other methods as errors of up to 15% may occur. [28]

$$P_{pc} = \sum_i y_i P_{c_i} \text{ and } T_{pc} = \sum_i y_i T_{c_i} \quad (3-35)$$

3.4.2.2 Stewart, Burkhardt and Voo (SBV) (1959)

Stewart Burkhardt and Voo (1959) [36] developed and compared different mixing rules for natural gases and found that the method described in Equations (3-43) to (3-45) to be the best solution for estimating the pseudocritical pressure and temperature. [28] The SBV is amongst one of the most widely used mixing rules in the petroleum industry. [32]

$$J = \frac{1}{3} \left[\sum y_i \left(\frac{T_c}{p_c} \right)_i \right] + \frac{2}{3} \left[\sum y_i \left(\frac{T_c}{p_c} \right)_i^{0.5} \right]^2 \quad (3-36)$$

$$K = \sum y_i \left(\frac{T_c}{p_c^{0.5}} \right)_i \quad (3-37)$$

$$T_{pc} = \frac{K^2}{J} \text{ and } p_{pc} = \frac{T_{pc}}{J} \quad (3-38)$$

3.4.2.3 Sutton (SSBV) (1985)

Sutton examined the effect of high concentrations of the heptane plus fraction on the calculation of z-factors. It was found that applying Kay's rule for higher-molecular-weight mixtures of hydrocarbon gases resulted in errors in the z-factor as high as 15%. An alternate method for calculating pseudocritical properties from gas composition as well as new pseudocritical property - gas gravity relationships were therefore developed. Data from 275 individual PVT reports covering wide temperature and pressure ranges, with some of the gases containing significant carbon dioxide amounts, were evaluated.[28]

For calculating the pseudocritical properties from gas composition Sutton proposed a modification of the method first proposed by Stewart, Burkhardt, and Voo (1959) [36] who developed and compared 21 different sets of mixing rules to determine pseudocritical properties. By introducing empirically derived adjustment factors (Equations (3-39) to (3-42)) and applying these to the original equation, Sutton claims a significant accuracy improvement in calculating the z-factor can be achieved.[28]

The adjustment factors proposed by Sutton are applied to the "J" and "K" terms:

$$J' = J - \varepsilon_J \quad (3-39)$$

$$K' = K - \varepsilon_K \quad (3-40)$$

The terms ε_J ε_K used to calculate the adjusted J and K value are given by the Equations (3-41) and (3-42). [28]

$$\varepsilon_J = 0,6081F_j + 1,1325F_j^2 - 14,004F_j y_{C7+} + 64,434F_j y_{C7+}^2 \quad (3-41)$$

$$\varepsilon_K = \left(\frac{T_c}{p_c^{0,5}} \right)_{C7+} (0,3129y_{C7+} - 4,8156y_{C7+}^2 + 27,3751y_{C7+}^3) \quad (3-42)$$

Resulting in following calculation procedure:

$$F_j = \frac{1}{3} \left(\frac{y T_c}{p_c} \right)_{C7+} + \frac{2}{3} \left(y \sqrt{\frac{T_c}{p_c}} \right)_{C7+}^2 \quad (3-43)$$

$$J = \frac{1}{3} \sum_{i=1}^n \left(\frac{y_i T_{ci}}{p_{ci}} \right) + \frac{2}{3} \left[\sum_{i=1}^n \left(y_i \sqrt{\frac{T_{ci}}{p_{ci}}} \right) \right]^2 - 0,6081F_j - 1,1235F_j^2 + 14,004F_j y_{C7+} + 64,434F_j y_{C7+}^2 \quad (3-44)$$

$$F_K = \left(\frac{T_c}{\sqrt{p_c}} \right)_{C7+} (0,3129y_{C7+} - 4,8156y_{C7+}^2 + 27,3751y_{C7+}^3) \quad (3-45)$$

$$K = \sum_{i=1}^n \left(\frac{y_i T_{ci}}{\sqrt{p_{ci}}} \right) - F_k \quad (3-46)$$

$$T_{pc} = \frac{K^2}{J} \quad (3-47)$$

$$p_{pc} = \frac{T_{pc}}{J} \quad (3-48)$$

The critical properties T_c and p_c of the C7+ fraction are estimated using correlations by Lee-Kessler given in Equation (3-51) which were found to be more accurate than other equations. [28]

$$p_c = e^{\left[\begin{array}{l} 8,3634 - \frac{0,0566}{\gamma} - \left(0,24244 + \frac{2,2898}{\gamma} + \frac{0,11857}{\gamma^2} \right) 10^{-3} T_b + \\ \left(1,4685 + \frac{3,648}{\gamma} + \frac{0,47227}{\gamma^2} \right) 10^{-7} T_b^2 - \\ \left(0,42019 + \frac{1,6977}{\gamma^2} \right) 10^{-10} T_b^3 \end{array} \right]} \quad (3-49)$$

In connection with the above equation, Whitson and Torp [37] provide a method suitable for estimating the boiling point from specific gravity and molecular weight:

$$T_b = (4,5579M^{0,15178}\gamma^{0,15427})^3 \quad (3-50)$$

Sutton concludes that the Stewart et al. mixing rules combined with the introduced adjustment factors provides results almost three times more accurate than those obtained using Kay's mixing rules. This is especially pronounced with high molecular weight gases where the derived z-factors are eight times more accurate. It is therefore recommended not to use Kay's rule to determine pseudocritical properties for gases with specific gravities of more than about 0.75. [28]

3.4.2.4 Corredor et al. (1992)

Corredor et al. [38] used the DAK equation to determine the inferred pseudocritical constants which were then used to develop a new correlation for J and K through multiple regression analysis. A strong correlation between the J and K values and the mass of the heptane plus in the mixture was observed. This led to the C7+ mass being directly included in the correlation. A total of 896 values of J and K were used to empirically find the correlation represented by Equations (3-51) and (3-52). The coefficients can be found in Table 3-7.

In a subsequent study Piper et al. [31] changed the coefficients while using the same basic formula. The great departure from previous methods is that the proposed method does not

require the use of other correlations to account for the effects of the heptane plus fraction (i.e. Wichert and Aziz correction).

Table 3-7: Coefficients for Equations (3-51) and (3-52). [31]

i	α_i	β_i
0	1.5303E-1	2.6662E0
1	9.0991E-1	9.7778E-1
2	9.5869E-1	9.7607E-1
3	6.6612E-1	7.4161E-1
4	4.7920E-1	5.2672E-1
5	3.4198E-1	1.6886E-2
6	2.0370E-2	4.5333E-1
7	-8.4700E-5	-3.1884E-3

3.4.2.5 Piper et al. (1993)

Based on earlier work by Corredor et al., Piper et al. proposed an updated version of a gas composition correlation similar in form to the SBV equations. The new study adds 586 data points to the original 896 data points with more gases in a higher specific gravity range. In addition, the data contains significantly more gas with non-hydrocarbon impurities than the data used by Sutton (1985). [31]

$$J = \alpha_0 + \sum_{i=1}^3 \alpha_i y_i \left(\frac{T_c}{p_c} \right)_i + \alpha_4 \sum_j y_j \left(\frac{T_c}{p_c} \right)_j + \alpha_5 \left[\sum_j y_j \left(\frac{T_c}{p_c} \right)_j \right]^2 + \alpha_6 y_{C_{7+}} M_{C_{7+}} + \alpha_7 (y_{C_{7+}} M_{C_{7+}})^2 \quad (3-51)$$

$$K = \beta_0 + \sum_{i=1}^3 \beta_i y_i \left(\frac{T_c}{\sqrt{p_c}} \right)_i + \beta_4 \sum_j y_j \left(\frac{T_c}{\sqrt{p_c}} \right)_j + \beta_5 \left[\sum_j y_j \left(\frac{T_c}{\sqrt{p_c}} \right)_j \right]^2 + \beta_6 y_{C_{7+}} M_{C_{7+}} + \beta_7 (y_{C_{7+}} M_{C_{7+}})^2 \quad (3-52)$$

Where $\gamma_i \in \{\gamma_{H_2S}, \gamma_{CO_2}, \gamma_{N_2}\}$, $\gamma_j \in \{\gamma_{C_1}, \gamma_{C_2}, \dots, \gamma_{nC_6}\}$ and T_{pc} and p_{pc} are given by:

$$T_{pc} = \frac{K^2}{J} \quad (3-53)$$

$$p_{pc} = \frac{T_{pc}}{J} \quad (3-54)$$

The evaluation of the extended data set resulted in updated coefficients which can be found in Table 3-8. Compared to previous works, such as Sutton (1985), this correlation does not require the use of other correlations for the calculation of the heptane plus fraction or the effect of non-hydrocarbon impurities. [31]

When employed for calculation of the z-factor in combination with the DAK equations an average absolute error of 1.1 and a maximum error of 5.8 were found. [31]

Table 3-8: Coefficients for Equations (3-51) and (3-52). [31]

i	α_i	β_i
0	5.2073E-2	-3.9741E-1
1	1.0160E0	1.0503E0
2	8.6961E-1	9.6592E-1
3	7.2646E-1	7.8569E-1
4	8.5100E-1	9.8211E-1
5	0	0
6	2.0818E-2	4.5536E-1
7	-1.5060E-4	-3.7684E-3

3.4.2.6 Elsharkawy et al. (2000)

Elsharkawy et al. developed, as they claim, a simpler, more consistent correlation which accounts for the presence of the heptane plus fraction in an easier way compared to previously available methods. Same as for the other discussed methods the proposed correlation for calculating the pseudocritical properties of a gas condensate was developed on the basis of the SBV mixing rule and uses the DAK correlation to arrive at the inferred values of J and K. [32]

$$J = \left[\sum y_i \left(\frac{T_c}{p_c} \right)_i \right]_{C_1-C_6} + \left\{ a_0 + \left[a_1 \left(\frac{yT_c}{p_c} \right) \right] \right\}_{C_{7+}} \quad (3-55)$$

$$K = \left[\sum y_i \left(\frac{T_c}{p_c^{0.5}} \right)_i \right]_{C_1-C_6} + \left\{ b_0 + \left[b_1 \left(\frac{yT_c}{p_c^{0.5}} \right) \right] \right\}_{C_{7+}} \quad (3-56)$$

Equations (3-55) and (3-56) with their appropriate coefficients listed in Table 3-9 can be applied to pure gas mixtures while Equations (3-57) and (3-58) are recommended for gas condensates that contain some non-hydrocarbon components. [32]

$$J = \left[\sum y_i \left(\frac{T_c}{p_c} \right)_i \right]_{C_1-C_6} + \left\{ a_0 + \left[a_1 + \left(\frac{yT_c}{p_c} \right) \right] \right\}_{C_{7+}} + \left[a_2 \left(\frac{yT_c}{p_c} \right) \right]_{N_2} \left[a_3 \left(\frac{yT_c}{p_c} \right) \right]_{CO_2} \left[a_4 \left(\frac{yT_c}{p_c} \right) \right]_{H_2S} \quad (3-57)$$

$$\begin{aligned}
K = & \left[\sum y_i \left(\frac{T_c}{p_c^{0,5}} \right) \right]_{i, C_1-C_6} \\
& + \left\{ b_0 + \left[b_1 \left(\frac{yT_c}{p_c^{0,5}} \right) \right]_{C_{7+}} + \left[b_2 \left(\frac{yT_c}{p_c^{0,5}} \right) \right]_{N_2} + \left[b_3 \left(\frac{yT_c}{p_c^{0,5}} \right) \right]_{CO_2} \right. \\
& \left. + \left[b_4 \left(\frac{yT_c}{p_c^{0,5}} \right) \right]_{H_2S} \right\}
\end{aligned} \tag{3-58}$$

Table 3-9: Coefficients for equations (3-57) and (3-58). [32]

i	a	b
0	-0,040279933	-0,776423332
1	0,881709332	1,030721752
2	0,800591625	0,734009058
3	1,037850321	0,909963446
4	1,059063178	0,888959152

3.4.3 Adjustment methods for accompanying non-hydrocarbons

While concentrations of up to 5% will not seriously affect the accuracy of pseudocritical gas correlations, errors as large as 10% may occur in the calculation of the z-factor for higher concentrations of non-hydrocarbon components. The Wichert-Aziz and the Carr-Kobayashi-Burrows methods are two available adjustments that account for the presence of non-hydrocarbon components. [12]

3.4.3.1 Wichert and Aziz (1972)

When the gas contains acid gas fractions i.e. hydrogen sulphide or carbon dioxide, the Wichert and Aziz correlation should be used to adjust the pseudocritical parameters T_c and p_c . Wichert and Aziz examined the effect of acid fractions on the z-factor over a wide range of acid gas fractions (Table 3-10) and proposed equations to adjust the pseudocritical properties that will yield reliable Z-factors. [31] [28]

$$T_{pc} = T_{pc}^* - \varepsilon \tag{3-59}$$

$$p_{pc} = \frac{p_{pc}^* (T_{pc}^* - \varepsilon)}{T_{pc}^* + y_{H_2S} (1 - y_{H_2S}) \varepsilon} \tag{3-60}$$

$$\varepsilon = 120 \left[(y_{H_2S} + y_{CO_2})^{0,9} - (y_{H_2S} + y_{CO_2})^{1,6} \right] + 15 (y_{H_2S}^{0,5} - y_{H_2S}^4) \tag{3-61}$$

If only the gas gravity and non-hydrocarbon content are known, the hydrocarbon portion and its gravity are determined as follows [14]:

$$y_{HC} = 1 - y_{H_2S} - y_{CO_2} - y_{N_2} \tag{3-62}$$

$$\gamma_{gHC} = \frac{\gamma_g - (y_{H_2S}M_{H_2S} + y_{CO_2}M_{CO_2} + y_{N_2}M_{N_2})/M_{air}}{y_{HC}} \quad (3-63)$$

The hydrocarbon pseudocritical properties of the entire mixture are then calculated on the basis of Kay's mixing rule: [35]

$$p_{pc}^* = y_{HC}p_{pcHC} + y_{H_2S}p_{pcH_2S} + y_{CO_2}p_{pcCO_2} + y_{N_2}p_{pcN_2} \quad (3-64)$$

$$T_{pc}^* = y_{HC}T_{pcHC} + y_{H_2S}T_{pcH_2S} + y_{CO_2}T_{pcCO_2} + y_{N_2}T_{pcN_2} \quad (3-65)$$

In order to arrive at T_{pc} and p_{pc} , T_{pc}^* and p_{pc}^* must be further modified by inserting them into Equation (3-59) and (3-60) to account for the presence of the acid components.

The Wichert and Aziz method was developed based on a study of 1085 Z-factors from 91 gas mixtures with the data ranges shown in Table 3-10. [28]

Table 3-10: Data ranges for the Wichert and Aziz method. [28]

Property	Range
Pressure [psi]	154 - 7026
Temperature [°F]	40 - 300
Carbon dioxide [mole %]	0 - 54.46
Hydrogen sulphide [mole %]	0 - 73.85

3.4.3.2 Carr, Kobayashi, and Burrows (1954)

Carr, Kobayashi, and Burrows (1954) proposed a graphical correction method to adjust the pseudocritical properties displayed in Figure 3-4. [39] Reference [12] suggests that Equations (3-66) and (3-67) can be applied for this purpose.

$$T'_{pc} = T_{pc} - 80y_{CO_2} + 130y_{H_2S} + 250y_{N_2} \quad (3-66)$$

$$p'_{pc} = p_{pc} + 440y_{CO_2} + 600y_{H_2S} - 170y_{N_2} \quad (3-67)$$

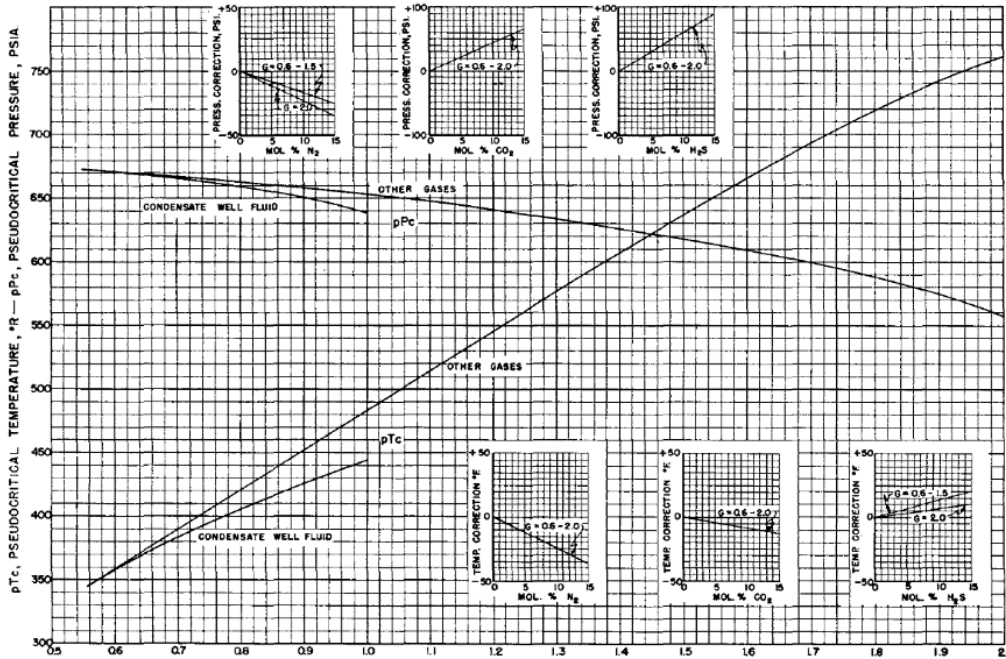


Figure 3-4: Carr-Kobayashi-Burrows's Correction Method for non-hydrocarbon components. [39]

3.4.4 Correlation of pseudocritical properties for the heptane plus fraction

Mixing rules such as the SBV or SSBV require the input of critical properties of the C7+ fraction. While the pure component critical properties are well known and readily available, the critical properties for heptane plus fraction must be estimated from correlations. Elsharkawy et al. [32] reviewed eight different such correlations and found methods by Lin-Chao, Lee-Kesler and Riazi-Daubert to deliver the most accurate results. Sutton [28] uses the Lee-Kesler equations, which were found to deliver slightly better results than other correlations. [28]

$$p_c = e^{\left[\begin{aligned} &8,3634 - \frac{0,0566}{\gamma} - \left(0,24244 + \frac{2,2898}{\gamma} + \frac{0,11857}{\gamma^2} \right) 10^{-3} T_b + \\ &\left(1,4685 + \frac{3,648}{\gamma} + \frac{0,47227}{\gamma^2} \right) 10^{-7} T_b^2 - \\ &\left(0,42019 + \frac{1,6977}{\gamma^2} \right) 10^{-10} T_b^3 \end{aligned} \right]} \quad (3-68)$$

$$T_c = 341,7 + 811\gamma + (0,4244 + 0,1174\gamma)T_b + \frac{(0,4669 - 3,2623\gamma)10^5}{T_b} \quad (3-69)$$

The Lee-Kessler equations establish a relationship between the pseudocritical properties, the specific gravity and the boiling point. As laboratory reports typically provide only the specific weight and gravity of the heptane plus fraction an additional equation for estimating the boiling point from specific gravity is necessary.[28] For this purpose Sutton recommends the use of a relationship proposed Whitson and Torp [18]:

$$T_b = (4,5579M^{0,15178}\gamma^{0,15427})^3 \quad (3-70)$$

In combination with Kay's mixing rule Whitson et al. [35] propose the use of the Matthews et al. [40] correlations to estimate the pseudocritical properties of the C7+ fraction:

$$T_{c_{C_{7+}}} = 608 + 364 \log(M_{C_{7+}} - 71,2) + (2450 \log M_{C_{7+}} - 3800) \log \gamma_{C_{7+}} \quad (3-71)$$

$$p_{c_{C_{7+}}} = 1188 + 431 \log(M_{C_{7+}} - 61,1) + [2319 - 852 \log(M_{C_{7+}} - 53,7)](\gamma_{C_{7+}} - 0,8) \quad (3-72)$$

3.5 Dynamic viscosity of natural gas mixtures

The dynamic viscosity μ and the kinematic viscosity ν represent two types of viscosity descriptions used in engineering calculations. Most petroleum engineering applications use the dynamic viscosity μ , which is expressed for Newtonian in Equation (3-73) as follows:

$$\mu = \frac{\tau g_c}{du/dy} \quad (3-73)$$

τ is defined as the shear stress per unit area in the shear plane parallel to the direction of flow, du/dy is the velocity gradient perpendicular to the plane of shear and g_c represents a units conversion from mass to force. [35]

The dynamic viscosity of a fluid is a measure of its resistance to flow, or in other words, a measure of the fluid's internal friction. Applying a shearing force to fluids with a small friction factor (meaning low viscosity) will result in a large velocity gradient. As the viscosity increases, the velocity gradient decreases as each fluid layer exerts a greater frictional drag on the adjacent layers.[12] Generally the viscosity is defined as the ratio of shear force per unit area to the local velocity gradient. A common unit for dynamic viscosity are poises, usually expressed in centipoises (cP) which is equivalent to the SI unit milliPascal seconds (mPa·s). Kinematic viscosity is obtained by dividing μ in cp by ρ in g/cm³. The SI unit for ν is mm²/s. [12,35]

The gas viscosity is not usually measured by PVT laboratories because it can be precisely estimated from empirical correlations. The viscosity of a natural gas can be completely described by the function $\mu_g = (p, T, y_i)$, which states that the viscosity is a function of pressure, temperature, and composition. In fact, a lot of the widely used gas viscosity correlations may be seen as modifications of that expression.[12] Viscosity of reservoir gases at standard and reservoir conditions typically ranges from 0.01 to 0.03 cp. It may reach up to 0.1 cp for near-critical gas condensates. The viscosity of a pure gas depends on temperature and pressure and for gas mixtures it is also a function of the composition of the gas. The composition of the gas plays a particularly important role if hydrocarbon components (such as N₂, CO₂ and H₂S) present in the gas. In such cases the viscosity has to be corrected for all non-hydrocarbon components. [41]

Predicting the gas viscosities at elevated pressure and temperature generally consists of two steps: First the mixture low-pressure viscosity μ_{gsc} at standard conditions is calculated and thereafter this viscosity value is corrected for the effect of pressure and temperature with a corresponding-states or dense-gas correlation. These methods either relate the actual viscosity μ_g at p and T to low-pressure viscosity through the ratio $\frac{\mu_g}{\mu_{gsc}}$ or the difference between those viscosities as a function of pseudoreduced properties p_{pr} and T_{pr} or as a function of pseudoreduced density ρ_r . [35, p. 5,35]

Two methods to estimate the gas viscosity that are commonly used in the petroleum industry are the Carr-Kobayashi-Burrows (1954) correlation and the Lee-Gonzalez-Eakin method.[12] Others include methods proposed by Carr et al. (Carr et al. 1954; Dempsey 1965; Dranchuk et al. 1986) (CKB), Jossi et al. (1962) (JST), Lohrenz et al. (1964) (LBC), Dean and Stiel (1965) (DS), Lee et al. (1966) (LGE), and Lucas (1981) (Poling et al. 2001).Londono et al. (LAB) (2002) updated LGE to provide a more accurate method for the prediction of pure-component and light natural-gas mixtures viscosities. The CKB method was used almost exclusively before mid-1980. After development of the LGE method, as a result of the API Project 65, laboratories changed to that method. [14]

3.5.1 Carr-Kobayashi-Burrows (1954)

Carr Kobayashi and Burrows developed a graphical correlation method to estimate the viscosity of natural gas. Carr et al. studied the viscosity of hydrocarbon mixtures, whether in the gas or liquid phase, as a function of pressure, temperature, and phase composition. They developed methods for predicting the viscosity of gas or a less dense fluid phase over the practical range of pressure, temperature, and phase compositions encountered in petroleum production operations. The proposed correlation is as two-step procedure based on graphical methods as a function of temperature, pressure, and gas specific gravity (molecular weight) and has a good accuracy with the experimental data at temperatures ranging from 32 to 400°F and a reduced pressure up to 20. [42]

In a first step the pseudocritical pressure, pseudocritical temperature, and apparent molecular weight from the specific gravity or the composition of the gas have to be found. This may be accomplished with pseudocritical properties correlations presented in the previous sections. Corrections for non-hydrocarbons should be made accordingly if they are present in concentration greater than 5%. [12]

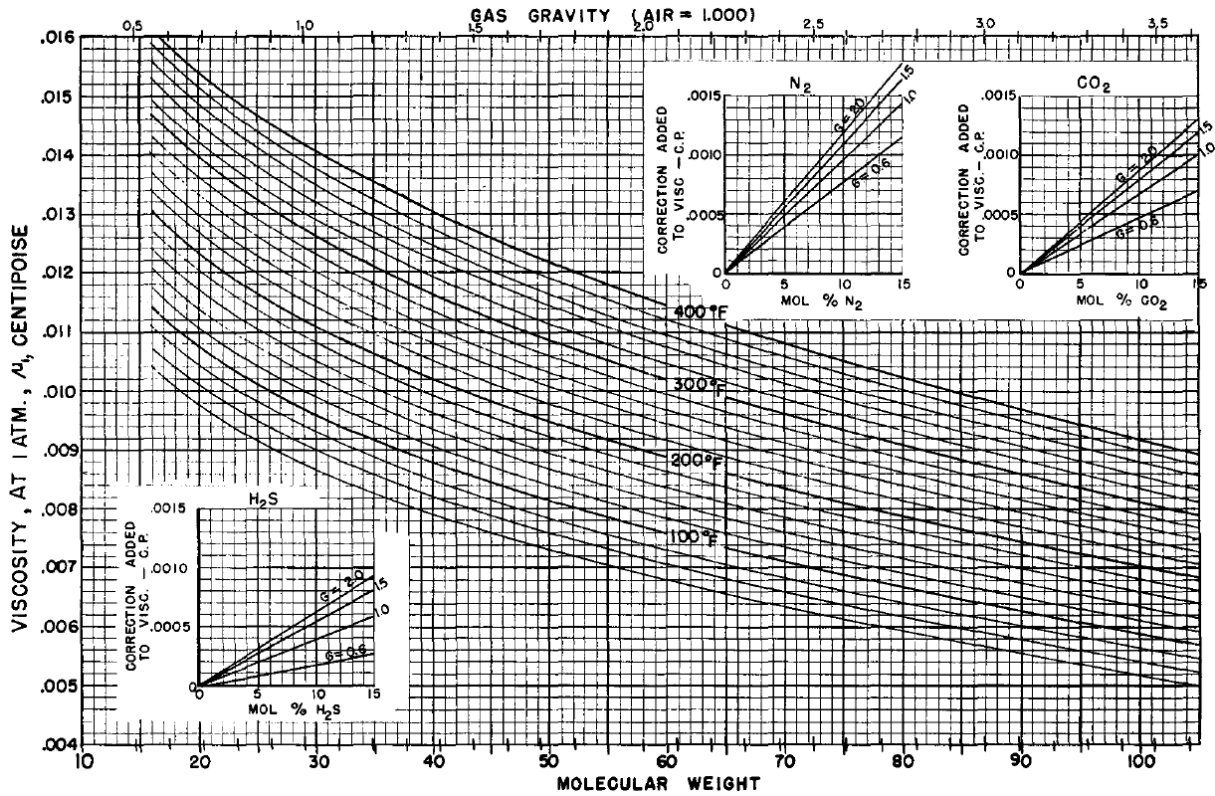


Figure 3-5: Viscosity of gas at 1 atmosphere vs. molecular weight [43]

Figure 3-5 allows the calculation of the gas viscosity at one atmosphere and the temperature of interest. Using the inserts in Figure 3-5 this viscosity, given as μ_1 , must be corrected for the presence of non-hydrocarbon components. The effects of non-hydrocarbon gases on μ_1 can be expressed as: [43]

$$\mu_1 = \mu_{1\text{ uncorrected}} + \Delta\mu_{N_2} + \Delta\mu_{CO_2} + \Delta\mu_{H_2S} \tag{3-74}$$

Once the pseudoreduced temperature is calculated through Equation (3-75). The viscosity ratio $\frac{\mu_g}{\mu_1}$ can be read from Figure 3-6.

$$T_r = \frac{T}{T_c} \text{ and } p_{pr} = \frac{p}{p_c} \tag{3-75}$$

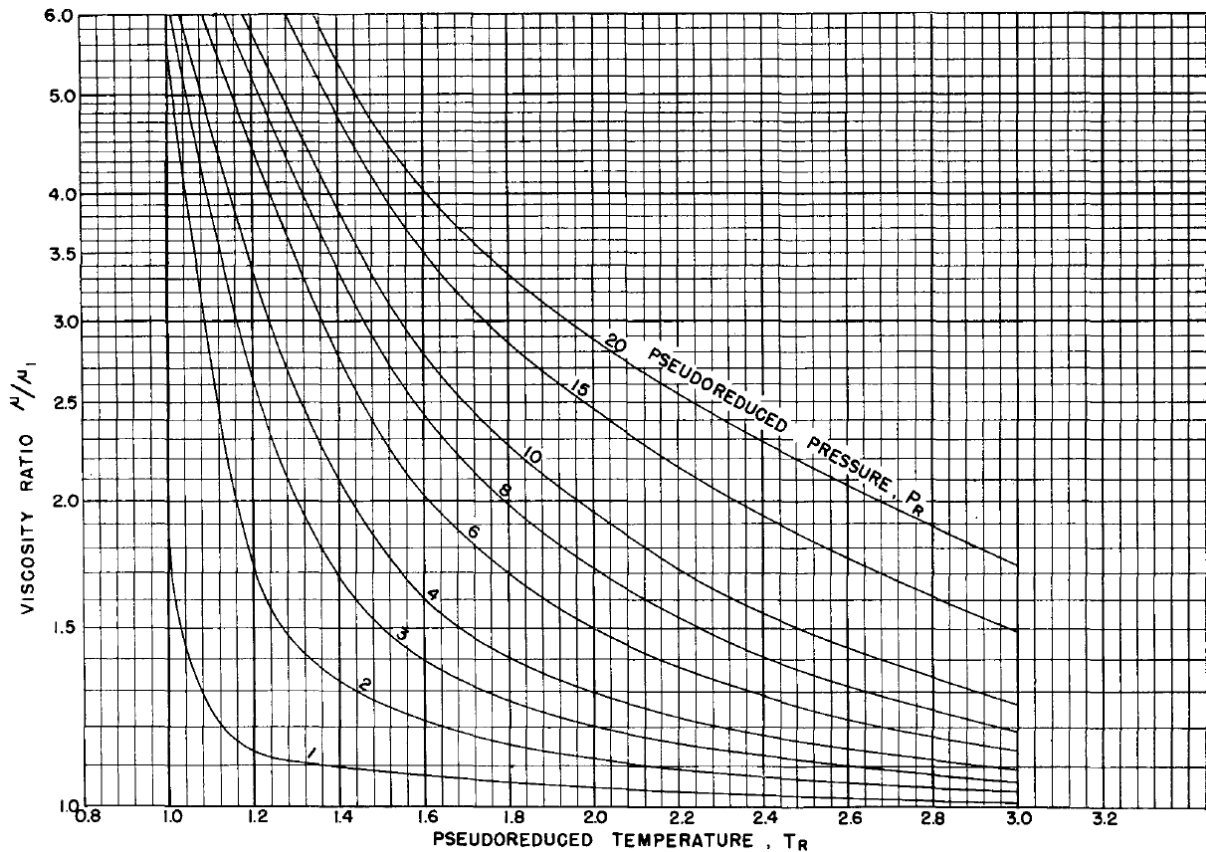


Figure 3-6: Viscosity ratio vs. pseudoreduced temperature.

Finally the viscosity ratio has to be converted to the absolute viscosity of the gas, μ_g by multiplying it with viscosity at 1 atmosphere μ_1 (generally given as μ_{gsc}):

$$\mu_g = \frac{\mu_g}{\mu_{gsc}} \mu_{gsc} \quad (3-76)$$

Standing [30] proposed mathematical expressions representing Carr et al.'s charts to calculate the viscosity of natural gas at atmospheric pressure and reservoir temperature. In addition to that Standing also presented equations to describe the effects of non-hydrocarbon components on the gas viscosity. These equations are valid for gas specific gravity and temperature are 0.55–1.55 and 100–300°F, respectively. Dempsey (1965) [44] presented a mathematical relationship to describe the $\frac{\mu_g}{\mu_{gsc}}$ ratio shown in Equation (3-82). [45]

The correlation proposed by Dempsey is valid in the range $1.2 \leq T_r \leq 3$ and $1 \leq p_r \leq 20$. [35]

$$\mu_{g \text{ uncorrected}} = [1,709(10^{-5}) - 2,062(10^{-6})\gamma_g]T_f + 8,188(10^{-3}) - 6,15(10^{-3}) \log \gamma_g \quad (3-77)$$

$$N_2 \text{ correction} = \gamma_{N_2} [8,43(10^{-3}) \log \gamma_g + 9,95(10^{-3})] \quad (3-78)$$

$$CO_2 \text{ correction} = \gamma_{CO_2} [9,08(10^{-3}) \log \gamma_g + 6,24(10^{-3})] \quad (3-79)$$

$$H_2S_{correction} = \gamma_{H_2S} [8,49(10^{-3}) \log \gamma_g + 3,73(10^{-3})] \quad (3-80)$$

$$\mu_g = \mu_{g_{uncorrected}} + N_2_{correction} + CO_2_{correction} + H_2S_{correction} \quad (3-81)$$

$$\ln \left[T_{pr} \frac{\mu_g}{\mu_{gsc}} \right] = a_0 + a_1 p_{pr} + a_2 p_{pr}^2 + a_3 p_{pr}^3 + T_{pr} (a_4 + a_5 p_{pr} + a_6 p_{pr}^2 + a_7 p_{pr}^3) \\ + T_{pr}^2 (a_8 + a_9 p_{pr} + a_{10} p_{pr}^2 + a_{11} p_{pr}^3) \\ + T_{pr}^3 (a_{12} + a_{13} p_{pr} + a_{14} p_{pr}^2 + a_{15} p_{pr}^3) \quad (3-82)$$

where a_0, \dots, a_{15} are the coefficients given in Table 3-11:

Table 3-11: Coefficients for Equation (3-82). [35]

Coefficient	Value	Coefficient	Value
a_0	-2.46211820	a_8	-7.93385648E-1
a_1	2.970547414	a_9	1.39643306
a_2	-2.86264054E-1	a_{10}	-1.49144925E-1
a_3	8.05420522E-3	a_{11}	4.41015512E-3
a_4	2.80860949	a_{12}	8.39387178E-2
a_5	-3.49803305	a_{13}	-1.86408848E-1
a_6	3.60373020E-1	a_{14}	2.03367881E-2
a_7	-1.044324E-2	a_{15}	-6.09579263E-4

3.5.2 Jossi et al. (1962)

Jossi, et al. developed a correlation for the viscosity of pure gases and gas mixtures. The pure components include gases such as argon, nitrogen, oxygen, carbon dioxide, sulphur dioxide, methane, ethane, propane, butane, and pentane. The correlation can be used to predict gas viscosity using the reduced density at a specific temperature and pressure, as well as the molecular weight. Further required input parameters are the critical temperature, critical pressure, and critical density. The Jossi, et al. correlation displayed in Equations (3-83) and (3-84) is rarely used for hydrocarbon gases as an estimate of the critical density is required. [46]

$$\left[(\mu_g - \mu_{gsc}) \xi + 10^{-4} \right]^{\frac{1}{4}} \\ = 0,1023 + 0,023364 \rho_r + 0,058533 \rho_r^2 - 0,40758 \rho_r^3 \\ + 0,0093324 \rho_r^4 \quad (3-83)$$

$$\xi_i = \left(\frac{T_{c_i}^{\frac{1}{6}}}{M_w^{\frac{1}{2}} p_c^{\frac{2}{3}}} \right) \quad (3-84)$$

Jossi, et al. stated that this correlation should only be applied for reduced densities with values below 2.0 and reported an approximate 4 percent average absolute error. [46]

Sutton [14] suggests following expression for the calculation of the reduced density:

$$\rho_r = \frac{0,27 p_{pr}}{Z T_{pr}} \quad (3-85)$$

3.5.3 Lohrenz et al. (1964)

Lohrenz et al. proposed a procedure to calculate the viscosity of reservoir gases based on previously published correlations. Over 300 calculated and experimental viscosities for high pressure gas mixtures were then used to evaluate the method. [47]

The procedure is divided in following steps [41,47]:

The first step consists of calculating the low-pressure, pure-component gas viscosities at the temperature of interest. This is accomplished by the use of the Stiel and Thodos correlations:

$$\mu_{gsc_i} \xi_i = 34(10^{-5}) T_{r_i}^{0,94} \quad \text{for } T_{r_i} \leq 1,50 \quad (3-86)$$

$$\mu_{gsc_i} \xi_i = 17,78(10^{-5}) (T_{r_i} - 1,67)^{\frac{5}{8}} \quad \text{for } T_{r_i} \leq 1,50 \quad \text{for } T_r > 1,50 \quad (3-87)$$

where the reduced temperature for each component is:

$$T_{r_i} = \frac{T}{T_{r_i}} \quad (3-88)$$

and the constant is:

$$\xi_i = \left(\frac{T_{c_i}^{\frac{1}{6}}}{M_i^{\frac{1}{2}} p_{c_i}^{\frac{2}{3}}} \right) \quad (3-89)$$

The units, Kelvin and atm, must be used in for the calculation for the pure component viscosity parameters ξ_i resulting in a table of values of μ_{gsc_i} for all pure components.

The heptane plus fraction is treated as mixture of hydrocarbons from C₇ to C₄₀ and given as:

$$x_{c_{7+}} = \sum_{i=7}^{40} x_{c_i} \quad \text{and} \quad x_{c_{7+}} M_{c_{7+}} = \sum_{i=7}^{40} (x_{c_i} M_{c_i}) \quad (3-90)$$

To find the low pressure mixture gas viscosity the equation of Herning and Zipperer is used:

$$\mu_{gsc} = \frac{\sum_{i=1}^n (x_i \mu_{gsc_i} \sqrt{M_i})}{\sum_{i=1}^n (x_i \sqrt{M_i})} \quad (3-91)$$

The viscosity at the temperature and pressure of interest is given by the relationship developed by Jossi, Stiel and Thodos for pure components and solved for the μ_g :

$$\begin{aligned} [(\mu_g - \mu_{gsc})\xi + 10^{-4}]^{\frac{1}{4}} \\ = 0,1023 + 0,023364\rho_r + 0,058533\rho_r^2 - 0,40758\rho_r^3 \\ + 0,0093324\rho_r^4 \end{aligned} \quad (3-92)$$

For the above relationship the reduced density has to be found. Sutton [14] suggests Equation (3-93):

$$\rho_r = \frac{0,27 p_{pr}}{Z T_{pr}} \quad (3-93)$$

Lohrenz et al. note that methods developed by Lee and Eakin and Dean and Stiel can simplify the calculation of the gas mixtures at low pressures (i.e. gas viscosity at standard conditions). Lee and Eakin provide an equation for μ_{gsc} as a function of the average molecular weight and temperature while Dean and Stiel give equations for μ_{gsc} similar to Equations (3-86) and (3-87) with the difference that the viscosity parameter ξ_i and the reduced temperature T_{r_i} are defined for mixtures. In addition to being easier to use, those methods should also be more accurate. [47]

The method by Lohrenz et al. for the viscosity prediction of gas mixture systems should be able to handle non-hydrocarbon gases if their contents do not exceed 7% for each. [41]

3.5.4 Dean and Stiel (1965)

The Dean and Stiel correlation is very similar to the method developed by Jossi et al. Same as that method it correlates the low-pressure gas viscosity with temperature, molecular weight, pseudocritical temperature, and pseudocritical pressure. [14]

$$\mu_{gsc} = 34(10^{-5}) \frac{(T_{pr})^{\frac{8}{9}}}{\xi} \quad \text{for } T_{pr} \leq 1,50 \quad (3-94)$$

$$\mu_{gsc} = 166,8(10^{-5}) \frac{(0,1338T_{pr} - 0,0932)^{\frac{5}{9}}}{\xi} \quad \text{for } T_{pr} > 1,50 \quad (3-95)$$

$$\xi = 5,4398 \left(\frac{T_{pc}}{M^3 p_{pc}^4} \right)^{\frac{1}{6}} \quad (3-96)$$

$$\rho_r = \frac{0,27 p_{pr}}{Z T_{pr}} \quad (3-97)$$

$$\mu_g = \mu_{gsc} + \frac{(10,8(10^{-5})) \left[e^{(1,439\rho_r)} - e^{(-1,111\rho_r^{1,858})} \right]}{\xi} \quad (3-98)$$

3.5.5 Lee-Gonzalez-Eakin (1966)

The Lee-Gonzalez-Eakin (LGE) method is a semi empirical relationship for the calculation the viscosity of natural gas. Based on experimental viscosity and density data of four natural gases for a temperature range of 100 to 340°F and pressure range of 100 to 8000 psia Lee et al. proposed a correlation shown in Equations (3-99) to (3-102). [45] This method is very popular and used by most PVT laboratories. [35,42] The terms K and X are expressed as functions of the molecular weight and Temperature of the concerned gas. The pressure is incorporated through the density ρ . [13]

$$\mu_g = 10^{-4} K e^{(X\rho^Y)} \quad (3-99)$$

$$K = \frac{(9,4 + 0,02M_w)T^{1,5}}{209 + 19M_w + T} \quad (3-100)$$

$$X = 3,5 + \left(\frac{986}{T} \right) + 0,01M_w \quad (3-101)$$

$$Y = 2,4 - 0,2X \quad (3-102)$$

The temperature T is in °R, the viscosity μ is in μP ($1 \mu\text{P} = 1.0 \times 10^{-6} \text{ g/cm/s}$) and the density ρ is g/cm^3 . The presented correlations reproduces the experimental data with a standard deviation of $\pm 2.69\%$ and a maximum deviation 8.99%. [45] Correction for non-hydrocarbon components are not mentioned. However Chen et al. [41] report that the correlation will yield accurate results if the H_2S content does not exceed 10%.

McCain [48] indicates that the accuracy of the Lee et al. correlation is within 2 to 4% for specific gas gravities smaller than 1. For gases of higher specific gravities the accuracy decreases, usually giving low estimates with errors up to 20% for retrograde gases that have specific gravities over 1.5. [48]

3.5.6 Lucas (1981)

Lucas proposes a gas viscosity correlation which correlates the low pressure gas viscosity with temperature, molecular weight, pseudocritical temperature, and pseudocritical pressure; same

as the Dean and Stiel correlation. [14] It is valid in a range of $1 < T_r < 40$ and $0 < p_r < 100$. [49] Sutton [14] gives following equations:

$$\mu_{gsc} \xi = \left[0,807T_{pr}^{0,618} - 0,357e^{(-0,449T_{pr})} + 0,340e^{(-4,058T_{pr})} + 0,018 \right] \quad (3-103)$$

$$\xi = 5,4398 \left(\frac{T_{pc}}{M^3 p_{pc}^4} \right)^{\frac{1}{6}} \quad (3-104)$$

$$\frac{\mu_g}{\mu_{gsc}} = 1 + \frac{A_1 p_{pr}^{1,3088}}{A_2 p_{pr}^{A_5} + (1 + A_3 p_{pr}^{A_4})^{-1}} \quad (3-105)$$

where

$$A_1 = \frac{1,245(10^{-3})e^{(5,1726T_{pr}^{-0,3286})}}{T_{pr}} \quad (3-106)$$

$$A_2 = A_1(1,6553T_{pr} - 1,2723) \quad (3-107)$$

$$A_3 = \frac{0,4489e^{(3,0578T_{pr}^{-37,7332})}}{T_{pr}} \quad (3-108)$$

$$A_4 = \frac{1,7368e^{(2,2310T_{pr}^{-7,6351})}}{T_{pr}} \quad (3-109)$$

$$A_5 = 0,9425e^{(-0,1853T_{pr}^{0,4489})} \quad (3-110)$$

Equation (3-111) can be used to find the pseudocritical pressure:

$$p_{pc} = RT_{pc} \frac{\sum_{i=1}^N Y_i Z_{ci}}{\sum_{i=1}^N Y_i v_{ci}} \quad (3-111)$$

If the composition is not available, pseudocritical correlations in terms of specific gravity can be used, e.g. Standing's equations given in equations (3-77) to (3-81).[49]

If polar compounds, such as H₂S and water, are present in a gas mixture special corrections should be applied to the correlation. The effect of H₂S on the correlation is always < 1% and can therefore be neglected. Appropriate corrections can be made to account for water if necessary. The Lucas correlation is recommended for general use, given its wide range of applicability.

In their work Poling et al. [10] provide a comparison of calculated versus experimental viscosity data for different gases at various temperatures and pressures. The error was found to be usually less than 5 % percent except for a few cases.

3.5.7 Gurbanov and Dadash-Zade (1986)

The Gurbanov and Dadash-Zade [50] approach is a two-step procedure. The first step consists of calculating the viscosity μ_{gsc} at atmospheric pressure and in the second step the viscosity ratio $\frac{\mu_{gsc}}{\mu_g}$ is considered as a function of T_{pr} and p_{pr} . Modified coefficients for Equation (3-112) and Equation (3-113) are provided by Chen and Ruth [41] and are given in Table 3-.

$$\mu_{gsc} = (a_1 + a_2T) - (a_3 + a_4T)\sqrt{M_w} \quad (3-112)$$

$$\frac{\mu}{\mu_{gsc}} = (b_1 + b_2p_r + b_3p_r^2)\frac{1}{T_r} + (b_4 + b_5p_r + b_6p_r^2)\frac{1}{T_r^4} + (b_7 + b_8p_r + b_9p_r^2) \quad (3-113)$$

where the temperature T is in Kelvin and the viscosity μ is cp.

Table 3- lists the coefficients determined by Chen and Ruth for the Gurbanov and Dadash-Zade viscosity model.

Table 3-12: Coefficients determined by Chen and Ruth. [41]

a₁	0.0038539	b₄	0.8266923
a₂	0.0000356	b₅	1.7124100
a₃	0.0004131	b₆	-0.0700968
a₄	0.0000016	b₇	1.2076900
b₁	-0.4888439	b₈	0.0301188
b₂	-0.0943952	b₉	-0.0048318
b₃	0.0199591		

The Gurbanov and Dadash-Zade viscosity model in combination with the coefficients developed by Chen and Ruth [41] is valid from reduced pressures p_r from 1 to 15 and reduced temperatures from 1,05 to 2,8. [19]

3.5.8 Londono et al. (2005)

Londono et al. developed a new model and calculation procedures for estimating hydrocarbon gas viscosity based on the Jossi et al. model. In addition new coefficients for the Jossi et al. and Lee et al. viscosity correlations are provided based an extensive database of measured gas viscosities. [46]

The original Jossi et al. formulation is given as follows:

$$\left[(\mu_g - \mu_{gsc})\xi + 10^{-4} \right]^{\frac{1}{4}} = f(\rho_r) \quad (3-114)$$

$$f(\rho_r) = f_1 + f_2\rho_r + f_3\rho_r^2 + f_4\rho_r^3 + f_5\rho_r^4 \quad (3-115)$$

$$\xi = \frac{T_c^{e_1}}{M_w^{e_2} p_c^{e_3}} \quad (3-116)$$

By using non-linear regression techniques on the pure component data the optimized coefficients obtained from the refitting are given in

Table 3-13: Coefficients by Londono et al. [46]

f₁	1.03671E-01	f₄	-3.12987E-02	e₂	3.91956E-01
f₂	1.31243E-01	f₅	8.84909E-03	e₃	-1.50857E-01
f₃	1.71893E-02	e₁	-1.21699E-01		

Londono et al. also updated the coefficients of the Lee et al. correlation, which is given by:

$$\mu_g = 10^{-4} K e^{(X\rho^Y)} \quad (3-117)$$

$$K = \frac{(k_1 + k_2 M_w) T^{k_3}}{k_4 + k_5 M_w + T} \quad (3-118)$$

$$X = x_1 + \left(\frac{x_2}{T}\right) + x_3 M_w \quad (3-119)$$

$$Y = y_1 - y_2 X \quad (3-120)$$

For the updated coefficients of the Lee et al. model data from both pure components and gas mixtures are used resulting in following updated coefficients given in Table 3-14.

Table 3-14: Coefficients by Londono et al. [46]

k₁	1.67175E+01	k₂	4.19188E-02	k₃	1.40256E+00
k₄	2.12209E+02	k₅	1.81349E+01	x₃	1.19260E-02
x₁	2.12574E+00	x₂	-2.06371E+03		
y₁	1.09809E+00	y₂	-3.92851E-02		

Londono et al. propose a new polynomial model that can be seen as an expansion of the Jossi, et al. model with additional temperature and density dependent terms. This model is given as:

$$\mu_g = \mu_{gsc} + f(\rho) \quad (3-121)$$

$$f(\rho) = \frac{a + b\rho + c\rho^2 + d\rho^3}{e + f\rho + g\rho^2 + h\rho^3} \quad (3-122)$$

$$a = a_0 + a_1 T + a_2 T^2 \quad (3-123)$$

$$b = b_0 + b_1 T + b_2 T^2 \quad (3-124)$$

$$c = c_0 + c_1T + c_2T^2 \quad (3-125)$$

$$d = d_0 + d_1T + d_2T^2 \quad (3-126)$$

$$e = e_0 + e_1T + e_2T^2 \quad (3-127)$$

$$f = f_0 + f_1T + f_2T^2 \quad (3-128)$$

$$g = g_0 + g_1T + g_2T^2 \quad (3-129)$$

$$h = h_0 + h_1T + h_2T^2 \quad (3-130)$$

The parameters for these equations are listed in Table 3-15

Table 3-15. Coefficients for the Londono et al polynomial model. [46]

a₀	9.53363E-01	a₁	-1.07384E+00	a₂	1.31729E-03
b₀	-9.71028E-01	b₁	1.12077E+01	b₂	9.01300E-02
c₀	1.01803E+00	c₁	4.98986E+00	c₂	3.02737E-01
d₀	-9.90531E-01	d₁	4.17585E+00	d₂	-6.36620E-01
e₀	1.00000E+00	e₁	-3.19646E+00	e₁	3.90961E+00
f₀	-1.00364E+00	f₁	-1.81633E-01	f₁	-7.79089E+00
g₀	9.98080E-01	g₁	-1.62108E+00	g₁	6.34836E-04
h₀	-1.00103E+00	h₁	6.76875E-01	h₁	4.62481E+00

It is necessary to determine the gas viscosity at standard conditions (1 atm) in order to utilize both the new and existing correlations. For this purpose Londono et al. provide Equation (3-131). [46]

$$\ln(\mu_{gsc}) = \frac{a_0 + a_1 \ln(\gamma_g) + a_2 \ln(T) + a_3 \ln(\gamma_g) \ln(T)}{1 + b_1 \ln(\gamma_g) + b_2 \ln(T) + b_3 \ln(\gamma_g) \ln(T)} \quad (3-131)$$

The new low pressure gas viscosity correlation has a reported average error of 1.36%. The values for the parameters a and b are listed Table 3-16: [46]

Table 3-16: Coefficients for Equation (3-131).

a₀	-6,39821E+00	a₁	-6,045922E-01	a₂	7,49768E-01
a₃	1,261051E-01	b₁	6,97180E-02	b₂	-1,013889E-01
b₃	-2,15294E-02				

Londono et al. report a an AAE of 4.43% and 2.29% for the “refitted” Jossi et al. and Lee et al. correlations respectively, compared to an AAE of 5.26% and 3.34% for the original correlations. The Jossi et al. correlations were developed for pure component data and therefor were only fitted to pure component data which comprised of 2494 data points. In contrast, the Lee et al. correlation was fitted using both, pure and gas mixture data (4909 points) and can be

considered appropriate for general use. The correlation for gas viscosity at low pressures yielded an AAE of 1.36 percent based on 135 pure component and 126 mixture data points. [46]

The new viscosity correlation, which is given as a function of density is supposed to be applicable over a wide range of temperatures, pressures and molecular weights for pure gases as well as for gas mixtures. The average absolute error for this model as is 3.05%. As only a limited amount of non-hydrocarbon impurities were present in the research database the modified correlations should perform well where relatively small amounts of non-hydrocarbon impurities are present. [46] Londono et al. do not mention any corrections for higher non-hydrocarbon contents.

3.5.9 Sutton (2007)

Sutton proposed a new method which is supposed to provide improved accuracy, especially for high gravity gas condensates. The low pressure gas viscosity is calculated through the method given by Lucas (Poling et al.). For the calculation of the viscosity ratio Sutton selected the LGE equation because of its simplicity and acceptability by the petroleum industry. Sutton provides updated coefficients for the LGE equation: [14]

$$\mu_g = \mu_{gsc} e^{[X\rho_g^Y]} \quad (3-132)$$

$$X = 3,47 + \frac{1588}{T} + 0,0009M \quad (3-133)$$

$$Y = 1,66278 - 0,04679X \quad (3-134)$$

$$\mu_{gsc}\xi = 10^{-4} \left[0,807T_{pr}^{0,618} - 0,357e^{(-0,449T_{pr})} + 0,340e^{(-4,058T_{pr})} + 0,018 \right] \quad (3-135)$$

$$\xi = 0,9490 \left(\frac{T_{pc}}{M^3 p_{pc}^4} \right)^{\frac{1}{6}} \quad (3-136)$$

Sutton reports improved results for the proposed method for gases containing higher levels of heptanes plus. The new correlation delivers results with an ARE of -0.5 % and an AARE of 6.3% when the LGE correlation is applied to the same data.[14]

3.5.10 Viswanathan (2007)

Viswanathan [51] proposed a viscosity correlation for a HPHT applications. The correlation is a modified LGE equations with coefficients that were fit to NIST [25] pure methane gas viscosity data in a pressure and temperature range from 5000 to 30000 psia and 100 to 400 °F. Although the correlations was developed for a one component gas without any non-hydrocarbon impurities McCain et al. (2011) indicate that correlation may be used with “some confidence” for HPHT calculations until better correlations are available. [15, p. 29]

$$\mu_g = 10^{-4} K e^{(X\rho^Y)} \quad (3-137)$$

$$K = \frac{(5,0512 - 0,2888M_w)T^{1,832}}{-443,8 + 12,9 + T} \quad (3-138)$$

$$X = -6,1166 + \left(\frac{3084,9437}{T}\right) + 0,3938M_w \quad (3-139)$$

$$Y = 0,5893 - 0,1563X \quad (3-140)$$

The temperature T is in °F, the gas density ρ is in g/cm³ and the resulting gas viscosity μ_g is in centipoise.

3.5.11 Elsharkawy (2006)

Elsharkawy proposes a correction method for the original LGE equation to account for the presence of the heptane plus fraction and the non-hydrocarbons components CO₂ and H₂S. As most PVT laboratories use the LGE method to report gas viscosities and it is simple to use, LGE correlation was chosen for modification. [18]

The corrections are calculated as follows:

$$\Delta\mu_g = y_{H_2S}(-3,2268(10^{-3}) \log \gamma_g + 2,1479(10^{-3})) \quad (3-141)$$

$$\Delta\mu_g = y_{CO_2}(6,4366(10^{-3}) \log \gamma_g + 6,7255(10^{-3})) \quad (3-142)$$

$$\Delta\mu_g = y_{C7+}(-3,2875(10^{-3}) \log \gamma_g + 1,2885(10^{-3})) \quad (3-143)$$

With the original LGE Equations given as: [18]

$$\mu_g = D_1 10^{-4} K e^{(D_2 \rho^{D_3})} \quad (3-144)$$

$$D_1 = \frac{(9,379 + 0,01607M_w)T^{1,5}}{209,2 + 19,26M_w + T} \quad (3-145)$$

$$D_2 = 3,448 + \left(\frac{986,4}{T}\right) + 0,01009M_w \quad (3-146)$$

$$D_3 = 2,447 - 0,224D_2 \quad (3-147)$$

Compared to the original LGE and other methods such as the Dean-Stiel and CKB methods, Elsharkawy claims an improved accuracy with an ARE of 1.9% and an AARE of 8.9%. [18] The composition of the study reference data i.e. the heptane plus and non-hydrocarbon content is not mentioned.

3.5.12 Galliéro et al. (2009)

Based on the Lennard Jones fluid (LJ) Galliéro et al. employed a corresponding states (CS) approach to predict the viscosity of for acid gas mixtures. The developed model therefore has a strong physical background and is able to predict the viscosity as a function of temperature and density. [52]

In the LJ fluid model (see also 4.2.2 - Zabaloy et al. (2005) - Lenard Jones fluid model) molecules are represented by simple spheres, without internal degrees of freedom, interacting through a LJ potential. The individual species of this non-polar fluid model are characterized by their molecular weight M and two molecular parameters, the potential depth ε and the molecular diameter σ . The latter two parameters are closely related to the critical temperature T_c and critical Volume V_c . [52]

The parameters described above can be found through following mixing rules:

$$M_x = \sum_{i=1}^N x_i M_i \quad (3-148)$$

$$\sigma_x^3 = \sum_{i=1}^N \sum_{j=1}^N x_i x_j \sigma_{ij}^3 \quad (3-149)$$

$$\varepsilon_x \sigma_x^3 = \sum_{i=1}^N \sum_{j=1}^N x_i x_j \varepsilon_{ij} \sigma_{ij}^3 \quad (3-150)$$

where the cross-molecular parameters between compounds i and compounds j are defined as:

$$\sigma_{ij} = \left(\frac{\sigma_{ii}^3 + \sigma_{jj}^3}{2} \right)^{1/3} \quad (3-151)$$

$$\varepsilon_{ij} = \left(\frac{\varepsilon_{ij} \sigma_{ii}^3 + \varepsilon_{ij} \sigma_{jj}^3}{2 \sigma_{jj}^3} \right)^{1/3} \quad (3-152)$$

It is necessary to define the reduced variables in which all fluids are equivalent in terms of thermodynamic and transport properties. The reduced thermodynamic variables T^* , ρ^* and μ^* are defined as:

$$T^* = \frac{k_B T}{\varepsilon_x}; \quad \rho^* = \frac{\rho \sigma_x^3}{M_x}; \quad \mu^* = \frac{\mu \sigma_x^2}{\sqrt{M_x \varepsilon_x}} \quad (3-153)$$

Incorporating the LJ fluid model leads to

$$\mu^* = \frac{4,75}{16(a_1 T^{*a_2} + a_3 e^{a_4 T^*} + a_5 e^{a_6 T^*})} \sqrt{\frac{T^*}{\pi}} + b_1 (e^{b_2 \rho^*} - 1) b_4 (e^{b_5 \rho^*} - 1) + \frac{b_5}{T^{*2}} (e^{b_6 \rho^*} - 1) \quad (3-154)$$

From which then can be inserted into Equation (3-155) to calculate the viscosity of the mixture:

$$\mu = \frac{\mu^* \sqrt{M_x \varepsilon_x}}{\sigma_x^2} \quad (3-155)$$

All necessary coefficients for the above equations can be found in Table 3-17, Table 3-18 and Table 3-19.

Galliéro et al. used three natural gas datasets in a temperature and pressure range from 240 to 450K and pressure 0.1 to 25 MPa respectively to evaluate the proposed method. The AAD ranges from 0.83 to 4.04% with a maximum error of 6.9%. The authors also claim a high consistency of the model applying the correlation to a methane mixtures containing a mole fraction of up 0.7 H₂S. [52]

Table 3-17: Coefficients for Equations proposed by Galliéro et al.[52]

i	1	2	3	4	5	6
a	1.16145	-0.14874	0.52487	-0.7732	2.16178	-2.43787
b	0.062692	4.095577	-8.743269E-6	11.12492	2.542477E-6	14.86398

Table 3-18: Optimized molecular parameters of some n-alkanes. [52]

n-alkane	σ [10 ⁻¹⁰ m]	ε [J mol ⁻¹]	T _{min} -T _{max} [K]	p _{min} -p _{max} [MPa]	AAAD [%]	Δ_{max} [%]
C ₁	3.6325	1258.1	200–500	0,1–100	1.3	3.6
C ₂	4.2093	2015.8	200–500	0,1–60	3.4	8.6
C ₃	4.6717	2442	200–450	0,1–30	6.5	10.7
C ₄	5.0741	2806.7	250–450	0,1–30	5.2	8.7
C ₅	5.4009	3101	303–383	0,1–100	5.5	10.4
C ₆	5.7051	3351.2	303–348	0,1–250	4.9	9.9
C ₇	5.9916	3566.4	293–343	0,1–100	4.5	9.4
C ₁₀	6.7285	4078.1	293–373	0,1–140	3.3	9.6
C ₁₆	7.9044	4773.3	298–348	0,1–150	5.4	9.9

Table 3-19: Molecular parameters of some petroleum compounds of interest. [52]

Compounds	σ [10^{-10} m]	ϵ [J mol ⁻¹]	T _{min} -T _{max} [K]	ρ_{\min} - ρ_{\max} [MPa]	AAD [%]	Δ_{\max} [%]
H₂S+dipole	3.688	2320	200–500	0.1–6	2.9	11.9
H₂S	3.667	2355	200–500	0.1–6	4.5	18.7
CO₂	3.6641	2007.9	250–500	0.1–100	4.3	8.7
N₂	3.5734	833.1	200–500	0.1–100	1.3	2.5
O₂	3.3269	1020.6	200–500	0.1–80	2.1	4.0
C₆H₆	5.1202	3710.7	283–393	0.1–200	4.7	11.5
C₇H₈	5.3897	3906.8	293–373	0.1–140	2.6	6.5

3.5.13 Sanaei et al. (2015)

A recent correlation developed by Sanaei et al. aims at estimating the viscosity of hydrocarbon gas mixtures with or without non-hydrocarbon component, using a one-step procedure. The input parameters of the correlation were found by using artificial neural network to determine which parameters have the most effect on the viscosity. Based on 2300 data points of Iranian and worldwide wet, dry, and condensate reservoir gases, non-linear multivariable regression combined with multivariable optimization was then employed to obtain the correlation form and to optimize its coefficients. A summary of the different gas property ranges of the data used for the study can be found in Table 3-21. [42]

The proposed correlation is given as follows:

$$\mu_g = P_3(\rho) + P_3\left(\frac{M_w}{T_f}\right) + P_3(T_{f\rho}) + P_3(P^\rho) + P_3(M_w\rho) \quad (3-156)$$

$$P_3(\rho) = a_0 + a_1\rho + a_2\rho^2 + a_3\rho^3 \quad (3-157)$$

$$P_3\left(\frac{M_w}{T_f}\right) = b_1\left(\frac{M_w}{T_f}\right) + b_2\left(\frac{M_w}{T_f}\right)^2 + b_3\left(\frac{M_w}{T_f}\right)^3 \quad (3-158)$$

$$P_3(T_{f\rho}) = c_1(T_{f\rho}) + c_2(T_{f\rho})^2 + c_3(T_{f\rho})^3 \quad (3-159)$$

$$P_3(P^\rho) = d_1(P^\rho) + d_2(P^\rho)^2 + d_3(P^\rho)^3 \quad (3-160)$$

$$P_3(M_w\rho) = e_1(M_w\rho) + e_2(M_w\rho)^2 + e_3(M_w\rho)^3 \quad (3-161)$$

With the coefficients given in Equation (3-20).

Table 3-20: Coefficients for the Equations proposed by Sanaei et al. [42]

a₀	1.977132 E-2	a₁	2.274942 E-2	a₂	-2.726357 E-2
a₃	4.218326 E-1				
b₁	-1.290755E-1	b₂	5.052971E-1	b₃	-6.643018E-1
c₁	0.00358553	c₂	-3.939443E-4	c₃	7.274715E-6
d₁	5.501917E-4	d₂	-2.12763E-6	d₃	1.946208E-9
e₁	-0.002651898	e₂	2.93349E-4	e₃	5.214413E-5

The correlation developed by Sanaei et al. shows an AARE of 2.49% and an ARE of -0.07% compared to an AARE of 4.48% and an ARE of 3.28% for the LGE equation.

Table 3-21: Ranges of different gas properties

Gas Property	Minimum	Maximum
Temperature (°F)	100	460
Pressure (psia)	14.7	10,000
Molecular weight (lb/lb-mole)	16.043	53.915
Density (g/cc)	0.001	0.571
CO ₂ content	0%	3.2%
N ₂ content	0%	4.8%

3.6 Thermal conductivity of natural gas mixtures

The thermal conductivity of a medium describes the proportionality between the heat flux ϕ in a given direction and the temperature gradient $\partial T/\partial x$ in the same direction. It is defined by the Fourier equation:[13, p. 101]

$$\phi = -\lambda \frac{\partial T}{\partial x} \quad (3-162)$$

In SI units the thermal conductivity is expressed in W/mK and in Btu/[(hr ft² °F)/ft] in oilfield units.

An example of values for common gases are Hydrogen = 0.142 W/mK, Helium = 0.129 W/mK, Oxygen = 0.025 W/mK, Air 0.024 W/mK, Nitrogen = 0.024 W/mK and Carbon dioxide = 0.014 W/mK. With increasing temperature the thermal conductivity normally rises. [13, p. 101]

One of the most common methods to measure the thermal conductivity is through the hot wire method. The difference in temperature between two coaxial cylinders which are separated by a thin film of gas is measured. The inner cylinder thereby consists of an electrical resistor acting as a heating element. Several parameters such as convection effects, radiant effects and wall effects have to be taken account of. [13, p. 101]It is not very practicable to measure the thermal conductivity of natural gas. Therefore thermal conductivities of natural gases or components of natural gases have been studied in detail in the past.

Correlations for the thermal conductivity of pure gases such methane, nitrogen, propane and ethylene have been published by Holland et al. (1979) [53] Holland et al. (1983) [54] and Hanley et al. (1973) [55]. Further works on natural gas conductivities include those by Pátek et al. (2003) [56] and Pátek et al.(2005) [57] who investigated Carbon Dioxide–Methane and Nitrogen-methane mixtures. Based on the kinetic gas theory Chung et al. (1988) [58] correlated the thermal conductivity as a function of molecular weight, acentric factor, reduced temperature, reduced density, critical volume, heat capacity at constant volume and low-pressure gas viscosity. [3]

In research associated with NIST, Ely and Hanley developed the TRAPP [59] (transport property prediction) method and later Ely and Huber introduced SUPERTRAPP [60], which are a computer databases for the prediction of thermodynamic and transport properties of fluid mixtures. Both Hanley et al.(1976) [61] and Pedersen et al. (1989) [62] present methods based on the corresponding states method to calculate the thermal conductivity of hydrocarbon mixtures. Guo et al. (2001) [63] developed two thermal conductivity correlations based on Peng and Robinson (PR) and Patel and Teja (PT) to correlate the viscosity and thermal conductivity of hydrocarbons and CO₂ and N₂ as well as their mixtures EOS thermal conductivity of hydrocarbons and CO₂ and N₂ as well as their mixtures. [3]

In the following chapters three estimation methods for hydrocarbon gas mixtures are presented while pure fluid data is available in detail from the NIST database.

3.6.1 Gas processors suppliers association engineering data book

The thermal conductivity of a natural gas mixture may be calculated using graphical correlations in a two-step procedure as described in the “Gas Processors Suppliers Association Engineering Data Book” [64]. First the thermal conductivity at atmospheric pressure is estimated using one of the charts shown in Figure 3-7 where the thermal conductivity at the desired temperature is correlated with the molecular weight of the gas mixture. For pure hydrocarbon and miscellaneous gases Figure 3-8 and [64]

Figure 3-9 are available. The second step consists of reading the ratio of the thermal conductivity of the gas at the desired temperature and pressure to that at atmospheric pressure from the chart in Figure 3-8. For this the pseudo reduced pressure and pseudo reduced temperature of the gas is required. [16] [64, p. 23:34]

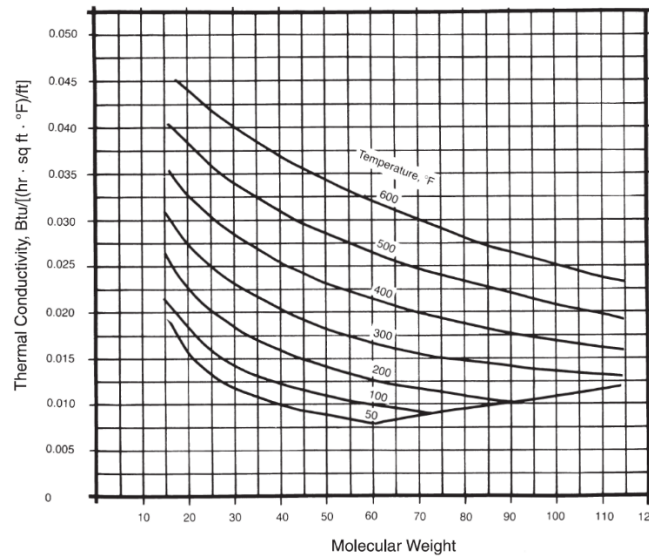


Figure 3-7: Thermal conductivity of natural and hydrocarbon gases at one atmosphere (14,696 psia). [64]

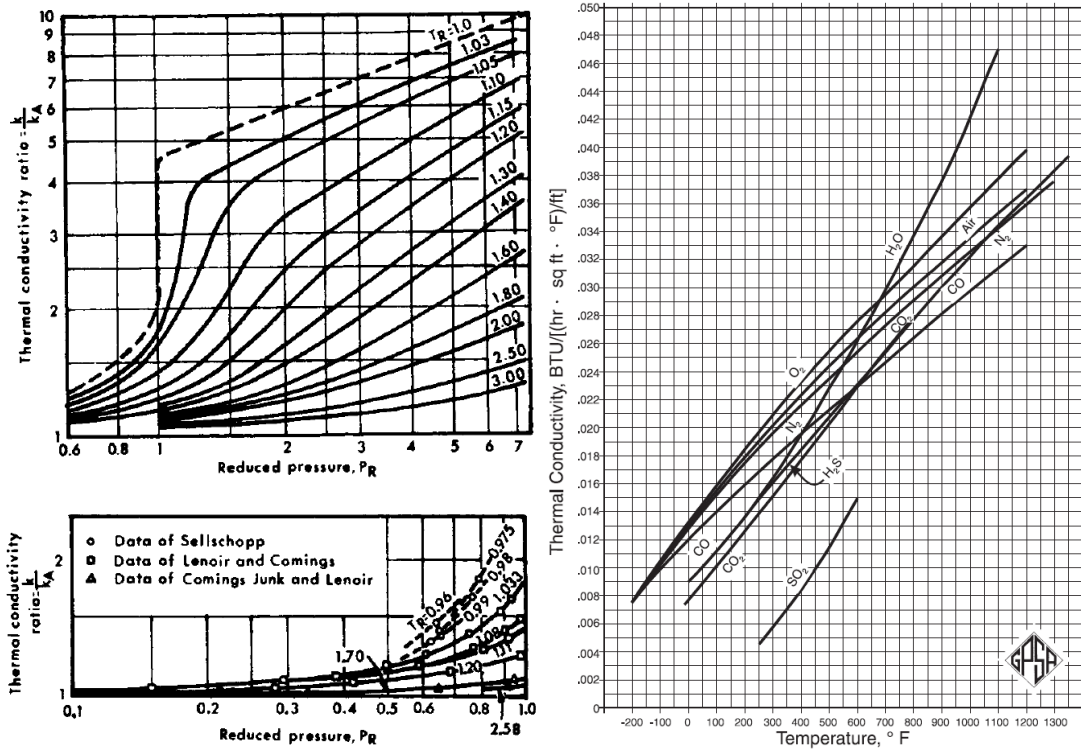


Figure 3-8: Thermal conductivity ratio for gases. [64]

Figure 3-9: Thermal conductivity of miscellaneous gases at one atmosphere. [64]

Another method for estimating the thermal conductivity of a gas mixture is by using the mixing rule given in Equation (3-163). The conductivity of each component at the given temperature is read from the charts in and [64]

Figure 3-9. This rule is only applicable to simple gas mixtures and cannot be applied to mixtures containing CO₂. [64, p. 23:36] It has to be noted that this method will only yield the thermal conductivity at one atmosphere.

$$k_m = \frac{\sum_i y_i k_i \sqrt[3]{M_{wi}}}{\sum_i y_i \sqrt[3]{M_{wi}}} \quad (3-163)$$

The thermal conductivity k is given in Btu/[(hr ft² °F)/ft].

3.6.2 Pedersen et al. (1989)

Based on the kinetic gas theory Pedersen et al. derived an approximate analytical expression for the thermal conductivity given by:

$$\lambda = \frac{1}{3} n v L C_v \quad (3-164)$$

Where n is the number of molecules per unit, v the average molecular speed, C_v the molar heat capacity at constant volume and L the mean free path between two molecules.

Applying the corresponding states theory in terms of pressure and temperature the thermal conductivity ($\lambda_r = f(p_r, T_r)$) of a component x at the temperature T and the pressure P may be found from Equation (3-167). [62, p. 189]

$$\lambda_x(p, T) = (T_{cx}/T_{co})^{-1/6} (P_{cx}/P_{co})^{2/3} (MW_x/MW_o)^{-1/2} \lambda_o(P_o/T_o) \quad (3-165)$$

Where $P_o = PP_{co}/P_{cx}$ and $T_o = TT_{co}/T_{cx}$ and λ_o is the thermal conductivity of the reference substance at the temperature T_o and pressure P_o .

Methane is used as the reference substance and contributions for the transport of translation energy and transport of internal energy. In addition a correction term α accounting for the deviations from the simple corresponding states theory is introduced leading to the final expression for the mixture thermal conductivity: [62, p. 188]

$$\begin{aligned} &\lambda_{mix}(p, T) \\ &= (T_{c,mix}/T_{co})^{-1/6} (P_{cx}/P_{co})^{2/3} (MW_x/MW_o)^{-1/2} \lambda_o(P_o/T_o) (\alpha_{mix}/\alpha_o) \left(\lambda_o(T_o, P_o) \right. \\ &\quad \left. - \lambda_{int,o}(T_o) \right) + \lambda_{int,mix}(T) \end{aligned} \quad (3-166)$$

The terms of Equation are defined in Reference [62, p. 188ff.].

Pedersen et al. state that it was not possible to compare the developed model with experimental values due to a lack of data for multicomponent hydrocarbon mixtures. However a comparison with petroleum fluid fractions data showed model deviations of up to 13%. [62, p. 193]

3.6.3 Jarrahan and Heidaryan (2014)

A simple to use method to estimate the thermal conductivity as a function of temperature and pressure was developed by Jarrahan and Heidaryan. Their study is based on literature data

at various pressures, temperatures and specific gravities with 731 data points of 42 binary mixtures and pressures ranges of 0.1 to 300 MPa, temperatures ranges from 220 to 425 K and specific gravities from 0.626 to 1.434. [16]

The thermal conductivity of natural gas is expressed as a function of pseudocritical pressure and temperature and the low pressure gas conductivity ($\lambda_{1 atm}$):

$$\lambda = f(\lambda_{1 atm}, p_{pr}, T_{pr}) \quad (3-167)$$

Jarrahian and Heidaryan use Sutton's (2007) correlations and the Wichert and Aziz (1972) non-hydrocarbon adjustment method to find the pseudocritical pressure and temperature of the gas mixture: [16]

$$\gamma_{gMIX} = \frac{\sum y_i M_i}{M_{air}} \quad (3-168)$$

$$\gamma_{gHC} = \frac{\gamma_{gMIX} - (\gamma_{H_2S} M_{H_2S} + \gamma_{CO_2} M_{CO_2} + \gamma_{N_2} M_{N_2}) / M_{air}}{1 - \gamma_{H_2S} - \gamma_{CO_2} - \gamma_{N_2}} \quad (3-169)$$

$$p_{pcHC} = 671,1 + 14\gamma_{gHC} - 34,3\gamma_{gHC}^2 \quad (3-170)$$

$$T_{pcHC} = 120,1 + 429\gamma_{gHC} - 62,9\gamma_{gHC}^2 \quad (3-171)$$

The adjusted pseudocritical pressure and temperature are defined as:

$$p_{pc}^* = (1 - \gamma_{H_2S} - \gamma_{CO_2} - \gamma_{N_2})p_{pcHC} + \gamma_{H_2S}p_{cH_2S} + \gamma_{CO_2}p_{cCO_2} + \gamma_{N_2}p_{cN_2} \quad (3-172)$$

$$T_{pc}^* = (1 - \gamma_{H_2S} - \gamma_{CO_2} - \gamma_{N_2})T_{pcHC} + \gamma_{H_2S}T_{cH_2S} + \gamma_{CO_2}T_{cCO_2} + \gamma_{N_2}T_{cN_2} \quad (3-173)$$

Where the pressure and temperature are in psia and °R.

$$T_{pc} = T_{pc}^* - \varepsilon \quad (3-174)$$

$$p_{pc} = \frac{p_{pc}^*(T_{pc}^* - \varepsilon)}{T_{pc}^* + \gamma_{H_2S}(1 - \gamma_{H_2S})\varepsilon} \quad (3-175)$$

$$\varepsilon = 120 \left[(\gamma_{H_2S} + \gamma_{CO_2})^{0,9} - (\gamma_{H_2S} + \gamma_{CO_2})^{1,6} \right] + 15(\gamma_{H_2S}^{0,5} - \gamma_{H_2S}^4) \quad (3-176)$$

The pseudo reduced properties can then be calculated:

$$T_{pr} = \frac{T}{T_{pc}} \quad \text{and} \quad p_r = \frac{p}{p_{pc}} \quad (3-177)$$

The thermal conductivity at atmospheric pressure is determined through Equation (3-178) where the temperature is in °R and thermal conductivity is in Btu/ft.hr°F.

$$\lambda_{1 atm} = \lambda_{1 atm}^{uncorrected} + \Delta\lambda_{N_2} + \Delta\lambda_{CO_2} + \Delta\lambda_{H_2S} \quad (3-178)$$

with:

$$\lambda_{1 atm}^{uncorrected} = \left(A_{1 atm} \gamma_{gMix}^{A_2} \right) (T - 459,67) + A_3 + A_4 \log(\gamma_{gMix}) \quad (3-179)$$

$$\Delta\lambda_{N_2} = y_{N_2} (A_5 \log(\gamma_{gMix}) + A_6) \quad (3-180)$$

$$\Delta\lambda_{CO_2} = y_{CO_2} (A_7 \log(\gamma_{gMix}) + A_8) \quad (3-181)$$

The sample data contained CO₂ and N₂ up to 87.8 and 82.8 of mole percent respectively, however due to lack of data for mixtures containing H₂S no correction was developed for that component. [16]

Finally, the natural gas thermal conductivity can be estimated by applying Equation (3-182):

$$\lambda = \lambda_{1 atm} \left(1 + \frac{A_9}{T_{pr}^5} \left(\frac{p_{pr}^4}{T_{pr}^{20} + p_{pr}^4} \right) + A_{10} \left(\frac{p_{pr}}{T_{pr}} \right)^2 + A_{11} \left(\frac{p_{pr}}{T_{pr}} \right) \right) \quad (3-182)$$

The coefficients for the equations above can be found in Table 3-22. Jarrahan and Heidaryan claim an acceptable accuracy for the models application in engineering calculations and with an ARE of 0.1232%, an AARE of 5.6932% and 0.9718 for R² in reference to the model input data. [16]

Table 3-22: Coefficients for the correlation of the thermal conductivity. [16]

A₁	3.095251494612E-5
A₂	-3.054731613002E-1
A₃	1.205296187262E-2
A₄	-2.155542603544E-2
A₅	1.695938319680E-2
A₆	1.983908703280E-3
A₇	1.469572516483E-2
A₈	-7.570807856000E-4
A₉	1.854452341597
A₁₀	-1.275798197236E-3
A₁₁	1.925784814025E-1

3.7 Heat capacity of natural gas mixtures

The heat capacity is an important parameter when dealing with problems involving gas flow with heat transfer and reasonably accurate estimates are necessary. Calculations of the bottom hole flowing pressures and temperatures will require isobaric heat capacities estimates for example. [65]

Heat capacities for pure substances are for example easily available through the free NIST web data base [25] whereas methods for the estimation of natural gas mixture heat capacities are presented in the following sections.

3.7.1 Abou-Kassem and Dranchuk (1982)

Abou-Kassem and Dranchuk developed an ideal isobaric heat capacity correlation for sweet and sour natural gases and a generalized correlation to estimate the heat capacity departures, for such gases. [65]

In a first step the ideal isobaric heat capacity is expressed as a function of specific gravity in Equation: [65]

$$c_{p_{mHC}}^o = A + BT_r \quad (3-183)$$

For gases containing CO₂, N₂ and H₂S following expression is used:

$$c_{p_m}^o = \frac{c_{p_{mHC}}^o}{F_{CO_2} + F_{N_2} + F_{H_2S}} \quad (3-184)$$

where

$$A = B_1 + B_2\gamma_g + B_3\gamma_g^2 \quad (3-185)$$

$$B = B_4 + B_5\gamma_g + B_6\gamma_g^2 \quad (3-186)$$

$$F_{CO_2} = 1 + y_{CO_2}(B_7 + B_8T) \quad (3-187)$$

$$F_{H_2S} = 1 + y_{H_2S}(B_9 + B_{10}T) \quad (3-188)$$

$$F_{N_2} = 1 + (B_{11}y_{N_2} + B_{12}y_{N_2}^2) + (B_{13}y_{N_2} + B_{14}y_{N_2}^2)T \quad (3-189)$$

The temperature is in °R and the corresponding coefficients B₁-B₁₄ for Equations (3-185) to (3-189) are listed in Table 3-24.

The ideal heat capacity model can be applied to sweet natural gases in a specific gravity range fro 0.55 to 1, in a temperature range of 32°F < T < 2240°F and for sour natural gases in the temperature range 32°F < T < 300°F.

In order to obtain the isobaric heat capacity Abou-Kassem and Dranchuk present the following expression for the isobaric heat capacity departure which is based on BWR EOS fitted to the Standing and Katz z-factor chart: [65]

$$(c_p - c_p^o) = R \frac{\left[-1 - 6A_3 \frac{\rho_r}{T_r^3} - \frac{6A_7}{A_8 T_r^3} + \left(\frac{6A_7}{A_8 T_r^3} + 3A_7 \frac{\rho_r^2}{T_r^3} \right) e^{(-A_8 \rho_r^2)} T_r \right]}{\left[1 + \left(A_1 - \frac{2A_3}{T_r^3} \right) \rho_r + A_4 \rho_r^2 - 2A_7 \frac{\rho_r^2}{T_r^3} (1 + A_8 \rho_r^2) e^{(-A_8 \rho_r^2)} \right]^2} \quad (3-190)$$

$$\left[T_r + 2 \left(A_1 T_r + A_2 + \frac{A_3}{T_r^2} \right) \rho_r + 3(A_4 T_r + A_5) \rho_r^2 \right]$$

$$+ A_7 \frac{\rho_r^2}{T_r^2} e^{(-A_8 \rho_r^2)} (3 + 3A_8 \rho_r^2 - 2A_8^2 \rho_r^4)$$

Where the molal isobaric heat capacity c_p , has the unit Btu/lb mol.

A_1 - A_8 in Table 3-23 represent the constants of the reduced BWR equation, which can be found in Reference [66].

Table 3-23: Coefficients for the specific isobaric heat capacity departure calculation.

A₁	0.31506237	A₅	-0.61232032
A₂	-1.0467099	A₆	-0.10488813
A₃	-0.57832729	A₇	0.68157001
A₄	0.53530771	A₈	0.68446549

Finally the the specific isobaric heat capacity can be calculated as the sum of the ideal specific isobaric heat capacity and the specific isobaric heat capacity departure from the ideal state:

$$C_{pm} = c_{pm}^o + (c_p - c_p^o) \quad (3-191)$$

The coefficients for Equation (3-190) are listed in Table 3-24 and are subject to following restrictions: $32^\circ\text{F} < T < 300^\circ\text{F}$, $0.0 < \gamma_{H_2S} < 0.40$ mole fraction, $0.0 < \gamma_{CO_2} < 0.20$ mole fraction and $0.0 < \gamma_{N_2} < 0.25$ mole fraction. Equation (3-190) may be used in the range $0.2 < p_r < 15$ and $1.05 < T_r < 3.0$. [65]

Table 3-24: Coefficients for the calculation of the isobaric heat capacity. [65]

B₁	5.596695	B₆	5.758700	B₁₁	0.3623622
B₂	-2.233480	B₇	0.4258600	B₁₂	-0.4661581
B₃	0.807265	B₈	1.24323E-3	B₁₃	0.97570E-3
B₄	-1.003900	B₉	-0.0405600	B₁₄	2.708217E-3
B₅	3.141600	B₁₀	1.00889E-3		

3.7.2 Moshfeghian (2011)

Moshfeghian developed a simple correlation to estimate the heat capacity of natural gases as a function of pressure, temperature, and specific gas gravity γ_g . The proposed correlation covers pressure ranges of from 0.10 to 20 MPa, (14.5 to 2,900 psia), temperature ranges of 20 to 200° C (68 to 392° F/293 to 473 K), and specific gravities from 0.60 to 0.80. [67]

$$C_p = (ab^T T^c + de^p p^f) \left(\frac{\gamma_g}{0,60} \right)^{0,025} \quad (3-192)$$

The values for the coefficients in Equation (3-192) are found in Table 3-25. In addition to that the applicable ranges and the average absolute percentage error and the maximum absolute percent deviations are listed. [67]

Table 3-25: Parameters for the correlation. [67]

γ_g	a	b	c	d	e	f	AAPD	MAPD	T-range [°C]
0,60	0.9426	1.0106	-0.5260	2.1512	1.0140	0.0155	3.43	12.10	15-200
0,65	1.1684	1.0123	-0.6476	2.1436	1.0146	0.0188	3.94	16.05	15-200
0,70	0.2533	1.0200	-0.7330	2.2486	1.0146	0.0204	4.39	20.44	20-200
0,75	1.8455	1.0194	-1.0665	2.1972	1.0148	0.0246	4.83	22.88	30-200
0,80	0.0133	1.0053	0.3912	2.1488	1.0155	0.0234	4.45	21.34	40-200
Generalized parameters									
0.60-0.80	0.900	1.014	-0.700	2.170	1.015	0.0214	3.34	23.19	

Moshfeghian evaluated the correlation accuracy by comparing it to results generated by the NIST REFPROP [68] software. For the generalized set of parameters and a total of 715 data points the average absolute percentage error and the maximum absolute percent deviations are 4.34 and 23.61, respectively. [67]

3.7.3 Lateef and Omeke (2011)

Based on the specific heat capacity description as a function of temperature given in Equation (3-193), and experimental data from three different gas fields Lateef and Omeke developed a correlation which can be applied to find the specific heat capacity of natural gas mixtures in a range from $0.55 < \gamma_g < 1$ and $150^\circ\text{F} < T < 2000^\circ\text{F}$ ($338.706\text{K} < T < 1366.483\text{K}$). [69]

$$C_p = a + bT + cT^2 + dT^3 \quad (3-193)$$

where a, b, c, and d are the specific heat coefficients.

The correlation for the estimation of the specific heat capacity of a natural gas requires the input of the temperature T (in °F), the pressure p (in psia), and the specific gas gravity γ_g . and is expressed as Equation (3-194). [69]

$$C_p = (0,000156p_r^3 - 0,005435p_{pr}^2 + 0,060528p_{pr} + 0,942510)^{0,7} \left[(6,0050\gamma_g^2 - 0,0416\gamma_g 6,1719) + (-1,3498(10^{-2})\gamma_g^2 + 4,0381(10^{-2})\gamma_g - 1,1206(10^{-2})T + (8,6856(10^{-6})\gamma_g - 2,0784(10^{-6})\gamma_g^2 + 9,2702(10^{-6})T^2 + (-1,8749(10^{-9})\gamma_g^2 + 4,0319(10^{-9}) - 2,1300(10^{-9})T^3) \right] \quad (3-194)$$

The assumption for the model developed by Lateef and Omeke is that natural gases with the same specific gravity have the same components in identical proportions. For example a mixture of 80 % methane and 20 % ethane would have the same specific gravity as a mixture of 90 % methane and 10 % propane. It is claimed that this assumption simplifies the calculation yet does not negatively affect the result. [69]

4 Supercritical carbon dioxide

Supercritical carbon dioxide describes the fluid condition of CO₂ above its critical temperature of 304.13 K and pressure of 7.38 MPa (Figure 4-1).

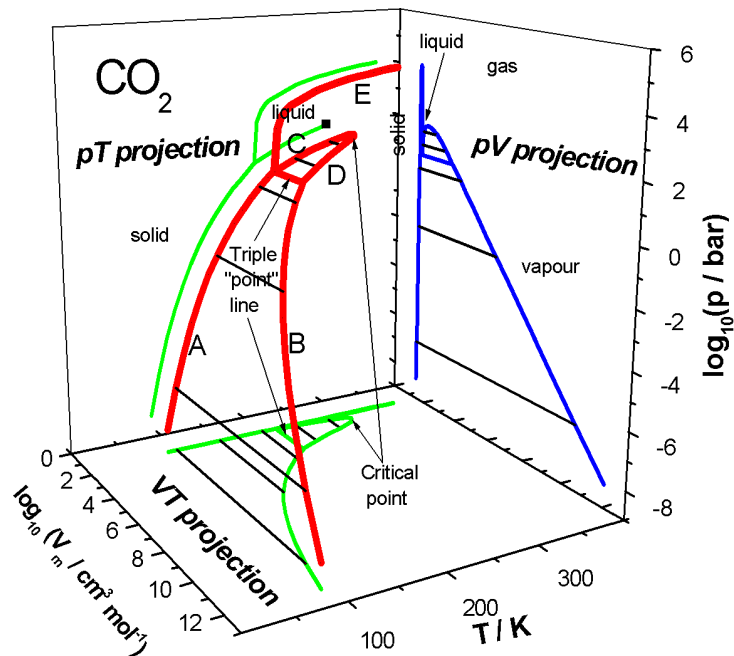


Figure 4-1: Phase diagram of carbon dioxide. [70]

Generally the thermodynamic properties of carbon dioxide can be predicted using correlations, equations of state (EOS) and black oil models. The latter have been developed for oil and natural gas containing typically less than 3% CO₂. Substantial errors may therefore result if such methods are applied to pure CO₂. While empirical correlations typically offer a straightforward approach, further parameters such as density are often needed for the estimation of properties. In addition correlations might not offer the required accuracy when applied to carbon dioxide at supercritical conditions. Because EOS or models based on EOS require extensive and complex numerical computations they may not be the preferred choice for a lot of engineering applications. The main EOS applied to carbon dioxide include the Peng-Robinson (PR), Soave-Redlich-Kwong (SRK) and Span & Wagner. The Span & Wagner EOS was specifically developed for the prediction of CO₂ properties and is widely considered the best choice for that application. However, it is not implemented in a lot of software packages used for evaluating carbon dioxide flow dynamics in wellbores and pipelines. [2]

4.1 National Institute of Standards and Technology (NIST) web database.

CO₂ properties recorded in the NIST database are mainly based on the Span & Wagner equation of state and a number of auxiliary models such as Fenghour et al, Ely et al and Vesovic et al. [63] The NIST data base can be found through the link in Reference [15].

4.2 Supercritical CO₂ dynamic viscosity

The viscosity of CO₂, as a function of temperature and pressure, is shown in Figure 4-2. While the temperature has little effect on the viscosity in the higher temperature ranges this changes in vicinity of the critical temperature a as can be observed from the almost vertical isobars in that region. The CO₂ viscosity diverges at the critical point and assumes a greater value than might be expected. However the increase in viscosity is only around 1% and relative small compared to that of the thermal conductivity, which can increase by a factor of two near the critical point. The T-p region for which a pronounced change of viscosity is observed, coincides with the area where the density changes rapidly with pressure, suggesting that density is an important variable when describing the viscosity behaviour of CO₂ at high pressures. [10, p. 9.30]

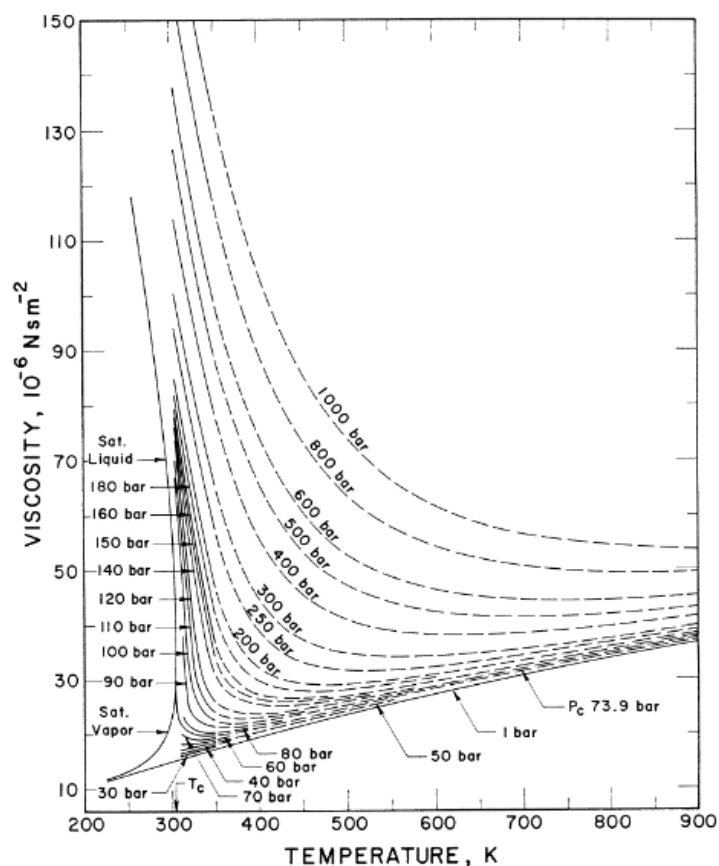


Figure 4-2: Viscosity of carbon dioxide. [71, p. 78]

There are several methods available for the estimation of high pressure pure gas components viscosity. The methods proposed by Lucas and Chung et al. both utilize a correlation for the estimation of the dense gas viscosity. Zabaloy et al. developed a model for viscosity prediction based on the description of a Lennard-Jones fluid which is able to correlate the pure compound viscosity of supercritical fluids over a wide range of conditions.[30] The TRAPP (transport property prediction) method is a method to calculate viscosities as well as thermal conductivities of pure fluids and mixtures. Some methods such as the Chung et al. and TRAPP method require the input of temperature and density which in turn calls for the use of EOS to obtain the necessary volumetric if not available otherwise.[22] Recently published correlations

by Bahadori and Vuthaluru and also Heidaryan et al were specifically developed for the estimation of supercritical CO₂ viscosities. These methods are simple to use and only require the temperature and pressure of interest as input parameters.

4.2.1 Lucas Method (1980)

Lucas [71] recommend a method somewhat similar to that first published by Reichenberg [72] for the calculation of viscosities for dense fluids. The input parameters required for this method are the critical temperature, critical pressure, critical compressibility factor, and dipole moment, as well as the system temperature and pressure. [10, p. 9.35]

The first step consists of calculating the parameter Z_1 for the reduced temperature of interest.[10]

$$Z_1 = \eta^0 \xi = [0,807T_r^{0,618} - 0,357e^{-0,449T_r} + 0,340e^{-4,058T_r} + 0,018]F_P^0 F_Q^0 \quad (4-1)$$

η^0 refers to the low-pressure viscosity. If $T_r \leq 1.0$ and $P_r \leq (P_{vp}/P_c)$, then the parameter Z_2 is calculated as follows:

$$Z_2 = 0,600 + 0,760P_r^\alpha + (6,990P_r^\beta - 0,6)(1 - T_r) \quad (4-2)$$

With $\alpha = 3,262 + 14,98P_r^{5,508}$ and $\beta = 1,390 + 5,746P_r$. If $1 \leq T_r \leq 40$ and $0 \leq P_r \leq 100$ then Z_2 is found through:

$$Z_2 = \eta^0 \xi \left[1 + \frac{aP_r^e}{bP_r^f + (1 + cP_r^d)^{-1}} \right] \quad (4-3)$$

$\eta^0 \xi$ is equal to Z_1 previously calculated and the coefficients are calculated as follows:

$$a = \frac{a_1}{T_r} e^{\alpha_2 T_r^\gamma}; \quad b = a(b_1 T_r - b_2); \quad c = \frac{c_1}{T_r} e^{c_2 T_r^\delta}; \quad d = \frac{d_1}{T_r} e^{d_2 T_r^\varepsilon}; \quad e = 1,2088; \quad (4-4)$$

$$f = f_1 e^{f_2 T_r^\zeta}$$

and

$$\begin{aligned} a_1 &= 1,245(10^{-3}); \quad a_2 = 5,1726; \quad \gamma = -03286; \quad b_1 = 1,6553; \quad b_2 = 1,2723; \\ c_1 &= 0,4489; \quad c_2 = 3,0578; \quad \delta = -37,7332; \quad d_1 = 1,7368; \quad d_2 = 2,2310; \\ \varepsilon &= -7,6351; \quad f_1 = 0,9425; \quad f_2 = -0,1853; \quad \zeta = 0,4489 \end{aligned} \quad (4-5)$$

After obtaining Z_1 and Z_2 , Y is defined as:

$$Y = \frac{Z_2}{Z_1} \quad (4-6)$$

Then the correction factors F_P and F_Q are calculated:

$$F_P = \frac{1 + (F_P^0 - 1)Y^{-3}}{F_P^0} \quad (4-7)$$

$$F_Q = \frac{1 + (F_Q^0 - 1)[Y^{-1} - (0,007)(\ln Y)^4]}{F_Q^0} \quad (4-8)$$

F_P^0 and F_Q^0 are low-pressure polarity and quantum factors determined can be determined by following the steps presented next: [10]

$$F_P^0 = 1 \text{ for } 0 \leq \mu_r \leq 0,022 \quad (4-9)$$

$$F_P^0 = 1 + 30,55(0,292 - Z_c)^{1,72} \text{ for } 0,022 \leq \mu_r \leq 0,075 \quad (4-10)$$

$$F_P^0 = 1 + 30,55(0,292 - Z_c)^{1,72}|0,96 + 0,1(T_r - 0,7)| \text{ for } 0,075 \leq \mu_r \quad (4-11)$$

where μ is the dipole moment and μ_r is the dimensionless dipole moment defined as:

$$\mu_r = 52,46 \frac{\mu^2 P_c}{T_c^2} \quad (4-12)$$

where μ is in debyes, P_c is in bars, and T_c is in °K.

F_Q^0 is used only for the quantum gases He, H₂, and D₂.

$$F_Q^0 = 1,22Q^{0,15}\{1 + 0,00385[(T_r - 12)^2]^{1/M} \text{sign}(T_r - 12)\} \quad (4-13)$$

where $Q = 1,38$ (He), $Q = 0,76$ (H₂), $Q = 0,52$ (D₂). The $\text{sign}(T_r - 12)$ means that one +1 or -1 are to be inserted depending on whether the value of the argument within () is greater than or less than zero. [10]

Once the above parameters are determined the gas viscosity can be calculated as

$$\eta = \frac{Z_2 F_P F_Q}{\xi} \quad (4-14)$$

where ξ is the reduced inverse viscosity defined as:

$$\xi = 0,176 \left(\frac{T_c}{M^3 P_c^4} \right)^{1/6} \quad (4-15)$$

ξ is given in $(\mu\text{P})^{-1}$, T_c in K, M in g/mol, and P_c in bars.

At low pressures, Y is almost 1, $F_P = 1$ and $F_Q = 1$. Consequently Z_2 then also equals $\eta^0 \xi$. The error was found to be less than 5% for most cases when comparing the Lucas method to experimental data. [10]

4.2.2 Zabaloy et al. (2005) - Lennard Jones fluid model

Zabaloy et al. proposed a model for the viscosity of pure component supercritical fluids, which uses molecular simulation results for the Lennard–Jones (LJ) fluid. The proposed model allows the calculation of the fluid viscosity at temperature and density conditions which correspond to LJ dimensionless temperature and density values beyond the range of the supporting molecular simulation data. This was achieved through setting up according interpolation and extrapolation schemes and makes viscosity prediction in the supercritical range possible.[73]

The Lennard-Jones Fluid model qualitatively reproduces the viscous behavior for real fluids over a wide range of conditions and is expressed as Lennard–Jones intermolecular potential as follows: [73]

$$u(r) = 4\varepsilon \left[\left(\frac{\sigma}{r} \right)^{12} - \left(\frac{\sigma}{r} \right)^6 \right] \quad (4-16)$$

r is the intermolecular distance, u the intermolecular potential energy, ε the depth of the LJ potential well and σ is the LJ separation distance at zero energy.

The LJ reduced temperature T^+ , reduced pressure P^+ , reduced density ρ^+ and reduced viscosity η^+ are defined as follows: [73]

$$T^+ = \frac{kT}{\varepsilon} \quad (4-17)$$

$$P^+ = \frac{P\sigma^3}{\varepsilon} \quad (4-18)$$

$$\rho^+ = \frac{N}{V}\sigma^3 = N_A\rho\sigma^3 \quad (4-19)$$

$$\eta^+ = \eta \frac{\sigma^2}{\sqrt{m\varepsilon}} \quad (4-20)$$

The input of the temperature and pressure is in K and bar respectively.

T is the absolute temperature, P the absolute pressure, k is the Boltzmann constant, N the number of molecules, V the system volume, N_A Avogadro's number, ρ the mole density in units such as moles per litres, η the Newtonian shear viscosity and m is the mass of one molecule. [73]

LJ viscosity–temperature–density relationship analytical form is given through: [73]

$$\eta^+ = \eta_0^+ + \sum_{i=2}^{10} \sum_{j=1}^3 b_{ji} \frac{(\rho^+)^i}{(T^+)^{j-1}} \quad (4-21)$$

The term of the viscosity at zero density η_0^+ is defined as

$$\eta_0^+ = \frac{0,176288(T^+)^{1/2}}{\Omega_v(T^+)} \quad (4-22)$$

where Ω_v is the collision integral, which is a function of T^+ and is given in Reference [10] (Poling et al.) as follows:

$$\Omega_v = [A(T^+)^{-B}] + Ce^{-DT^+} + Ee^{-FT^+} \quad (4-23)$$

where $A = 1.16145$; $B = 0.14874$; $C = 0.52487$; $D = 0.77320$; $E = 2.16178$ and $F = 2.43787$. Equation (4-23) is applicable from $0.3 \leq T^+ \leq 100$. [10]

To calculate viscosities at given temperature and pressure the Kolafa and Nezbeda EOS, which interrelates the temperature, the pressure, and the density of the LJ fluid is needed. From this the dimensionless LJ reduced density ρ^+ can be found: [73]

$$z = \frac{P^+}{\rho^+ T^+} = f_{KN}(\rho^+, T^+) \quad (4-24)$$

f_{KN} is a function of ρ^+ and T^+ and its calculation is specified in Reference [74] in Appendix A. Equation (4-24) is valid in a range of $0.68 \leq T^+ \leq 10$.

The LJ separation distance at zero energy parameter σ is given as temperature dependent parameter with the adjustable parameter S_σ which is set to match the experimental viscosities slope. Values for S_σ are listed in Reference [73] for various pure gases and is given as -0,0085 for CO_2 .

$$\alpha_\sigma = \frac{\sigma}{\sigma_c} = 1 + S_\sigma(T_r - 1) \quad (4-25)$$

Equation (4-26) allows the calculating of the viscosity. F is another adjustable parameter listed in Reference [73] and given as $F=1.0285$ for CO_2 . [73]

$$\eta = \frac{F\eta^+ \sqrt{m\varepsilon}}{\sigma^2} \quad (4-26)$$

The parameters ε and σ_c can be calculated through following expressions:

$$\varepsilon = \frac{kT_c}{1,3396} \quad (4-27)$$

$$\sigma_c = \left(\frac{kT_c 0,1405}{P_c 1,3396} \right)^{1/3} \quad (4-28)$$

4.2.3 Bahadori and Vuthaluru (2009)

Bahadori and Vuthaluru developed a simple to use correlation for the prediction of CO₂ viscosity and thermal conductivity as a function of pressure and temperature. The correlations have no complex expressions and therefore offer a straightforward calculation. The correlation is applicable in a temperature range between 260 and 450 K and in a pressure range between 10 and 70 MPa. These are the temperature and pressure regions that are widely considered in CO₂ sequestration.[7]

$$\ln(\mu) = a + \frac{b}{P} + \frac{c}{p^2} + \frac{d}{p^3} \quad (4-29)$$

where

$$a = A_1 + \frac{B_1}{T} + \frac{C_1}{T^2} + \frac{D_1}{T^3} \quad (4-30)$$

$$b = A_2 + \frac{B_2}{T} + \frac{C_2}{T^2} + \frac{D_2}{T^3} \quad (4-31)$$

$$c = A_3 + \frac{B_3}{T} + \frac{C_3}{T^2} + \frac{D_3}{T^3} \quad (4-32)$$

$$d = A_4 + \frac{B_4}{T} + \frac{C_4}{T^2} + \frac{D_4}{T^3} \quad (4-33)$$

The units of viscosity are mPas whereas pressure (P) and temperature (T) are expressed in MPa and °K respectively. Compared to reported data by Vesovic et al. [75] the proposed correlation shows average absolute deviation of 1,1 % for the viscosity. [7]

Table 4-1: Coefficients for Equations (4-30) to (4-33) to predict viscosity of carbon dioxide. [7]

Symbol	Coefficients for viscosity of CO ₂ temperatures less than 340 °K	Coefficients for viscosity of CO ₂ at temperatures more than 340 °K
A ₁	-8.381727231932328E1	-6.304360942940384E1
B ₁	7.170262916398216E4	7.089412819202834E4
C ₁	-2.088352606491789E7	-2.729618206187531E7
D ₁	2.035238087953347E9	3.491954145885637E9
A ₂	7.688274861237018E3	5.392507286567643E3
B ₂	-6.832908603727831E6	-6.48675327864201E6
C ₂	2.00319868619153E9	2.543938513422521E9
D ₂	-1.94536522596535E11	-3.281228975928387E11
A ₃	-1.967260059076993E5	-1.182481836340281E5
B ₃	1.732142393454871E8	1.438608961427429E8
C ₃	-5.049067845006425E10	-5.738803284656972E10
D ₃	4.882358762211981E12	7.535042772730154E12
A ₄	1.3529778432466E6	6.947087585578619E5
B ₄	-1.19567721576674E9	-8.506349304338924E8
C ₄	3.498814034450212E11	3.424312685872325E11
D ₄	-3.395109635057981E13	-4.542379235870166E13

4.2.4 Heidaryan et al. (2010)

Based on experimental data and data reported by Stephan and Lucas [71], Heidaryan et al. developed a correlation valid for a temperature range of 310 to 900K and pressure range of 7.5 to 101.4 MPa. [76] The correlation parameters were fitted by minimizing the error between the correlation results from the literature and experimental data which were obtained using a rolling body viscometer in at temperature range from 313.15K to 523.15K and pressure range between 7.7MPa and 81.1MPa.

$$\mu = \frac{A_1 + A_2 p + A_3 p^2 + A_4 \ln(T) + A_5 \ln(T)^2 + A_6 \ln(T)^3}{1 + A_7 p + A_8 \ln(T) + A_9 \ln(T)^2} \quad (4-34)$$

The corresponding coefficients for Equation (4-34) can be found in Table 4-5. The unit of viscosity is expressed in centipoise (cp) while the temperature and pressure are given in K and bar(0.1 MPa), respectively. [76] Heidaryan et al. state an AAE of 1.71%, 3.64%, 1.45% and 1.82% when compared with experimental data obtained through their study, data by Stephan and Lucas [71], data by Pensado et al. [77] and NIST web book data [25], respectively.

Table 4-2: Coefficients for Equation (4-34). [76]

Coefficient	Value
A ₁	-1,146067E-1
A ₂	6,978380E-7
A ₃	3,976765E-10
A ₄	6,336120E-2
A ₅	-1,166119E-2
A ₆	7,142596E-4
A ₇	6,519333E-6
A ₈	-3,567559E-1
A ₉	3,180473E-2

4.3 Supercritical CO₂ thermal conductivity

The thermal conductivity behaviour of CO₂ as a function of pressure and temperature is shown in Figure 4-3. Around the critical point the thermal conductivity of a fluid diverges and this so called critical enhancement is observed in a large range of temperatures and densities around the critical point for CO₂. [75] From Figure 4-4 it can be seen that the thermal conductivity may increase by a factor of six as a result of the enhancement in the critical region. [10, p. 10.19] The region in which this enhancement is smaller than 1%, lies outside a pressure and density range which is approximately marked by $240 < T < 450$ °K and $25 \text{ kg/m}^3 < \rho < 1000 \text{ kg/m}^3$. Vesovic et al. present a mathematical description for this fluid behaviour in the critical region and implement it in their correlation. [35]

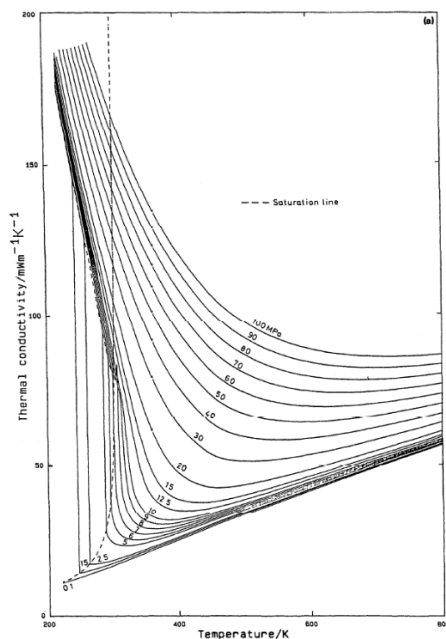
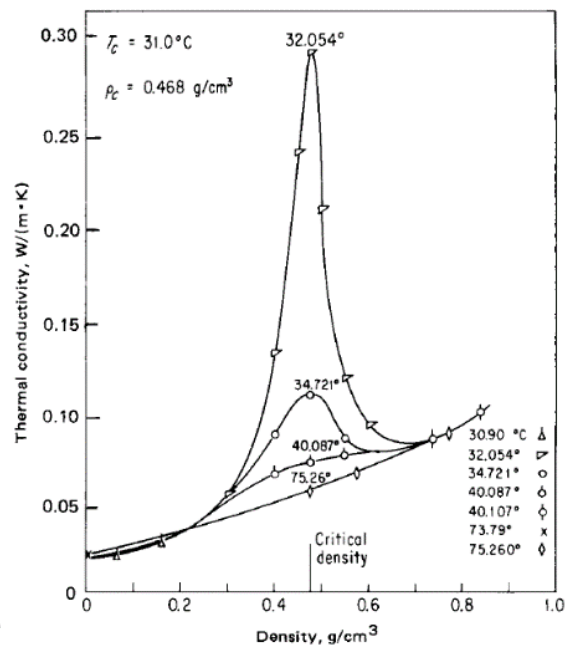
Figure 4-3: The thermal conductivity of CO₂ along isobars. [75]

Figure 4-4: Thermal conductivity of carbon dioxide near the critical point. [10, p. 10.21]

Mathematical models of real systems require the input of the thermal conductivity because of its influence on the heat transfer capability. It is not practical to measure this thermo-physical property and therefore accurate models are needed.[3] Several methods to predict the thermal conductivities of fluids at high pressures are published in the literature. Stiel and Thodos presented a generalized excess thermal conductivity concept in which thermal conductivity depends on critical temperature, critical pressure and critical volume. [3] Chung et al. [58] used the kinetic gas theory to obtain a relation for thermal conductivity. The TRAPP (transport property prediction) and later SUPERTRAPP was developed by Ely et al. as a corresponding states style approach to compute thermal conductivities of pure fluids and mixtures.[3] Guo et al [63] proposed two thermal conductivity correlations based on Peng and Robinson (PR) and Patel and Teja (PT) Equation of States. Vesovic et al. [75] presented reference data for thermal conductivity and viscosity relationships for CO₂, also in the critical range. There are also several recently published correlations available that are simple to use and were specifically developed for application in the supercritical temperature and pressure range of CO₂.

4.3.1 Vesovic (1990)

The thermal conductivity or viscosity represented by $X(\rho, T)$ are expressed as the sum of three independent contributions:

$$X(\rho, T) = X^0(T) + \Delta X(\rho, T) + \Delta_c X(\rho, T) \quad (4-35)$$

The first term $X^0(T)$ describes the transport property in the limit of zero density while the last term, named the critical enhancement, $\Delta_c X(\rho, T)$ represents the behaviour of a fluid near its critical point which contributes to the divergences of the thermal conductivity, and to a lesser extent the viscosity, around that point. The excess property $\Delta X(\rho, T)$ describes the contributions of all other effects on the transport property at elevated densities such as many-body collisions, molecular – velocity correlations and collisional transfer. While Vesovic et al. established theoretical models for the terms $X^0(T)$ and $\Delta_c X(\rho, T)$ that show good agreement with experimental data (see Figure 4-6) the description of excess property $\Delta X(\rho, T)$ is based entirely on data obtained from experiments. [75]

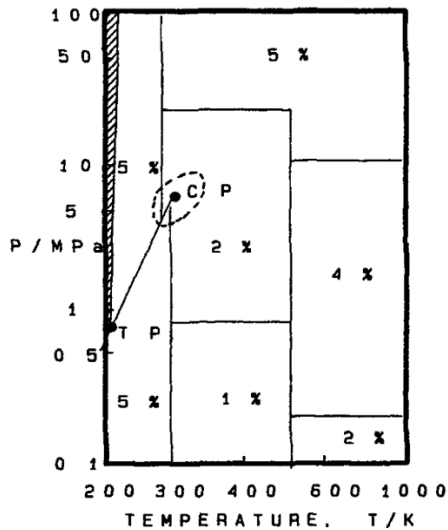


Figure 4-5: The extent of the thermal conductivity correlation and its estimated uncertainty. [75]

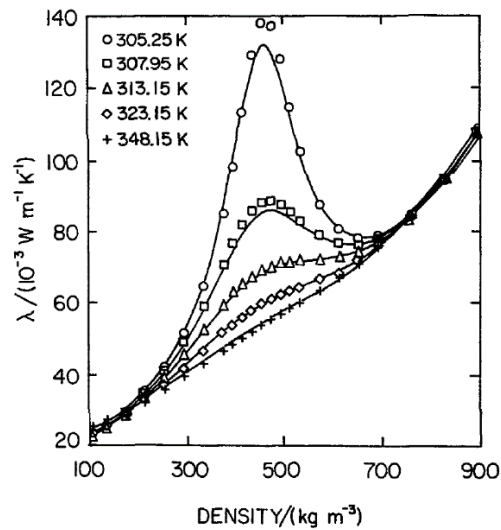


Figure 4-6: The thermal conductivity of CO₂ in the critical region as a function of density at different pressures. The solid curves represent the mathematical model developed by Vesovic et al. to describe the thermal conductivity changes around the critical point while the data points are experimental results. [75]

The correlations for the thermal conductivity cover a temperature range from 200K to 1000K and up to 100 MPa. Vesovic et al. provide the correlations results in tables for these property ranges. The uncertainties associated with the developed models are stated as ranging from $\pm 5\%$ for the thermal conductivity in the liquid phase and are displayed in detail in Figure 4-5.

4.3.2 Bahadori and Vuthaluru (2009)

The correlation proposed by Bahadori and Vuthaluru is applicable in a temperature range between 260 and 450 °K and in a pressure range between 10 and 70 MPa. [7]

$$\ln(\lambda) = a + \frac{b}{P} + \frac{c}{P^2} + \frac{d}{P^3} \quad (4-36)$$

Where

$$a = A_1 + \frac{B_1}{T} + \frac{C_1}{T^2} + \frac{D_1}{T^3} \quad (4-37)$$

$$b = A_2 + \frac{B_2}{T} + \frac{C_2}{T^2} + \frac{D_2}{T^3} \quad (4-38)$$

$$c = A_3 + \frac{B_3}{T} + \frac{C_3}{T^2} + \frac{D_3}{T^3} \quad (4-39)$$

$$d = A_4 + \frac{B_4}{T} + \frac{C_4}{T^2} + \frac{D_4}{T^3} \quad (4-40)$$

Table 4-3: Coefficients for Equations (4-37) to (4-40) to predict thermal conductivity of CO₂. [7]

A₁	2,511772164091
B₁	-4,61299395833E3
C₁	1,56039978824E6
D₁	-1,6486817476956E8
A₂	-6,7843586693162E2
B₂	5,9472900533367E5
C₂	-1,8136903173662E8
D₂	1,8606361834906E10
A₃	2,0648978571659E4
B₃	-1.9966713570538E7
C₃	6,4236725264301E9
D₃	-6,8021988393284E11
A₄	-1,095035226623E5
B₄	1,0878297025052E8
C₄	-3,575489373317E10
D₄	3,8549993712053E12

The units of the thermal conductivity are given in W/(mK) whereas pressure and temperature are expressed in MPa and °K respectively. Compared to data reported by Vesovic et al. (1990) [75] the proposed correlation shows average absolute deviation of 1,27 % for the thermal conductivity. [7]

4.3.3 Ouyang (2012)

Ouyang proposes the correlation given in Equations (4-41) and (4-42) based on data available through the National Institute of Standards and Technology (NIST) web data base [25].

$$k = G_0 + G_1p + G_2p^2 + G_3p^3 + G_4p^4 \quad (4-41)$$

$$G_i = m_{i0} + m_{i1}T + m_{i2}T^2 + m_{i3}T^3 + m_{i4}T^4 \quad (i = 0, 1, 2, 3, 4) \quad (4-42)$$

The correlation coefficients are listed in Table 4-4 and the carbon dioxide thermal conductivity (k) is in W/(m*K), pressure (p) in psia. The correlation is valid in a range from for pressure = 1100 – 9000 psia (7,6 - 62 MPa) and temperature = 40 – 100 °C (313 – 373 K). [2]

Table 4-4: Correlation coefficients. [2]

	m_{i0}	m_{i1}	m_{i2}	m_{i3}	m_{i4}
i=0	9.859639572733E-01	-5.503641864344E-02	1.057381020708E-03	-8.653773289916E-06	2.607146719869E-08
i=1	-8.219651988122E-04	5.199181579899E-05	-1.048105893468E-06	8.823897953704E-09	-2.706470092326E-11
i=2	2.622601305269E-07	-1.657328960394E-08	3.402817642542E-10	-2.907643931825E-12	9.015692452402E-15
i=3	-3.381016445331E-11	2.147179067610E-12	-4.458031806753E-14	3.845649305052E-16	-1.201102332048E-18
i=4	1.536208590758E-15	-9.799515356723E-17	2.051753162406E-18	-1.783790285298E-20	5.608187118410E-23

4.3.4 Jarrahan and Heidaryan (2012)

Jarrahan and Heidaryan [3] propose the following expression for the calculation of the CO₂ thermal conductivity as a function of pressure and temperature:

$$\lambda = \frac{A_1 + A_2p + A_3p^2 + A_4 \ln(T) + A_5 \ln(T)^2}{1 + A_6p + A_7 \ln(T) + A_8 \ln(T)^2 + A_9 \ln(T)^3} \quad (4-43)$$

where p is the pressure in MPa, T the temperature °K and the thermal conductivity is given in mW m⁻¹ K⁻¹. The coefficients for equation (4-43) are given in Table 4-5.

Table 4-5: Coefficients used for the calculation of the thermal conductivity.[3]

A₁	1.49288267457998E1
A₂	2.62541191235261E-3
A₃	8.77804659311418E-6
A₄	-5.11424687832727
A₅	4.37710973783525E-1
A₆	2.11405159581654E-5
A₇	-4.73035713531117E-1
A₈	7.36635804311043E-2
A₉	-3.76339975139314E-3

The method developed by Jarrahan and Heidaryan is based on 668 experimental measurements and is valid in a temperature range from 310 to 960 K, and a pressure range between 7.4 and 210 MPa. However the authors note that lack of data for temperature from 400 to 475 °K and pressure above 25 MPa as well as temperature from 575 to 650 °K and 875 to 950 K in the data they used to develop the correlation. The ARE and AARE are reported with 2.06% and 2.42% respectively when compared with 13467 thermal conductivity NIST [25] data points in temperature ranges of 310 to 960 °K and the pressure ranges from 7.4 to 210 MPa.

4.3.5 Amooy (2013)

Amooy presents a correlation for the estimation of thermal conductivity based on 600 data points for a temperature range of 290 to 800 °K and a density range between 1 and 1200 kg/m³. The correlation is given as Equation (4-44) with the corresponding coefficients given in Table 4-6, allows the calculation of the thermal conductivity (mW/(m K)) as a function of the CO₂ density (kg/m³) and the temperature (K). Amooy reports an AARE of 2.74%. [78]

$$\lambda = \frac{A_1 + A_2\rho + A_3\rho^2 + A_4\rho^3T^3 + A_5\rho^4 + A_6T + A_7T^2}{\sqrt{T}} \quad (4-44)$$

Table 4-6: Coefficients for Equation (4-44). [78]

A₁	-105.161
A₂	0.9007
A₃	0.0007
A₄	3.50E-15
A₅	3.76E-10
A₆	0.7500
A₇	0.0017

4.4 Supercritical CO₂ density

The density estimation of CO₂ may be calculated through a model based on an Equation of state or an empirical correlation. The latter type offers a somewhat simpler approach. The empirical correlations developed specifically for CO₂ do not require a large number of parameters or complicated and longer computations. Examples for such correlations are those published by Bahadori et al.[79] or Haghbakhsh et al [80].

4.4.1 Prediction of supercritical CO₂ properties through EOS

Modern EOS which allow highly accurate fluid descriptions are typically not simple cubic EOS such as the van der Waals or the Peng-Robinson EOS, but are given in a some form of a fundamental equation of the Helmholtz energy as function of temperature and density. These modern Helmholtz EOS are based on theoretical models but include many parameters that are adjusted to experimental data. While more complicated than the cubic equations of state the more modern EOS will predict the fluid properties with much greater accuracy.[81]

Thermodynamic properties are not only important as such, but also for the calculation of transport properties which are usually correlated as a function of temperature and density. Because experimental data is mostly measured as a function of temperature and pressure a EOS is needed to obtain the density. Also the description of the critical region in terms of transport properties (especially the thermal conductivity) requires some additional thermodynamic input quantities. [81]

Span and Wagner (1996) developed an EOS which allows calculations for CO₂ properties with uncertainties similar to those of the best experimental data. Compared to the EOS previously developed by Ely et al. (1987) improvements by up to a factor of ten are achieved, depending on the property or region. The EOS of Span and Wagner also represents properties near the critical point much more accurately and is recommended for pressures up to 800 MPa and temperatures up to 1100 K. [81]

Interestingly Bahadori (2008) notes:

“From a Process Engineer’s point of view utilizing a commercial soft-wares and using equations of state to predict properties is convenient and easy-to-use, but such approaches do not work equally very well for all properties. Experiences show that

equations of state are not suitable to predict thermal conductivities, viscosities and surface tensions ”[82]

The three major types of Equations of state that are commonly used for calculating the density of CO₂ are the Redlich-Kwong (RK-type), Benedict-Webb-Rubin (BWR-type), and Span-Wagner (SW-type) EOSs. The RK-type EOSs are modified to include the effect of temperature using the attractive term of the van der Waals EOS while BWR-type EOSs are multiple-parameter equations. The latter employ power series expansions to display the correlations with fluid pressure, volume, and temperature. SW-type EOSs which are known to accurately predict the density of CO₂ are based on the Helmholtz energy. [83]

4.4.2 Wang et al. (2015)

Although the published EOSs, such as the SW-EOS, with which the physical properties of CO₂ can be calculated from the triple-point temperature up to 1100 K at pressures up to 800 MPa, calculation errors remain. Wang et al. selected twelve commonly used EOSs and conducted a detailed study on their performance when applied to supercritical CO₂ density prediction. The study is based on density measurements ranges from 303 to 473 K and pressure from 3 to 60 MPa. [83]

In addition Wang et al. provide correction terms for the evaluated EOS and propose a simple to use of calculation method for supercritical CO₂ to determine the density at a known temperature and pressure. [83] A summary of the aforementioned EOSs is given in Table 4-7.

Table 4-7: Twelve commonly used EOSs. [83]

Name	Authors	Year	Type of equation
SRK	Soave	1972	SRK
SRK-Twu	Twu et al.	1995	SRK
PR	Peng and Robinson	1976	PR
PRSV	Stryjek and Vera	1986	PR
PR-Twu	Twu et al.	1995	PR
Twu-Sim-Tassone	Twu et al.	2002	RK
Zudkevitch-Joffee	Zudkevitch and Joffee	2004	RK
BWRS	Starling	1973	BWR
MBWR	Jacobsen Stewart	1973	BWR
Lee-Kesler	Lee and Kesler	1975	BWR
Span-Wagner	Span and Wagner	1996	SW
Sun-Kiselev-Ely	Sun et al.	2005	SW

Wang et al. identify three distinct regions in CO₂ density variations which become apparent when plotting the density versus the reduced temperature below a certain temperature. In the linear-growth interval (LGI) which is in the range $0.4 < p_r < 1$ and where the CO₂ has not yet become supercritical, density increases approximately linearly. For this interval the densities calculated with the use of the different EOSs agree with the measured values. The CO₂ density

increases abruptly in the he rapid-growth interval (RGI) where the fluid is in supercritical state which corresponds to a range of $1 < p_r < 10,596$ when $T_r > 1$. The density values calculated by using EOSs are all smaller than the measured ones in this region. Significant errors result with the largest absolute values being around 30%. There are also considerable calculation errors of up to 16% in the slow-growth interval (SGI) which corresponds to $p_r > 10.596$ and $T_r > 1$. [83]

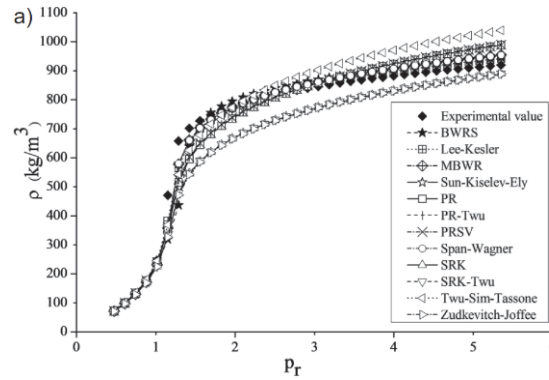


Figure 4-7: Variation curve for the density of supercritical CO₂ with reduced pressures when the reduced temperature is 1,03. [83]

Wang et al. claim to offer an accuracy improvement by providing the relative errors and introducing correction terms for every one of these intervals for the various different EOS in Reference [83]. Using the corrected Lee-Kesler, MBWR, Span-Wagner and Sun-Kiselev-Ely equations Wang et al. claim to restrict the relative error within 1.5 %.

Based on supercritical CO₂ density measurement data Wang et al. present a polynomial density calculation formula including 28 constant parameters as shown in Equation (4-45). The performance of the developed correlation is compared to the uncorrected EOS models and displayed graphically in Figure 4-8. [83]

$$\begin{aligned} \rho = & (a_1 T_r^3 + a_2 T_r^2 + a_3 T_r + a_4) p_r^6 + (b_1 T_r^3 + b_2 T_r^2 + b_3 T_r + b_4) p_r^5 \\ & + (c_1 T_r^3 + c_2 T_r^2 + c_3 T_r + c_4) p_r^4 + (d_1 T_r^3 + d_2 T_r^2 + d_3 T_r + d_4) p_r^3 \\ & + (e_1 T_r^3 + e_2 T_r^2 + e_3 T_r + e_4) p_r^2 + (f_1 T_r^3 + f_2 T_r^2 + f_3 T_r + f_4) p_r \\ & + (g_1 T_r^3 + g_2 T_r^2 + g_3 T_r + g_4) \end{aligned} \quad (4-45)$$

Supercritical CO₂ densities at known temperatures and pressures can be obtained through Equation (4-45) which is supposed to limit the average relative error of within 2.0% across the whole studied range, the interval RGI to within 1.3 %, and the interval SGI to within 0.8 %. The coefficients for Equation are given in Table 4-8.

The coefficients in Table 5 9 are not the same coefficients as given in the original paper by Wang et al. During the course of this thesis it was found that the correlation proposed by Wang et al did not deliver any realistic results. After this was brought to the authors attention new coefficients for the correlation equation were provided which are presented in Table 5 9.

This correlation can be applied in ranges of 303K to 473K and pressures from 3 to 60 MPa [83]. The density ρ is in kg/m^3 .

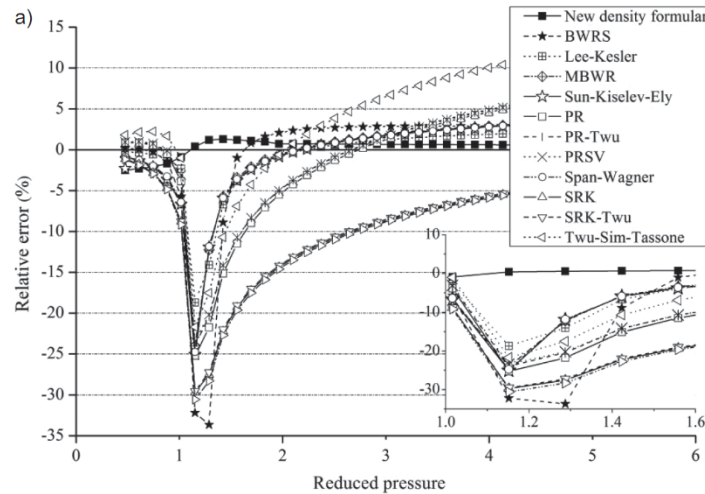


Figure 4-8: Variation curves for the relative errors of CO₂ density of various EOSs at a reduced temperature of 1.03. [83]

Table 4-8: Coefficients for Equation (4-45).

a ₁	104.99927	c ₁	2609.85387	e ₁	322904.61250	g ₁	126658.72654
a ₂	-268.74446	c ₂	-81317.55502	e ₂	-1109777.47493	g ₂	-454595.75086
a ₃	170.89810	c ₃	79364.40032	e ₃	1246290.30475	g ₃	538576.62754
a ₄	0.00000	c ₄	-23259.58953	e ₄	-455090.03042	g ₄	-21039.53100b1
b ₁	-2628.93255	d ₁	-128855.45993	f ₁	-365704.89550		
b ₂	755.01259	d ₂	425084.32981	f ₂	1294024.16922		
b ₃	-6379.90417	d ₃	-451931.52881	f ₃	-1507250.97083		
b ₄	132.32773	d ₄	152810.50157	f ₄	576924.52801		

4.4.3 Haghbakhsh et al. (2013)

Haghbakhsh et al. present a correlations for the prediction of supercritical carbon dioxide density based on the sensitivity analysis and mathematical regression using 1240 SC-CO₂ density data points. The proposed density model which requires the temperature and pressure as input is valid in a range of 308–523 °K and pressure between 75 and 468 bar. The coefficients for Equation (4-46) can be found in Table 4-9.[80]

$$\rho = \frac{A + B \ln(T) + C [\ln(T)]^2 + DP + EP^2}{1 + \ln(T) + G [\ln(T)]^2 + HP + IP^2} \quad (4-46)$$

where T, P and ρ are temperature (K), pressure (bar) and density (kg/m^3), respectively.

Table 4-9: Coefficients for Equation (4-46).[80]

A	153.3851466	F	-0.3524432
B	-53.044601	G	0.03140435
C	4.568413346	H	7.49768E-5
D	0.007191632	I	2.38083E-8
E	2.43117E-5		

Haghighbakhsh et al. report an absolute average relative deviation of 2.21% for their correlation as compared to 5.01% of the Bahadori et al correlation in a Temperature range of 308 to 433 °K and a pressure range from 75 to 468 bar. [80]

4.4.4 Bahadori et al. (2009)

The method developed by Bahadori et al. is a simple to use correlation as a function of temperature (T) and pressure (P). The correlation presented in Equation (4-47) was specifically developed for predicting supercritical carbon dioxide density and may be applied for pressures between 25 and 700 bar and temperatures between 293 and 433 °K. [79]

$$\rho = \alpha + \beta T + \gamma T^2 + \theta T^3 \quad (4-47)$$

where

$$\alpha = A_1 + B_1 P + C_1 P^2 + D_1 P^3 \quad (4-48)$$

$$\beta = A_2 + B_2 P + C_2 P^2 + D_2 P^3 \quad (4-49)$$

$$\gamma = A_3 + B_3 P + C_3 P^2 + D_3 P^3 \quad (4-50)$$

$$\theta = A_4 + B_4 P + C_4 P^2 + D_4 P^3 \quad (4-51)$$

The units of density is in kg/m³ while the temperature T is in °K and the pressure p is in bar. Table 4-10 provides the coefficients for the above equations.

Table 4-10: Coefficients for Equations (4-48) to (4-51). [79]

Coefficient	25 bar < P < 100 bar	100 bar < P < 700 bar
A ₁	2.089800972761597E5	1.053293651041897E5
B ₁	-1.456286332143609E4	-9.396448507019846E2
C ₁	2.885813588280259E2	2.397414334181339
D ₁	-1.597103845187521	-1.819046028481314E-3
A ₂	-1.675182353338921E3	-8.253383504614545E2
B ₂	1.16799554255704E2	7.618125848567747
C ₂	-2.31558333122805	-1.963563757655062E-2
D ₂	1.284012022012305E-2	1.497658394413360E-5
A ₃	4.450600950630782	2.135712083402950
B ₃	-3.10430147581379E-1	-2.02312885037391E-2
C ₃	6.157718845508209E-3	5.272125417813041E-5
D ₃	-3.420339567335051E-5	-4.043564072108339E-8
A ₄	-3.919844561756813E-3	-1.827956524285481E-3
B ₄	2.734973744483903E-4	1.768297712855951E-5
C ₄	-5.428007373890436E-6	-4.653377143658811E-8
D ₄	3.019572090945029E-8	3.586708189749551E-11

4.4.5 Ouyang (2011)

Based on CO₂ data supplied through the NIST database Ouyang developed a correlation as a function of temperature and pressure. It can be applied from 1100 to 9000 psia (7 to 62 MPa) and 40 to 100 °C (313 to 373 K).

$$\rho = A_0 + A_1p + A_2p^2 + A_3p^3 + A_4p^4 \quad (4-52)$$

$$A_i = b_{i0} + b_{i1}T + b_{i2}T^2 + b_{i3}T^3 + b_{i4}T^4 \quad (i = 0,1,2,3,4) \quad (4-53)$$

where the density ρ is in kg/m³, the pressure (p) in psia, and the temperature (T) in Celsius. The coefficients associated with the above equations are presented in Table 4-11.

Table 4-11: Value for b_{ij} coefficients in Equation (4-47) for pressures < 3000 Psia. [84]

	b ₁₀	b ₁₁	b ₁₂	b ₁₃	b ₁₄
i=0	2.148322085348E+05	1.168116599408E+04	-2.302236659392E+02	1.967428940167E+00	-6.184842764145E-03
i=1	4.757146002428E+02	-2.619250287624E+01	5.215134206837E-01	-4.494511089838E-03	1.423058795982E-05
i=2	-3.713900186613E-01	2.072488876536E-02	-4.169082831078E-04	3.622975674137E-06	-1.155050860329E-08
i=3	1.228907393482E-04	-6.930063746226E-06	1.406317206628E-07	-1.230995287169E-09	3.948417428040E-12
i=4	-1.466408011784E-08	8.338008651366E-10	-1.704242447194E-11	1.500878861807E-13	-4.838826574173E-16

Table 4-12: Value for b_{ij} coefficients in Equation (4-47) for pressures > 3000 psia. [84]

	b_{10}	b_{11}	b_{12}	b_{13}	b_{14}
i=0	6.897382693936E+02	2.730479206931E+00	-2.254102364542E-02	-4.651196146917E-03	3.439702234956E-05
i=1	2.213692462613E-01	-6.547268255814E-03	5.982258882656E-05	2.274997412526E-06	-1.888361337660E-08
i=2	-5.118724890479E-05	2.019697017603E-06	-2.311332097185E-08	-4.079557404679E-10	3.893599641874E-12
i=3	5.517971126745E-09	-2.415814703211E-10	3.121603486524E-12	3.171271084870E-14	-3.560785550401E-16
i=4	-2.184152941323E-13	1.010703706059E-14	-1.406620681883E-16	-8.957731136447E-19	1.215810469539E-20

Ouyang claims a very good agreement with the NIST data and the AREs for the proposed correlation are within +0.1% and -0.1%. [84] However it should be noted that the NIST data for CO₂ was generated through various EOS and correlations itself. Therefore the inherent uncertainties associated with the NIST data have to be taken into consideration.

4.5 Supercritical CO₂ heat capacity

Data for the heat capacity is available through the NIST WebBook database. However, no simple to use correlation or methods specifically developed for the prediction of the supercritical CO₂ heat capacity was found during the course of this research.

5 Evaluation and comparison

Selected Correlations from the previous chapters that offer simple to use models usually based on temperature, pressure, density and specific gravity dependent equations have been programmed in Microsoft Excel using Visual Basic. The programmed models are therefore readily available and can be accessed directly or be easily implemented into further MS Excel programs. Checking the applicable range is simple and evaluation of the different models is possible by using the tools in MS excel

The obtained correlation results are plotted against the respective NIST data which is used as a reference database for this study. For validation the data provided by NIST is also checked against experimental literature data for the CO₂ properties. The average relative errors of the different models are then displayed as a function of pressure and temperature.

Evaluation studies on pseudocritical properties, natural gas viscosity and CO₂ viscosity are available from the literature and the main findings of those studies are provided in a summarized form and are a part of this evaluation. A summary and ranking of all the evaluated correlation models, their respective performance and accuracy, is presented in the final section of this chapter in Table 5-6 to Table 5-14.

5.1 Natural gas correlation models

5.1.1 Pseudocritical properties correlations

A comprehensive evaluation study of z-factor, viscosity and pseudocritical properties correlations, can be found in McCain et al (2011) [15]. Data from 1434 PVT reports of worldwide origin resulting in 6000 lines of data that included variables was used. 145 samples contained more than 50 mol% non-hydrocarbons, 1214 gas samples had 5 mol% non-hydrocarbons or more and over three-quarters of the gases contained some non-hydrocarbon components. Regarding the pseudocritical correlations, the evaluation is limited to gas specific gravity correlations and does not include those based on mixing rules. The authors point out that the accuracies of the predicted properties are about the same regardless of which of the two types of correlations is used. Furthermore the gas specific gravity can be readily calculated when the gas composition is available. Table 5-1 and Figure 5-1 indicate that the Piper et al. correlations delivers the best results while the Sutton (2007) method in combination with the Wichert and Aziz correction is basically equivalent. [15]

Figure 5-5 and Figure 5-6 show the performance of pseudocritical temperature correlations which were programmed in the course of this study. It is evident that most of the correlations result in very similar predictions, especially in the lower specific gas gravity range. The plotted correlation results are representative for a natural gas mixture containing no non-hydrocarbon impurities.

Sutton (2007) [14] evaluated the accuracy of different pseudocritical properties - specific gas gravity correlations for varying amounts of CO₂ H₂S and N₂ in mixtures with methane to determine the suitability of each method. The following correlations were included: Standing

(1981), Sutton (1985), Piper (1993) Elsharkawy (2000) and Sutton (2005). The critical properties derived from the Standing and Sutton correlation were adjusted through the Wichert and Aziz correction. Sutton states:

“At low levels of impurities, all of the methods perform reasonably well, but errors can increase dramatically in the Piper or Elsharkawy methods as the non-hydrocarbon content level increases. Clearly, the modifications proposed by Wichert and Aziz are superior compared with the other available methods.” [14]

McCain et al [15] present a table displaying the average relative errors (ARE) and average absolute relative errors (AARE) of gas z-factor correlations compared with gases with non-hydrocarbon components. The Sutton (2007) correlation is the most accurate followed by the Piper et al. and Standing correlation as displayed in Table 5-2.

For this study the Piper et al., the Standing and the Sutton (2007) (the latter two including the correction by Wichert and Aziz (1972)) pseudocritical correlations are displayed as a function of the specific gas gravity for a hypothetical gas mixture containing 10% H₂S, 10% CO₂ and 5% N₂ in Figure 5-7 and Figure 5-8. As Sutton indicates, the Piper et al. correlation clearly shows a different behaviour when applied to gases with a relatively high non-hydrocarbon content.

Table 5-1: Relative errors of several gas z-factor correlations based on gas specific gravity. The Sutton (2007) correlations include the Wichert-Aziz correlation for hydrogen sulphide and carbon dioxide. [15]

Pseudocritical properties correlation	Z-factor correlation	ARE, % Error, %	AARE, % Relative Error, %
Piper et al. (1999)	Hall-Yarborough (1973)	0.307	1.562
Piper et al. (1999)	Dranchuk-Abou-Kassem (1975)	0.296	1.590
Piper et al. (1999)	Brill-Beggs (1974), (1977)†	-0.253	1.731
Sutton (2007)*	Hall-Yarborough (1973)	-0.548	1.621
Sutton (2007)*	Dranchuk-Abou-Kassem (1975)	-0.422	1.511
Elsharkawy-Elkamel (2000)	Dranchuk-Abou-Kassem (1975)	0.010	1.821
Elsharkawy-Elkamel (2000)	Hall-Yarborough (1973)	-0.014	1.812
Standing (1977)*	Hall-Yarborough (1973)	-1.084	1.968
Standing (1977)*	Dranchuk-Abou-Kassem (1975)	-1.010	1.949
Standing (1977)*	Brill-Beggs (1974), (1977) †	-1.609	2.320
Elsharkawy et al. (2000)	Hall-Yarborough (1973)	1.200	2.434
Elsharkawy et al. (2000)	Dranchuk-Abou-Kassem (1975)	1.185	2.452
Sutton (1985)*	Dranchuk-Abou-Kassem (1975)	1.746	2.878
Sutton (1985)*	Hall-Yarborough (1973)	1.769	2.887
Londono et al. (2005)	Dranchuk-Abou-Kassem (1975)	-1.044	3.254
Piper et al. (1999)	Nishuimi-Saito (2005)‡	5.646	5.911
Londono et al. (2005)	Nishuimi-Saito (2005) ‡	5.157	6.432
Piper et al. (1999)	Papay (1968)	15.113	16.166

Sutton also points out the importance of selecting the correct gas pseudocritical-property model i.e. gas condensates and associated gas correlations for high-gas-gravity scenario

gases. However the differences in the pseudocritical-property relationships are not significant and too small to create substantial errors in calculated Z factors for gases hydrocarbon-gas gravities less than 0.75 to 0.8. [14] This can also clearly be seen in Figure 5-5 in Figure 5-6. A graphical representation of Sutton's findings concerning non-hydrocarbon impurities is presented in Figure 5-2 to Figure 5-4.

Table 5-2: Average relative errors (ARE) Average absolute relative errors (AARE) of gas Z-factor correlations compared with gases with non-hydrocarbon components. [15]

Correlation	H ₂ S>5mol%		CO ₂ >5mol%		N ₂ >5mol%		H ₂ S+CO ₂ +N ₂ >10mol%	
	ARE	AARE	ARE	AARE	ARE	AARE	ARE	AARE
Sutton (2007)	-0.7	1.9	0.1	1.7	-0.8	2.1	-0.2	1.9
Piper et al. (1999)	1.9	2.9	0.6	1.8	0.3	2.7	0.6	2.2
Standing (1977)	-0.5	2.0	-0.3	2.2	-1.5	2.6	-0.4	2.2
Elsharkawy-Elkamel (2000)	1.3	2.8	-1.0	2.8	-3.9	4.7	-2.1	4.0
Londono et al. (2005)	9.7	13.5	-1.2	6.0	-2.5	6.5	-0.1	8.4
Elsharkawy et al. (2000)	16.6	17.4	2.9	4.4	-0.1	4.7	4.8	7.9
Sutton (1985)	30.4	30.6	6.6	6.8	1.7	4.5	11.5	12.6

Elsharkawy and Elkamel [33] also provide a review of the correlations based on gas composition and mixing rules as well as methods based on gas gravity. The methods were compared using sour gas data containing an average mole fraction of 7.45% H₂S and 4.04% CO₂. The results are summarized in Table 5-3. For methods based on gas composition the best accuracy and correlation coefficient is reported for the Piper et al. and Corridor et al. correlations, while for the methods based on gas gravity, the Sutton and Elsharkawy et al. Methods were the most accurate. [33]

Table 5-3: Accuracy of correlations using compositional data and gas gravity correlations. [33]

Method	ARE	AAD	SD	Coefficient. of correlation
Standing	-0.81	3.50	6.79	92.08
Sutton	-1.72	3.47	7.14	91.43
Elsharkawy et al.	-2.25	3.48	7.30	91.23
Elsharkawy and Elkamel	-0.26	1.69	3.12	97.66
Based on compositional data				
Kay- Wichert & Aziz	0.69	1.38	2.13	98.57
SSVB- Wichert & Aziz	0.65	2.14	2.85	97.65
Corredor et. al	0.25	1.36	2.51	98.8
Piper et. al	0.31	1.21	1.92	99.10

Comparing the evaluation results on the accuracy of the various pseudocritical property correlations presented by Elsharkawy and Elkamel (2000) [33], Sutton (2007) [14], McCain et al.(2011) [15], the Sutton (2007) correlation in combination with Wichert and Aziz non-hydrocarbon correction method stands out as one of the best. It is therefore recommended to employ this method for the estimation of the pseudocritical temperature and pressure.

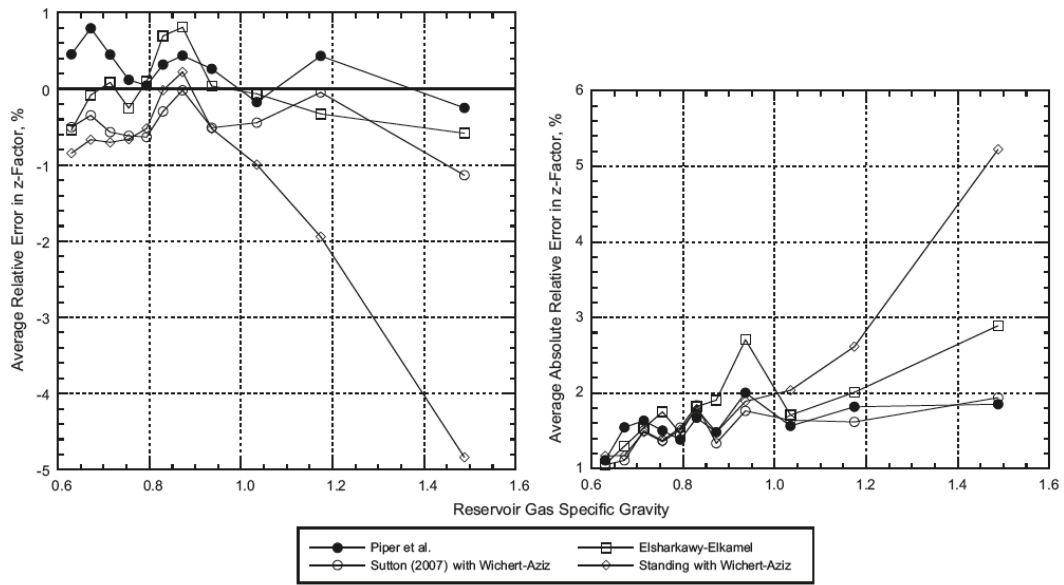


Figure 5-1: Comparisons of relative errors in gas z-factor correlations using data split by gas specific gravity. [15]

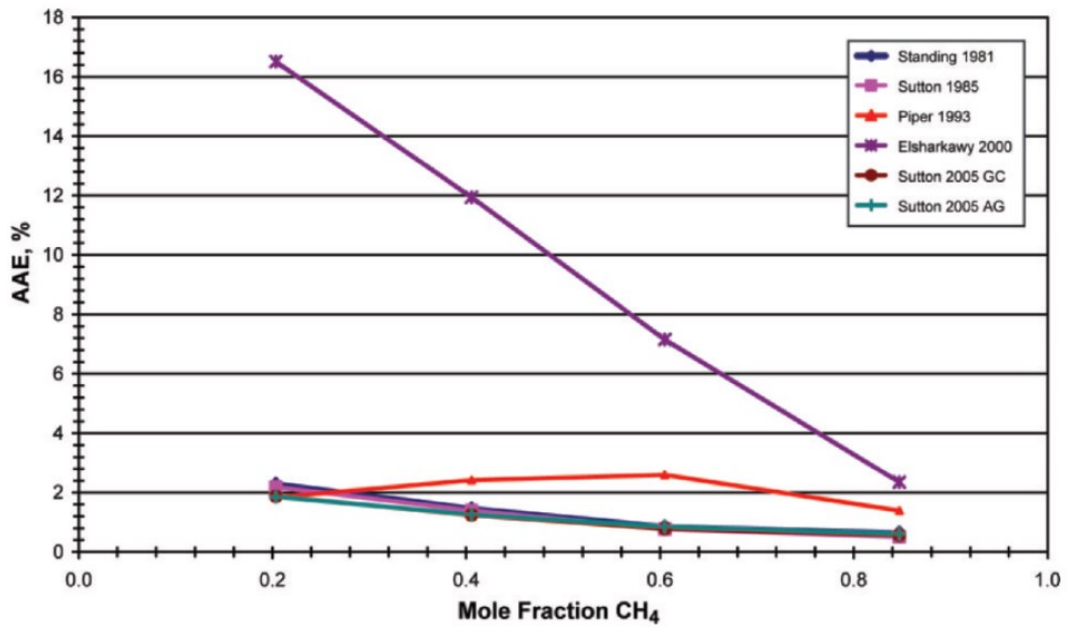


Figure 5-2: Error in calculated z factor from DAK for CH₄/H₂S mixture. [14]

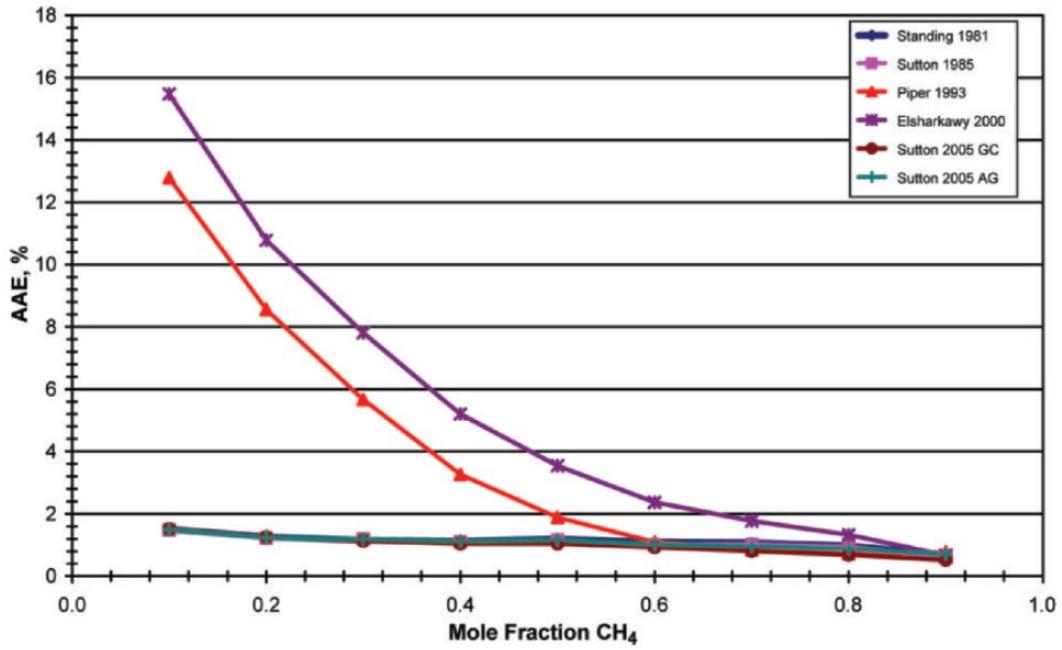


Figure 5-3: Error in the calculated z-factor from DAK for CH₄/CO₂ mixture. [14]

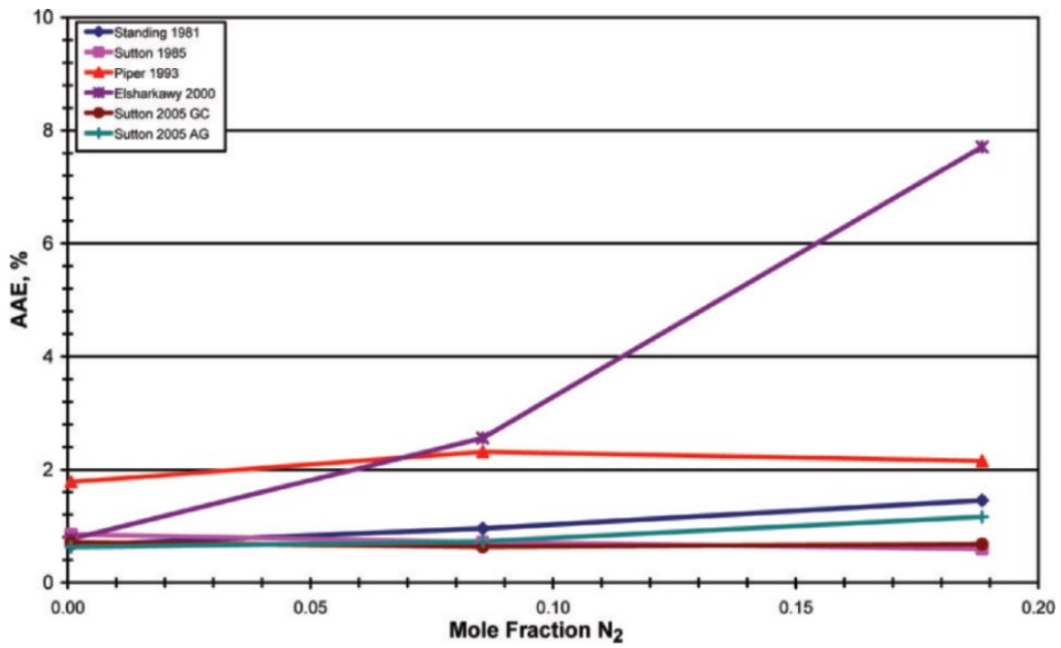


Figure 5-4: Error in the calculated z-factor from DAK for varying levels of N₂. [14]

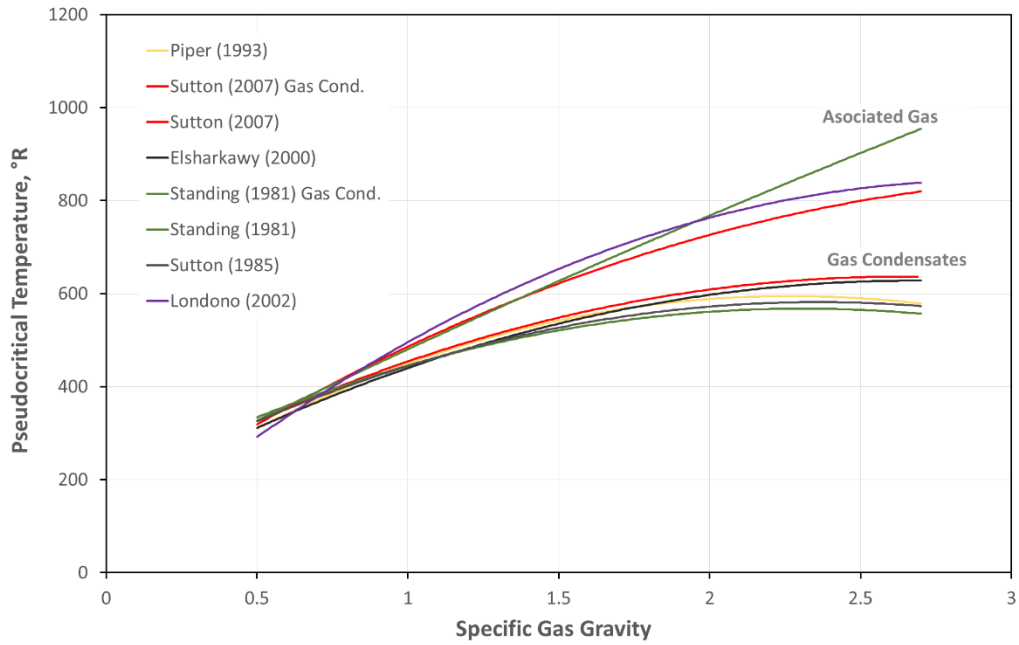


Figure 5-5: Pseudocritical temperature correlations as a function of the specific gas gravity.

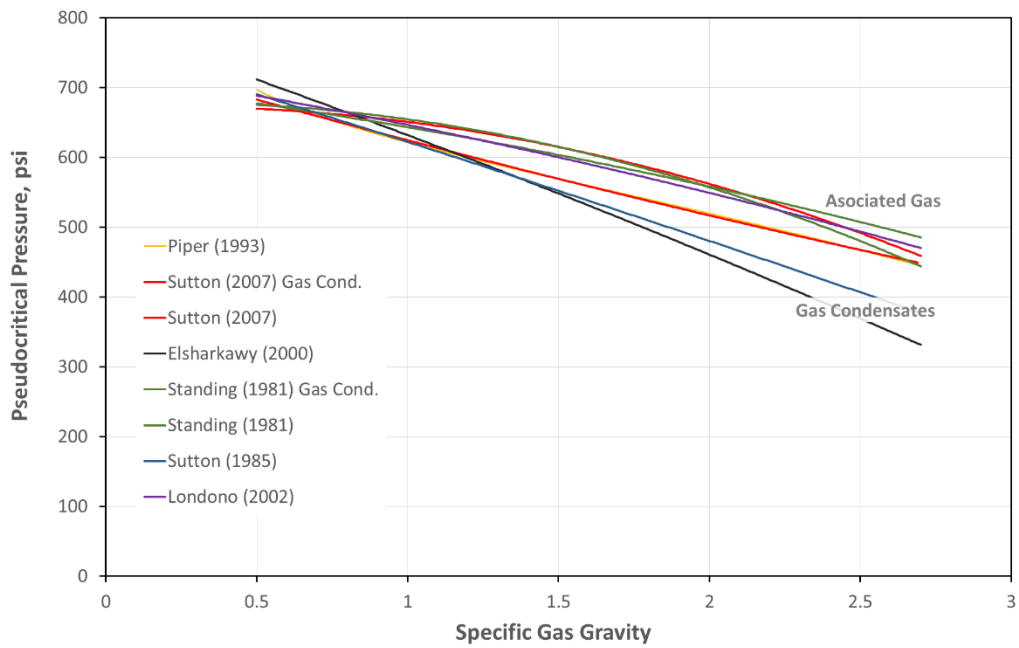


Figure 5-6: Pseudocritical pressure correlations as a function of the specific gas gravity.

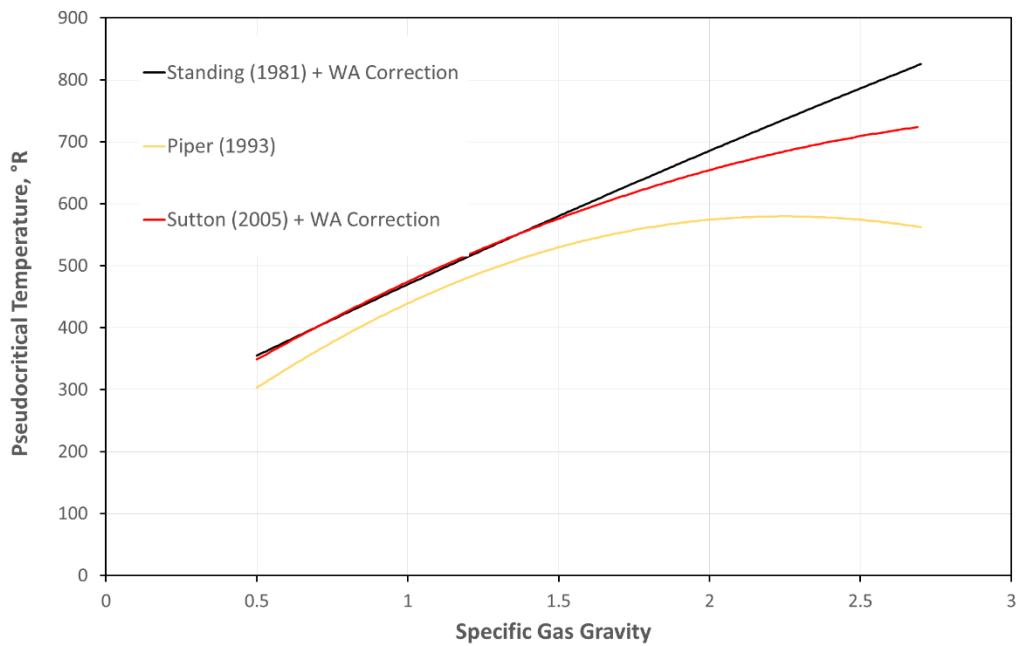


Figure 5-7: Pseudocritical temperature correlations including the correction by Wichert and Aziz (1972) as a function of the specific gas gravity for a hypothetical gas mixture containing 10% H₂S, 10% CO₂ and 5% N₂.

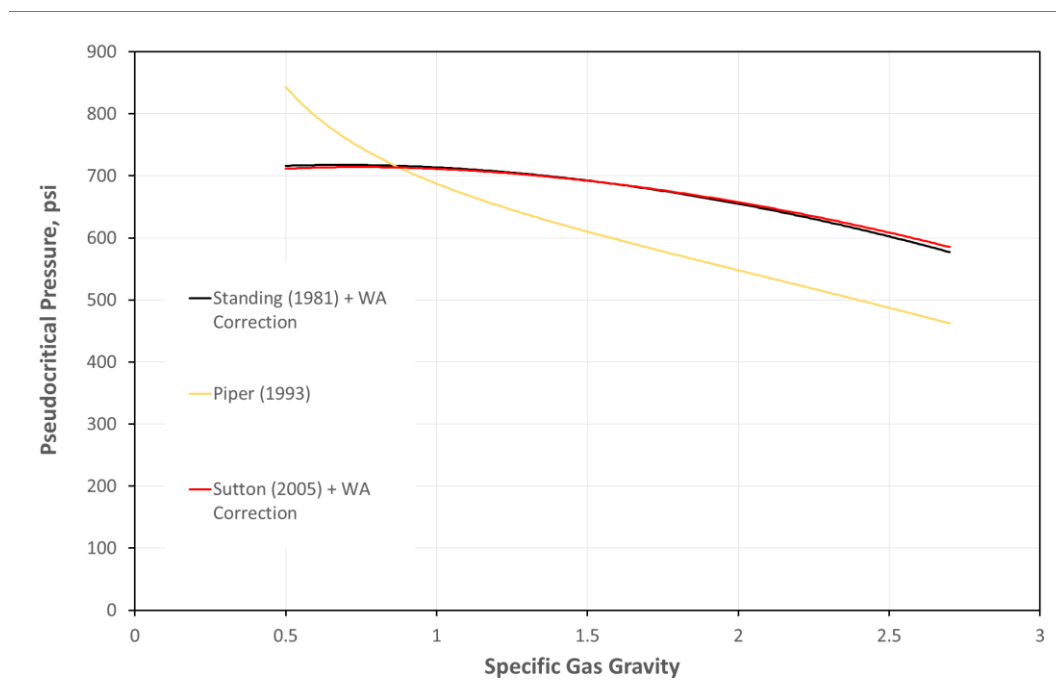


Figure 5-8: Pseudocritical pressure correlations including the correction by Wichert and Aziz (1972) as a function of the specific gas gravity for a hypothetical gas mixture containing 10% H₂S, 10% CO₂ and 5% N₂.

5.1.2 Dynamic viscosity of natural gas mixtures

McCain et al. [15] evaluated some commonly used gas viscosity equations for eight naturally occurring petroleum gases using 243 data points. This data covers temperature and pressure ranges from 200 to 8000 psi and 100 to 340 °F, respectively. The mean gas specific gravity is 0.66 and non-hydrocarbon impurities such as carbon dioxide do not exceed 0.1%. It is noted

that the data indicates dry gases and that no gas viscosity data for gas condensates appears to be available. The Piper et al. correlation was used to estimate pseudocritical properties while the DAK equation was used to estimate z-factor for cases where the density was needed. For high pressure high temperature gases McCain [15, p. 29] recommends the correlation developed by Viswanathan (2007) [51]. The correlations proposed by Jossi et al. and the Dean and Stiel equations were found to have a discontinuity at a pseudoreduced temperature of 1.5 which is the expected temperature region for petroleum reservoirs at moderate to higher pressures. Those two correlations were therefore not included by McCain. [15] The evaluated correlations and their relative errors are given in Table 5-4 and Figure 5-9 shows a comparison of relative errors as a function of temperature.

Sanaei et al. [42] evaluated different gas correlations for gases with up to 4.8% non-hydrocarbon content and found the LGE and their own correlation to have the best performance.

Chen and Ruth [20] indicate that the Gurbanov and Dadash-Zade [50] model best represents gas viscosity at atmospheric pressure and the viscosity ratio equation by the same researchers presents a “relatively fair match” with CKB data. Concerning non-hydrocarbon impurities Chen and Ruth [41] recommend using Standings correction. They also state that the greatest errors when calculating the viscosity may be introduced from the pseudocritical properties parameters. Therefore it is absolutely necessary to apply the Wichert and Aziz rule for non-hydrocarbon correction if compositional data is available. [41]

Table 5-4: Relative errors of the gas viscosity correlations evaluated by McCain et al. [15, p. 22]

Viscosity correlation	ARE, %	AARE, %
Lee et al. (1966)	-1.60	2.26
Londono et al. (2005)	-2.66	3.08
Sutton (2007)	2.05	3.10
Poling et al. (2001)	-0.61	3.34
Lee et al. (1964)	-3.23	3.70
Carr et al. (1954)	-9.81	9.81

The method proposed by Sutton 2007 [14] is based on a combination of the Poling et al. (2001) [10] and LGE method. The LGE equations were selected as a basis for the viscosity ratio calculation because of its simplicity and acceptability by the petroleum industry. Several other correlations are based on the LGE equations. These include the Elsharkawy (2006) [18] and Viswanathan (2007) [51] correlations and one method proposed by Londono et al. (2005) [34].

Figure 5-10 shows a comparison of the LGE and Londono et al. methods which both rank as the most accurate in the study presented by McCain et al. [15] The correlation results are plotted for gas pressures of 10, 20 and 40 MPa as a function of temperature.

Figure 5-11 compares the LGE and the Gurbanov and Dadash-Zade (1986) correlation which is not included in the table presented by McCain et al. Both correlations display a similar behaviour. Compared to the LGE correlation the Gurbanov and Dadash-Zade method does not require the density as an input. This may be seen as an advantage since the density has to be calculated through an EOS in the other cases.

Both the LGE and Gurbanov and Dadash-Zade correlations are simple to apply and are recommended for calculating the dynamic viscosity of natural gas mixtures. Based on the results described above the LGE is the most accurate.

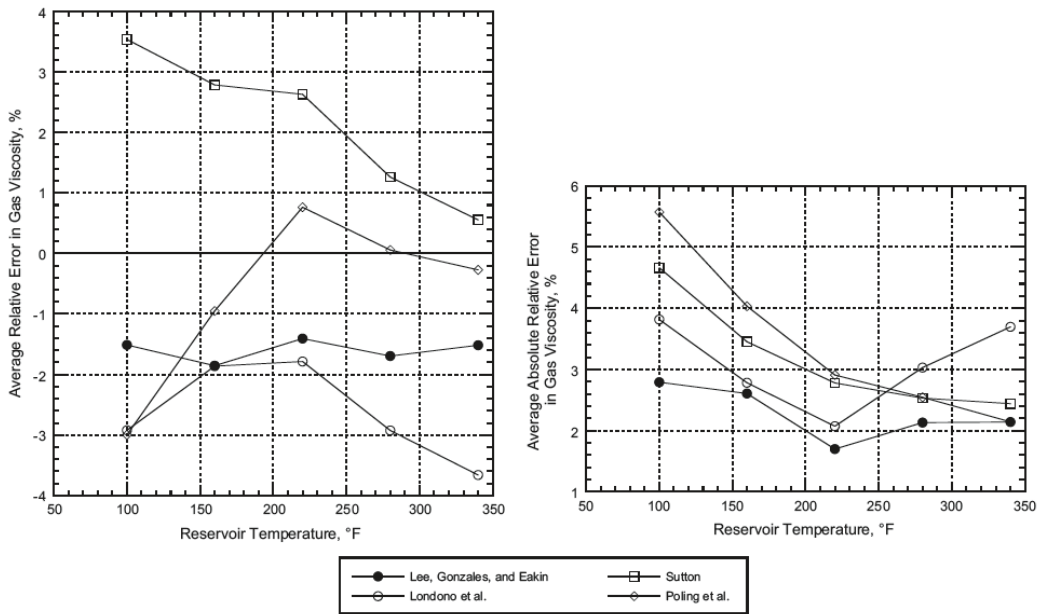


Figure 5-9: Comparisons of relative errors in gas viscosity correlations as a function of temperature. [15, p. 23]

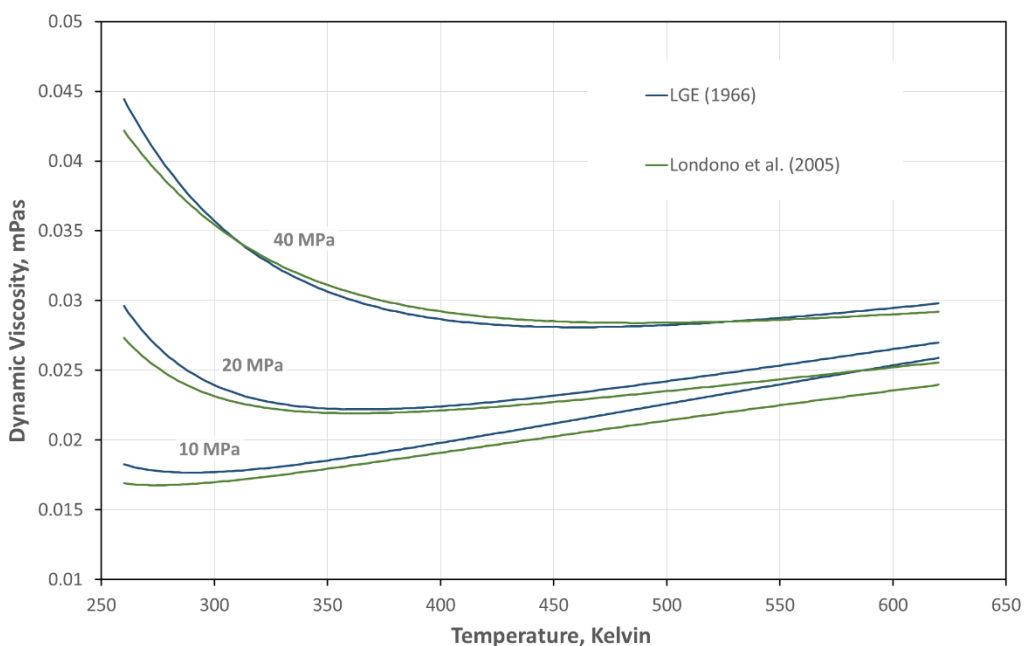


Figure 5-10: Comparisons of the LGE and Londono et al. gas viscosity correlations as a function of temperature.

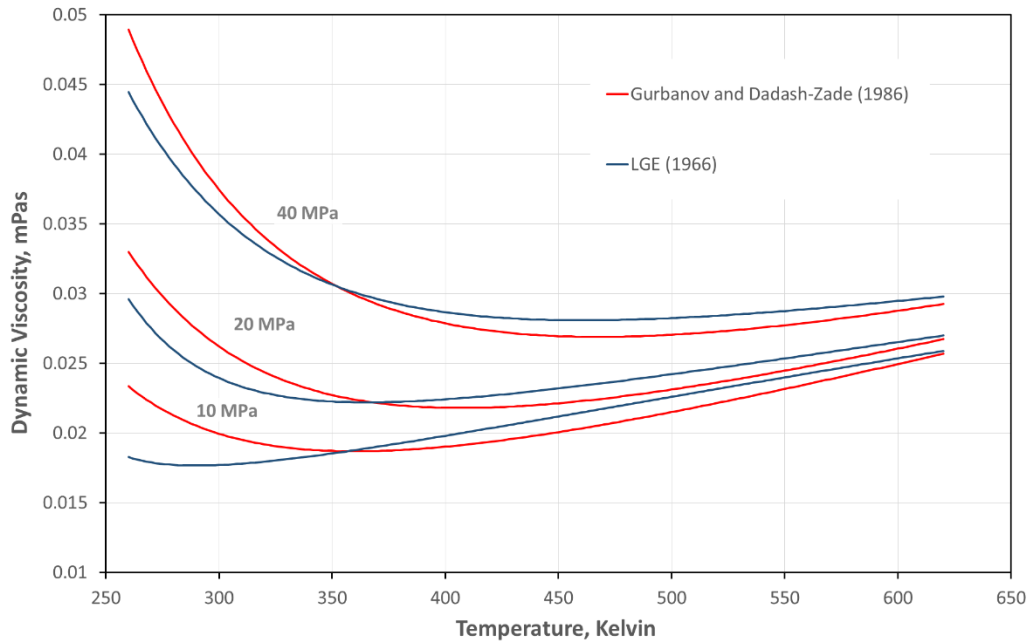


Figure 5-11: The LGE and Gurbanov and Dadash-Zade gas viscosity correlations as a function of temperature.

5.1.3 Thermal conductivity of natural gas mixtures

The Jarrahan and Heidaryan (2014) method to calculate the thermal conductivity of a natural gas mixture is simple to apply and was therefore selected for further investigation. It uses the specific gas gravity temperature and pressure as input parameters and contains corrections for CO_2 and N_2 . Figure 5-13 shows a comparison of correlation results with experimental data published by Pátek et al. (2003) [57] for a gas mixture composed of approximately 50% CH_4 and 50% CO_2 . While the general trend is represented by the model data there is only a modest match with the experimental values.

A comparison of the correlation results with methane thermal conductivity data obtained from the NIST WebBook [25] is displayed in Figure 5-12. Especially when looking at the lower temperature and also higher pressure areas it is clear that correlation performs poorly compared to the NIST data. Figure 5-15 and Figure 5-14 show the ARE and AARE in reference to the NIST data as a function of temperature and pressure. The overall ARE is 5.02% and the AARE is 8.55% for the entire recommended correlation range.

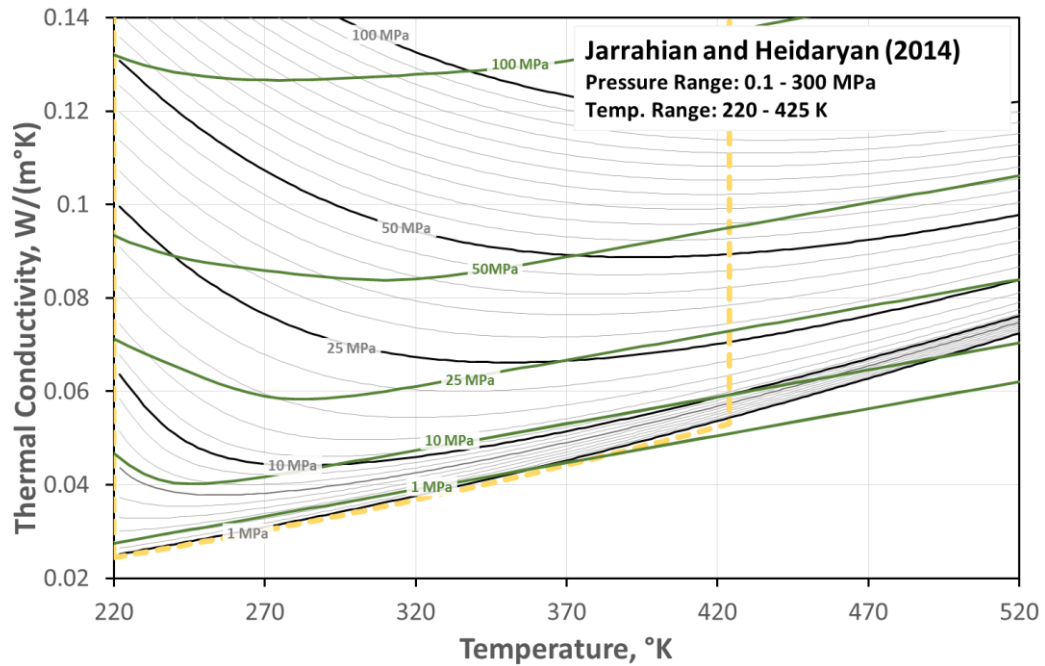


Figure 5-12: Comparison of the correlation results with methane data obtained from the NIST WebBook. The Jarrhian and Heidaryan correlation results are displayed in green for selected isobars. The yellow dotted line represents the range as recommended by the authors.

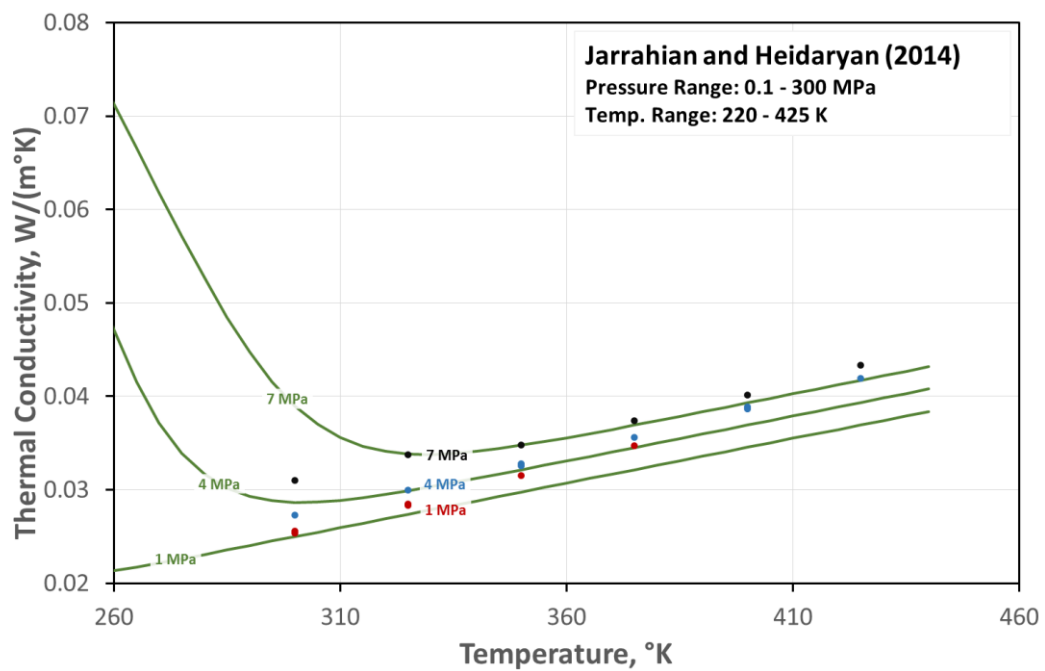


Figure 5-13: Comparison of the correlation results with data from Pátek et al for $x_{\text{CH}_4} = 0.4994$ and $x_{\text{CO}_2} = 0.5006$. The Jarrhian and Heidaryan correlation results are displayed in green for 1, 4 and 7 MPa.

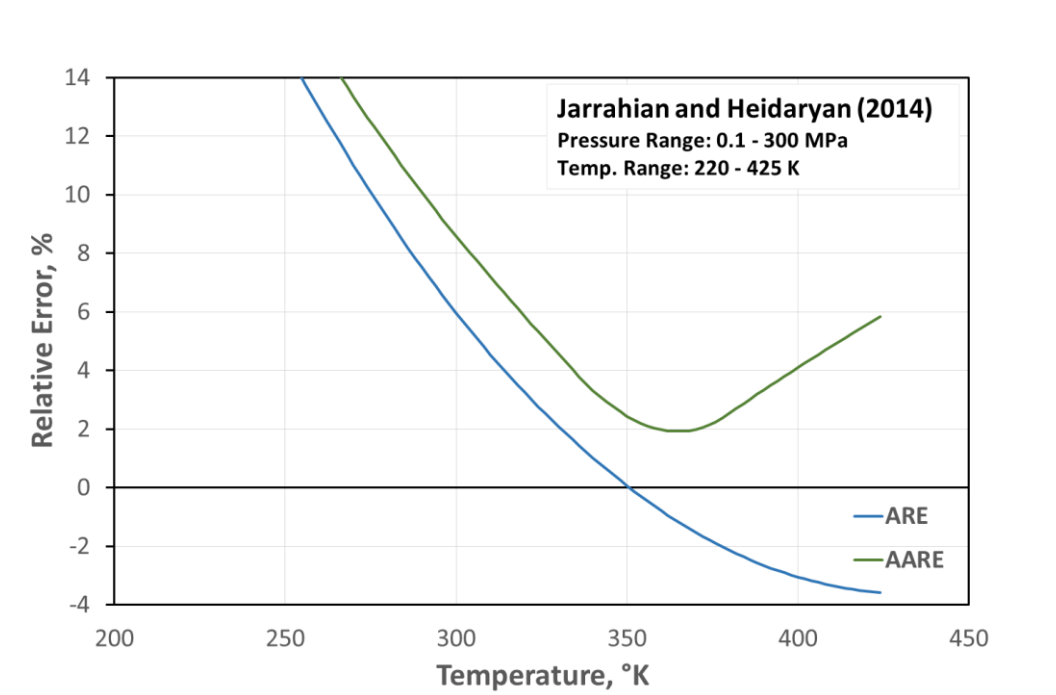


Figure 5-14: The average relative error (ARE) and absolute relative error (AARE) as a function of temperature for the thermal conductivity correlation developed by Jarrahan and Heidaryan (2014).

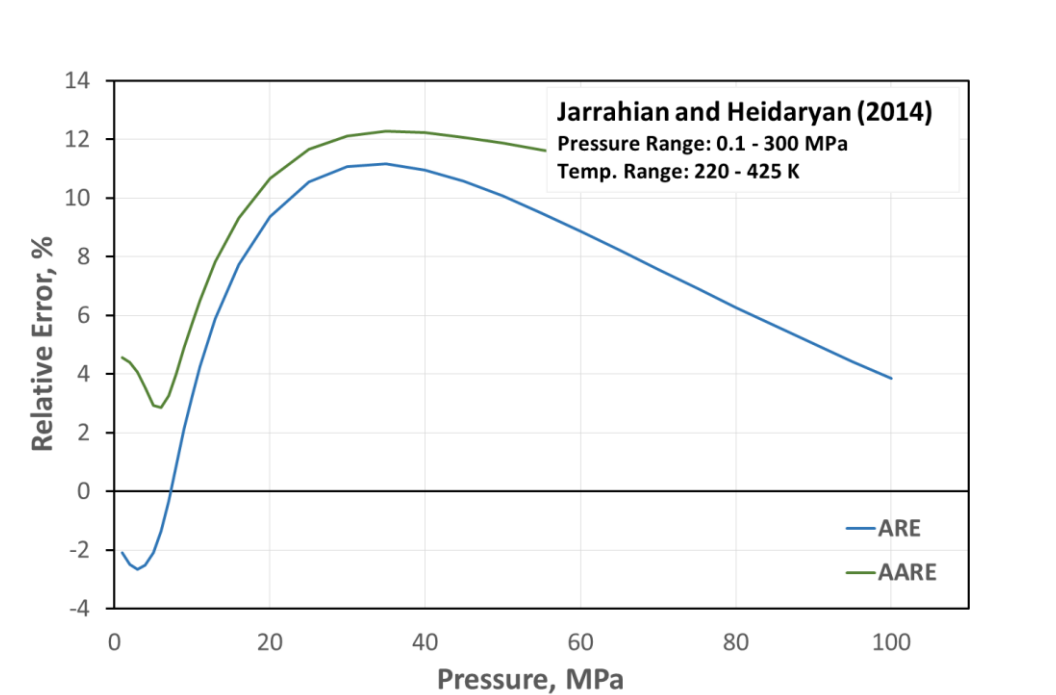


Figure 5-15: The average relative error (ARE) and absolute relative error (AARE) as a function of pressure for the thermal conductivity correlation developed by Jarrahan and Heidaryan (2014).

5.1.4 Heat capacity of natural gas mixtures

The methods presented by Moshfeghian (2011) [67] and Lateef and Omeke (2011) [69] were selected because of their simplicity. Both models only require the specific gas gravity, temperature and pressure to calculate the isobaric heat capacity of a natural gas mixture. The

method proposed by Lateef and Omeke however did not yield any representative results. That leaves the method proposed by Moshfeghian which is presented in Figure 5-16. The correlation model results are compared to methane data obtained through the NIST [25] data base. It can be seen there is only a modest match over a considerable part of the recommended range. The accuracy decreases for higher pressures and lower temperatures as showed by ARE and AARE development in Figure 5-18. In reference to the NIST data the overall ARE and AARE is 0.61% and 2.41 % respectively.

It is important to point out that Moshfeghian states a specific gas gravity range of 0.6 to 0.8 in which his correlation can be applied. The comparison with methane (specific gravity of 0.55) may therefore not be precise. However no other gas heat capacity data within the specified range was available for comparison.

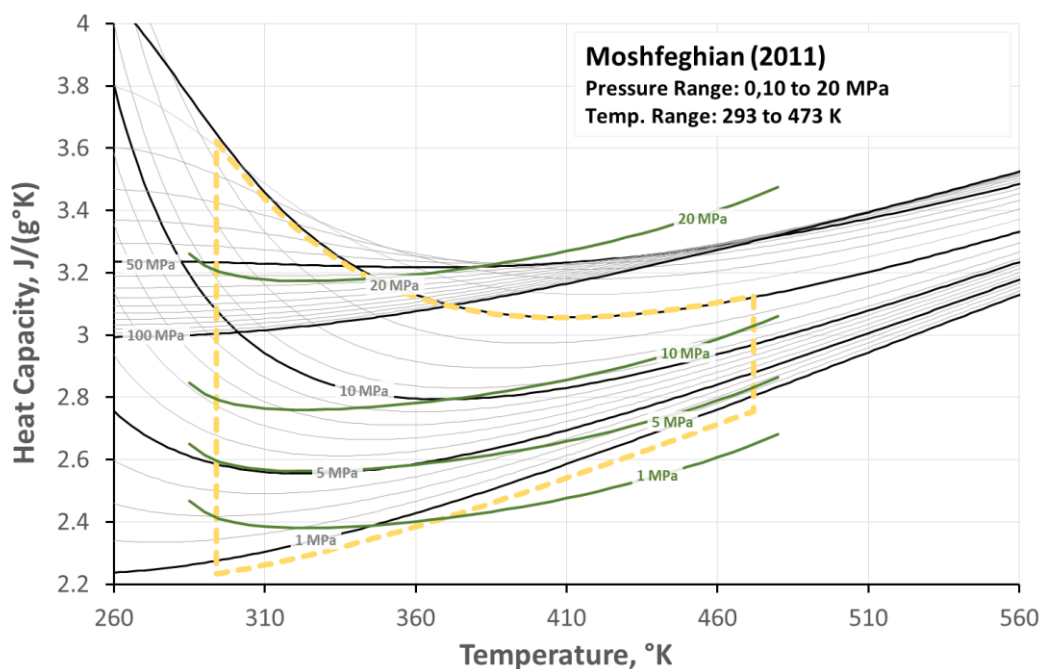


Figure 5-16: Comparison of the correlation results with NIST data. The Ouyang (2011) isobaric heat capacity correlation results are displayed in green for selected isobars. The yellow dotted line represents the range as recommended by the author.

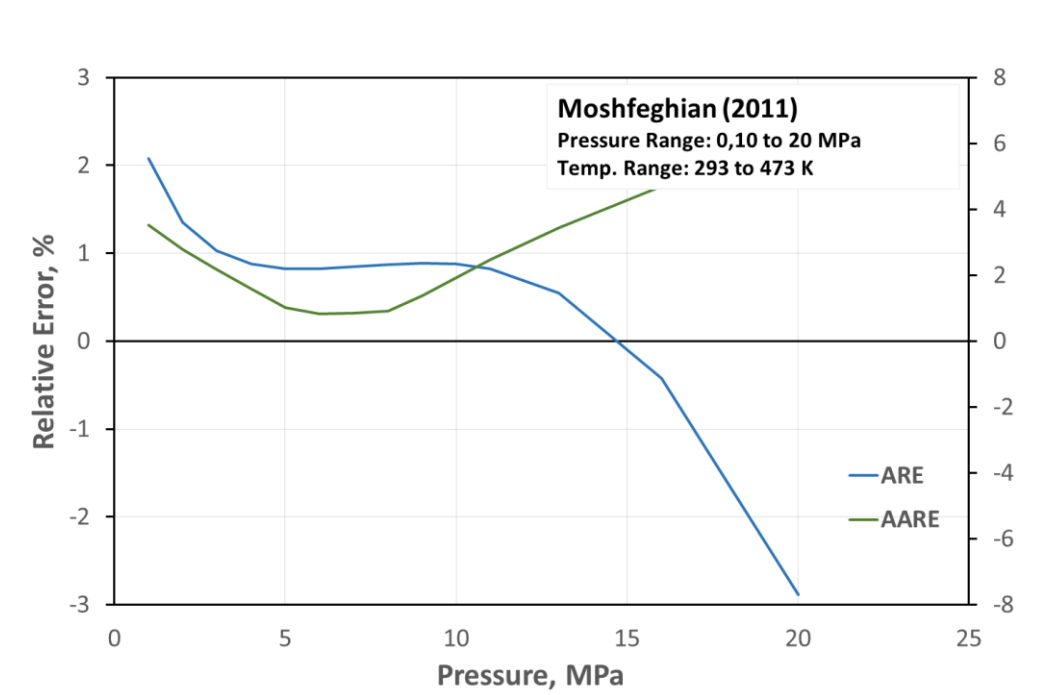


Figure 5-17: The average relative error (ARE) and absolute relative error (AARE) as a function of pressure for the isobaric heat capacity correlation developed by Moshfeghian (2011).

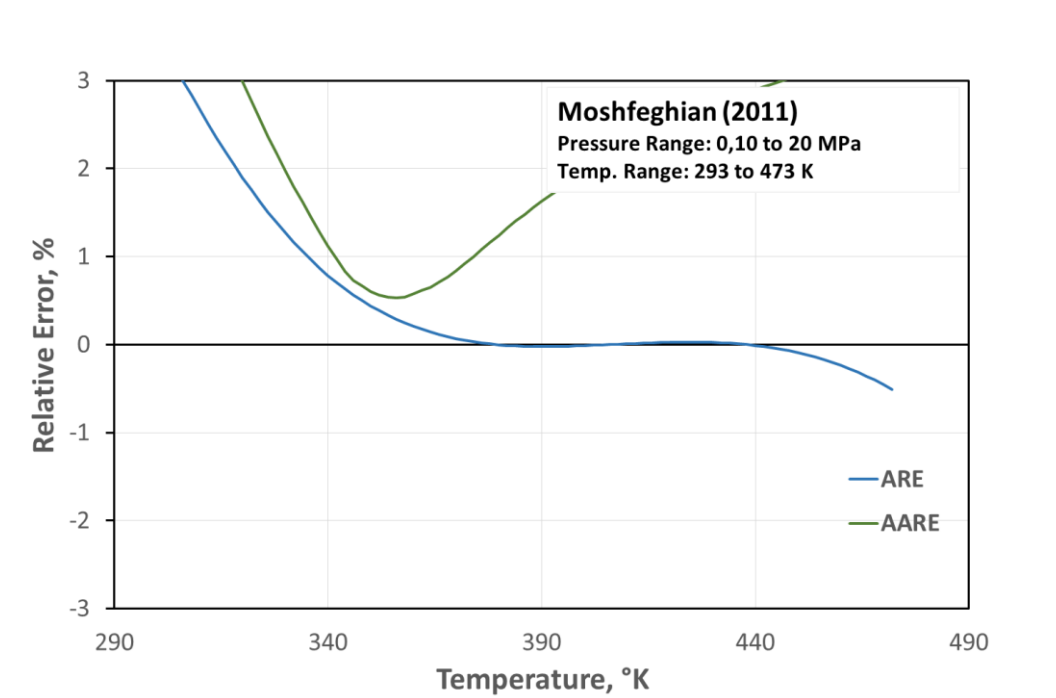


Figure 5-18: The average relative error (ARE) and absolute relative error (AARE) as a function of temperature for the isobaric heat capacity correlation developed by Moshfeghian (2011).

5.2 CO₂ correlation models

5.2.1 CO₂ viscosity correlation models

Heidaryan et al. present a comparison between different correlations that can be applied to supercritical CO₂. The investigated models are: Stephan and Lucas [71], Chung et al. [58], Lennard–Jones model [73], Bahadori and Vuthaluru [7] and the correlation proposed by Heidaryan et al [76]. The results are summarized in Table 5-5

Heidaryan et al. conclude that Bahadori and Vuthaluru correlation has the best results for isotherms from 370 °K to 450 °K, while for isotherm from 460 °K to 830 °K, the Heidaryan et al. approach delivers the least error. For temperature higher than 840 K the modified LJ has the best results. [76]

Table 5-5: Summary of AAREs for five different models and the proposed correlation versus validation data as presented by Heidaryan et al. [76] *The Bahadori and Vuthaluru correlation is only valid in a range from 260K to 450K as well as a pressure range between 10 MPa and 70 MPa. The presented AARE for that model was calculated as an average of the individual AAREs values within that range.

Validation data		AARE in % of the proposed thermal conductivity correlations					
Data base	Temperature and pressure range	Lucas	Chung et al.	LJ	Modified LJ	Bahadori and Vuthaluru	Heidaryan et al.
Pensado et al.	313-353 K 20-60 MPa	4.87	6.44	4.89	5.12	2.03	1.45
Heidaryan et al.	313.15K- 523.15K 7.7-81.1 MPa.	5.96	5.18	4.88	4.71	1.68*	1.71
Stephan and Lucas	310–900K 7.5–101.4 MPa	6.34	6.59	4.27	4.21	2.47*	3.64
NIST web book.	310–900K 7.5-101.5 MPa.	7.02	3.51	5.24	4.69	1.36*	1.82

For this study two viscosity models, the Bahadori and Vuthaluru and the Heidaryan et al models are compared to the NIST data. The reference data obtained through the NIST Chemistry WebBook [25] is validated by cross checking it with CO₂ experimental results provided by Stephan and Lucas (1979) [71]. The measured viscosities are available up to a pressure of 100 MPa and are generally in good agreement with the NIST data as displayed in Figure 5-19. The NIST webpage states that the uncertainty in viscosity ranges from 0.3% in the dilute gas near room temperature to 5% at the highest pressures.

The Bahadori and Vuthaluru (2009) [7] correlation shows consistently accurate results across the higher pressure ranges and is most accurate in the 15 to 25 MPa pressure region where it is in very good agreement with the reference data. There are some deviations in region of the

lower range boundary especially for temperatures below 340 °K as can be seen in Figure 5-20. This is also represented by the average relative error (ARE) and absolute average relative error (AARE) which is plotted against pressures within the given range and displayed in Figure 5-21. The overall ARE and AARE is -1.23% and 1.9% respectively.

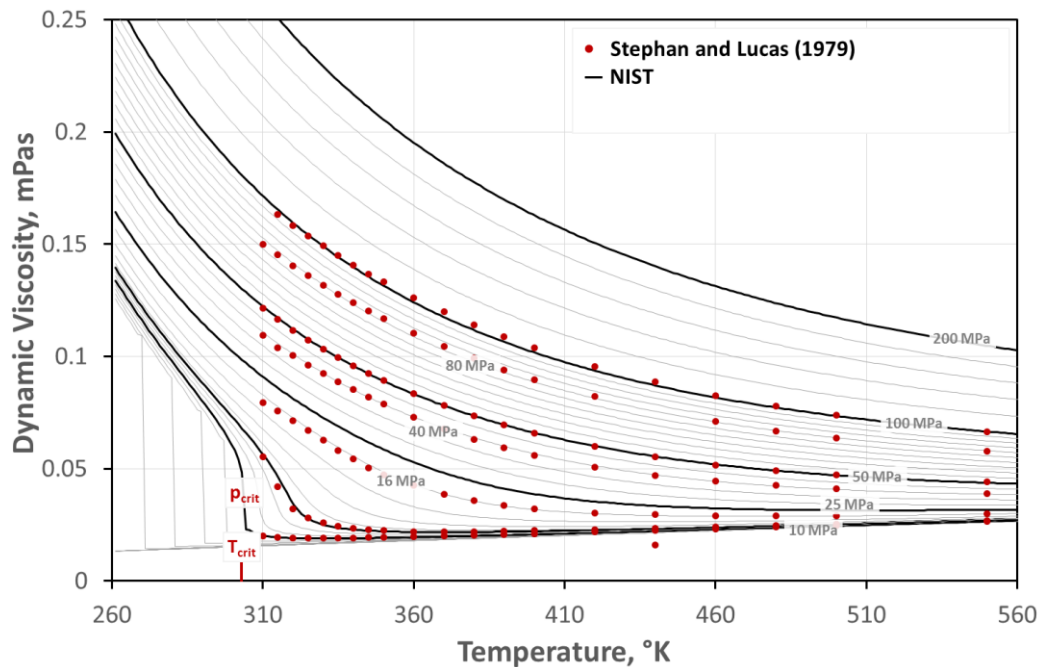


Figure 5-19: Experimental data from Stephan and Lucas (1979) plotted against the NIST reference data.

The Heidaryan et al. (2010) [76] correlation has a recommended temperature and pressure range of 310 to 900 °K and 7.5 to 101.4 MPa respectively. Compared to the Bahadori and Vuthaluru correlation with a stated temperature range between 260 and 450 °K and a pressure range between 10 and 70 MPa, this represents an extended range. The accuracy is best within a pressure range of 15 to 45 MPa. For higher or lower pressures the accuracy in reference to the NIST data decreases. As with the Bahadori and Vuthaluru correlation deviations increase in the lower pressure and temperature range around 10 MPa and temperatures smaller than 360 °K. (Figure 5-22). However, with an ARE of 0.5% and AARE of 1.9% compared to the NIST data the correlation has a good overall performance and a wide range in which it can be applied. The relative errors for this correlation are shown in Figure 5-23.

Both viscosity correlation show satisfactory accuracies with relatively small deviations. Care should be taken when applying the correlations close to the critical temperature and pressure. Depending on the desired P-T range both the Bahadori and Vuthaluru and the Heidaryan et al models can be recommended for use.

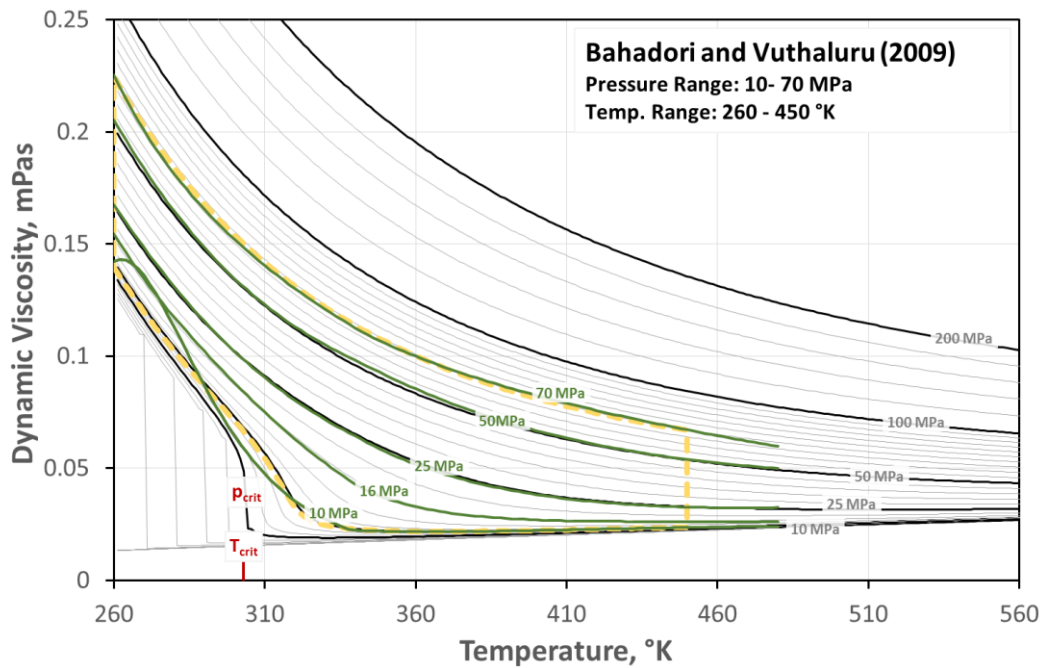


Figure 5-20: Comparison of the correlation results with NIST data. The Bahaduri and Vuthaluru (2009) viscosity correlation results are displayed in green for selected isobars. The yellow dotted line represents the range as recommended by the authors.

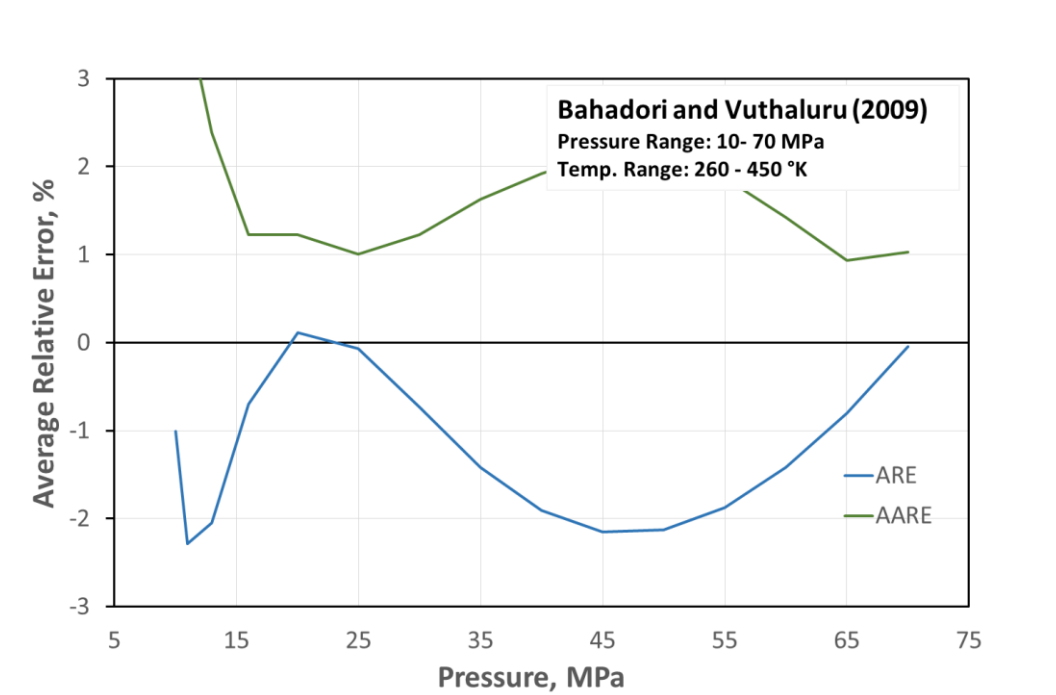


Figure 5-21: The average relative error (ARE) and absolute relative error (AARE) as a function of pressure.

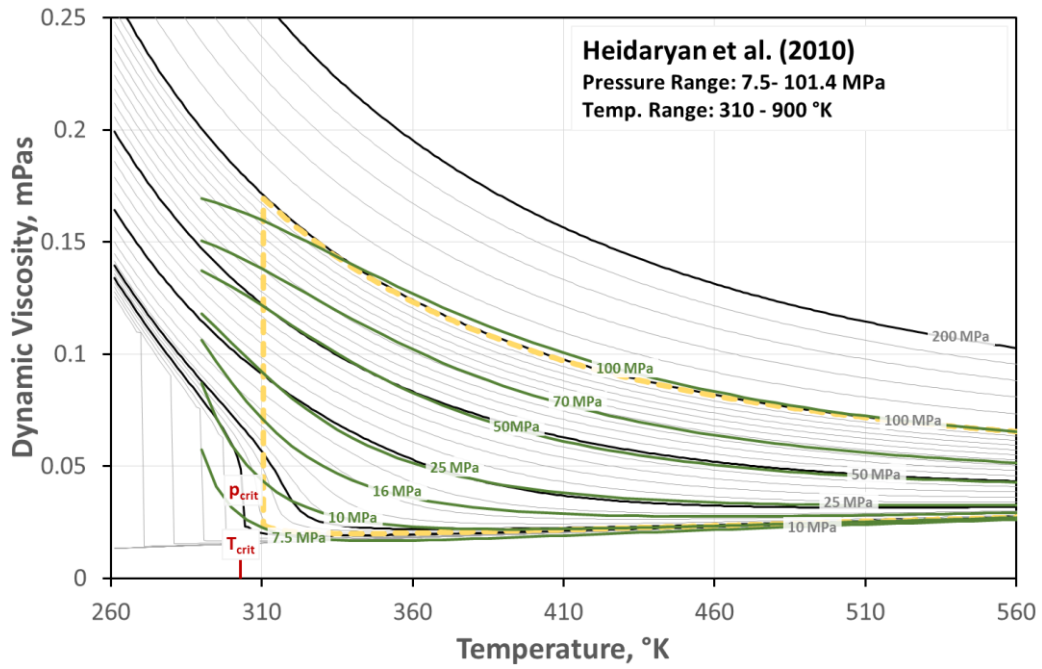


Figure 5-22: Comparison of the correlation results with NIST data. The Heidaryan et al. (2010) viscosity correlation results are displayed in green for selected isobars. The yellow dotted line represents the range as recommended by the authors.

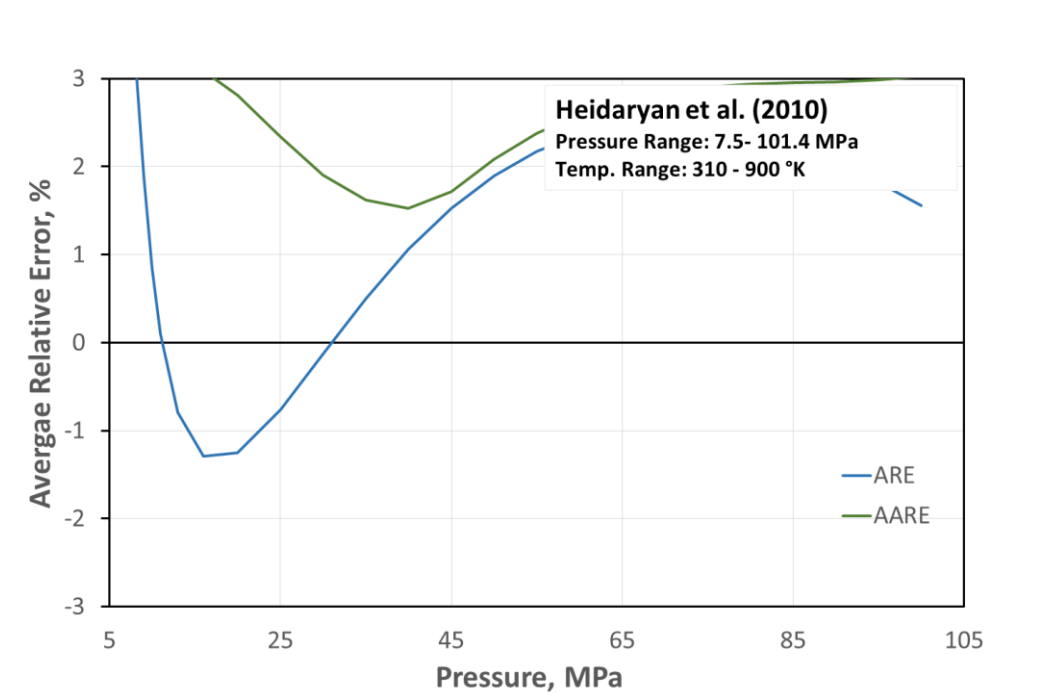


Figure 5-23: The average relative error (ARE) and absolute relative error (AARE) as a function of pressure.

5.2.2 CO₂ thermal conductivity

Four different correlation models for the estimation of CO₂ thermal conductivity by Bahadori and Vuthaluru (2009) [7], Ouyang (2012) [2], Jarrahan and Heidaryan (2012) [3] and Amooey (2013) [78] are evaluated. Same as for the CO₂ viscosity, reference data is available through the NIST data base. Le Neindre et al. (1973) [85] published measured CO₂ thermal conductivity values for temperatures ranging from 290 to 800 °K and pressures up to 100 MPa. These values are compared to the NIST data in Figure 5-24. As it can be seen, there is a good agreement between the reported experimental data and the NIST data. According to the NIST webpage the uncertainties associated with the published thermal conductivity data range within $\pm 5\%$.

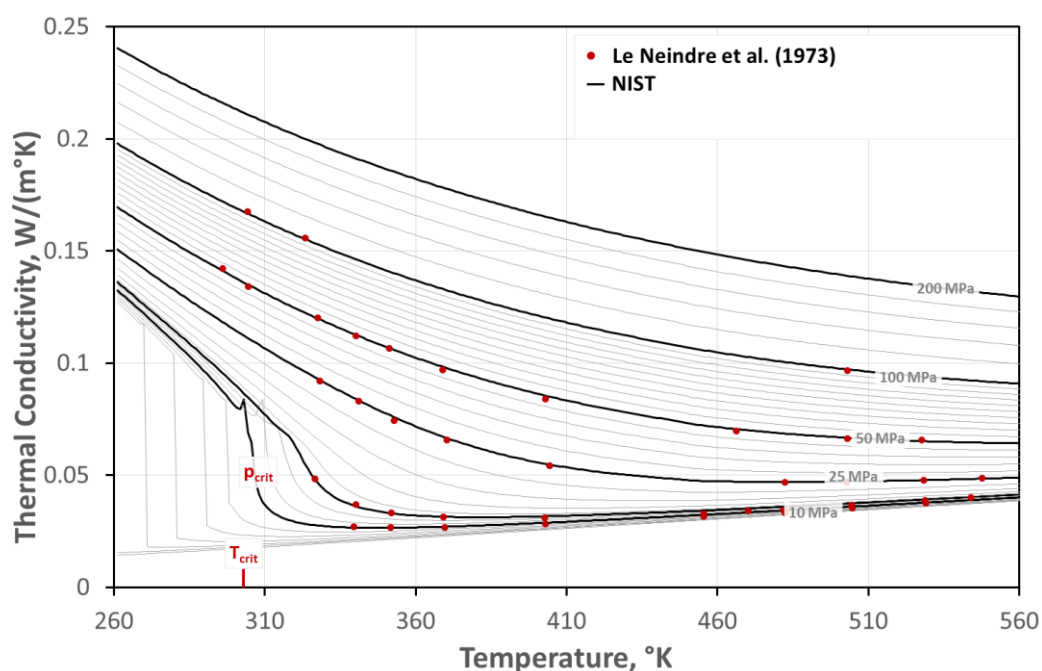


Figure 5-24: Experimental data from Le Neindre et al. (1973) plotted against the NIST reference data.

The Bahadori and Vuthaluru correlation displayed in Figure 5-25 shows a good correlation performance for the higher isobars but the accuracy decreases for pressures below 20 MPa as can also be seen by the development of the AARE in Figure 5-26. The ARE over the entire pressure range is -0.76% and the AARE is 1.95% . The correlation developed by Ouyang to predict the thermal conductivity of Carbon dioxide is displayed in Figure 5-27. It has a relatively narrow recommended temperature range from 313 to 373 °K. The correlation is based on NIST data and matches this very well over most of its recommended pressure range corresponding with a low ARE in Figure 5-28. However, for lower pressures, and temperatures smaller than 335 °K there are some deviations in relation to the NIST data. The resulting overall ARE and AARE in reference to the NIST data is -0.6% and 2.27% respectively.

The correlation presented by Jarrahan and Heidaryan (2012), which is recommended for temperatures from 310 to 960 °K, and pressures from 7.4 to 210 MPa, has the largest range of all the CO₂ thermal conductivity models. In reference to the NIST model, the accuracy of the

correlation decreases for pressures higher than 100 MPa. This is clearly visible in Figure 5-29 and also Figure 5-30 which displays the average relative error for different pressures within the correlation range. There is also a significant deviation in the area around the 10 MPa isobar. For pressures from approximately 15 to 110 MPa the model shows a good performance and the ARE is below 1% within this region. The overall ARE is -0.63% and the overall AARE is 1.67%.

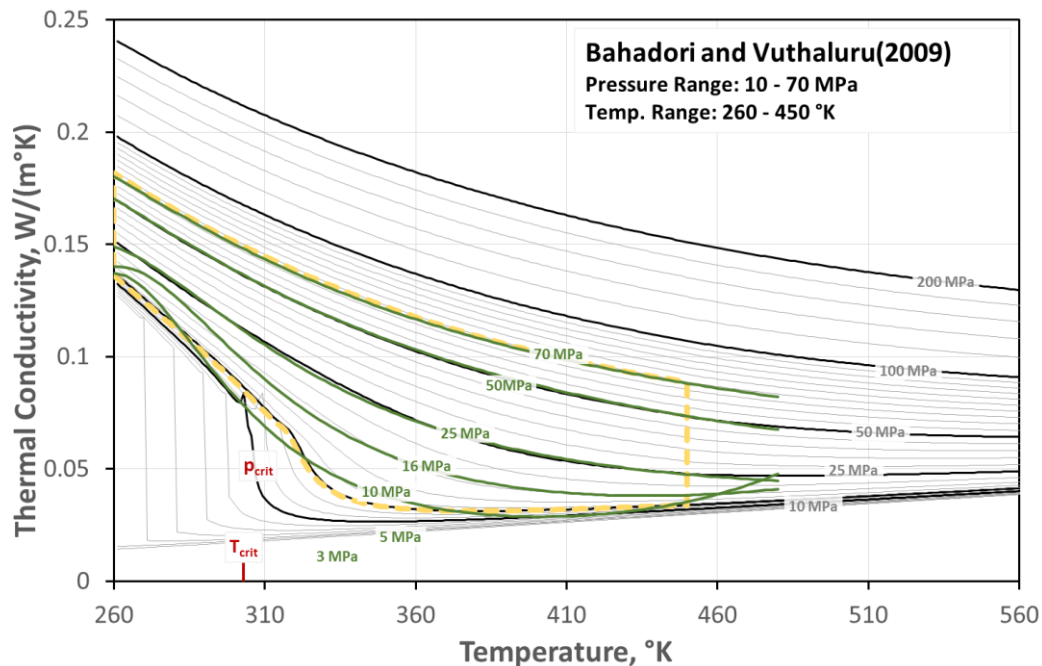


Figure 5-25: Comparison of the correlation results with NIST data. The Bahadori and Vuthaluru (2009) thermal conductivity correlation results are displayed in green for selected isobars. The yellow dotted line represents the range as recommended by the authors.

Amooey presents a correlation for the estimation of thermal conductivity with a recommended temperature range of 290 to 800 °K and a density range between 1 and 1200 kg/m³. In comparison to the other three thermal conductivity models, this correlation is a function of the CO₂ density and temperature as opposed to the pressure and density. For temperatures higher than 360 °K the correlation matches the NIST density data well and this is especially true for the lower density areas as can be seen in Figure 5-31. Figure 5-32 shows that the ARE is below 4% except for the lower and upper regions around the boundaries of the recommended pressure range for this correlation. Summing up the results described above, all of the models show deviations from the NIST data in the lower regions of the recommended pressure and temperature range close to the critical point. The Bahadori and Vuthaluru (2009), Ouyang (2012) and Jarrahan and Heidaryan (2012) correlations all have similar average relative errors of around 1% over most of their recommended range. The Model by Ouyang has the smallest ARE for pressures greater than 15 MPa but at the same time a limited temperature range of only 60 °K. The correlation developed by Jarrahan and Heidaryan seems to best represent the CO₂ thermal conductivity behaviour over a large pressure and temperature range. The correlation developed by Amooey shows a very good performance for temperatures greater than 360 °K. However, if the density is not available it has to be calculated using either an EOS

or another density correlation. This might make it less suitable for applications where only the pressure and temperature are desired as input parameters.

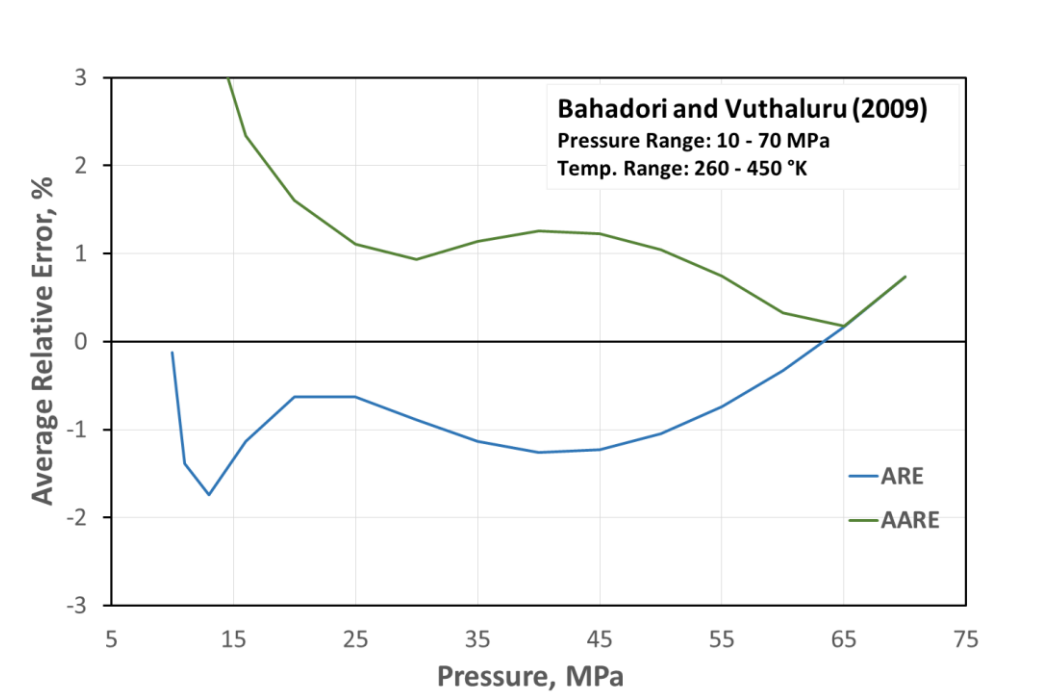


Figure 5-26: The average relative error (ARE) and absolute relative error (AARE) as a function of pressure for the thermal conductivity correlation developed by Bahadורי and Vuthaluru (2009).

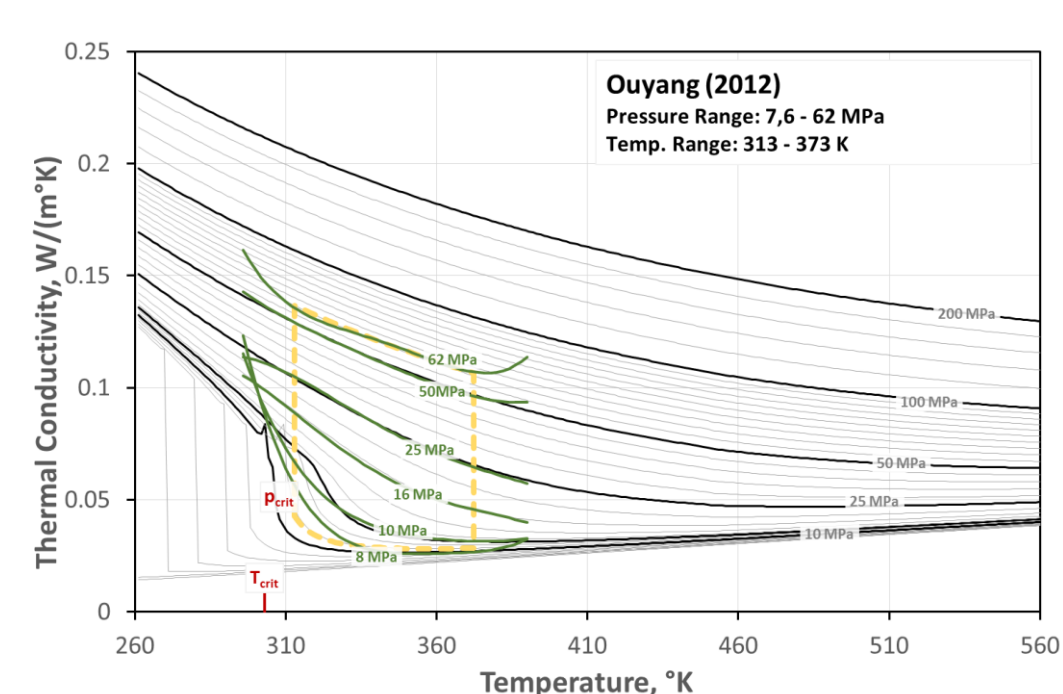


Figure 5-27 Comparison of the correlation results with NIST data. The Ouyang (2012) thermal conductivity correlation results are displayed in green for selected isobars. The yellow dotted line represents the range as recommended by the authors.

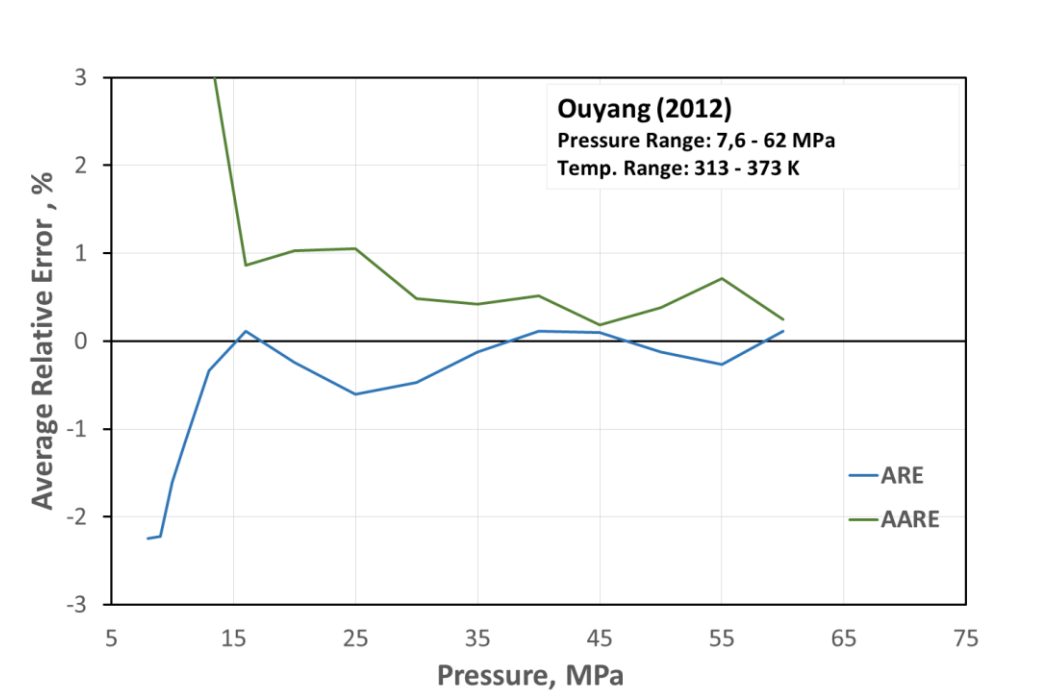


Figure 5-28: The average relative error (ARE) and absolute relative error (AARE) as a function of pressure.

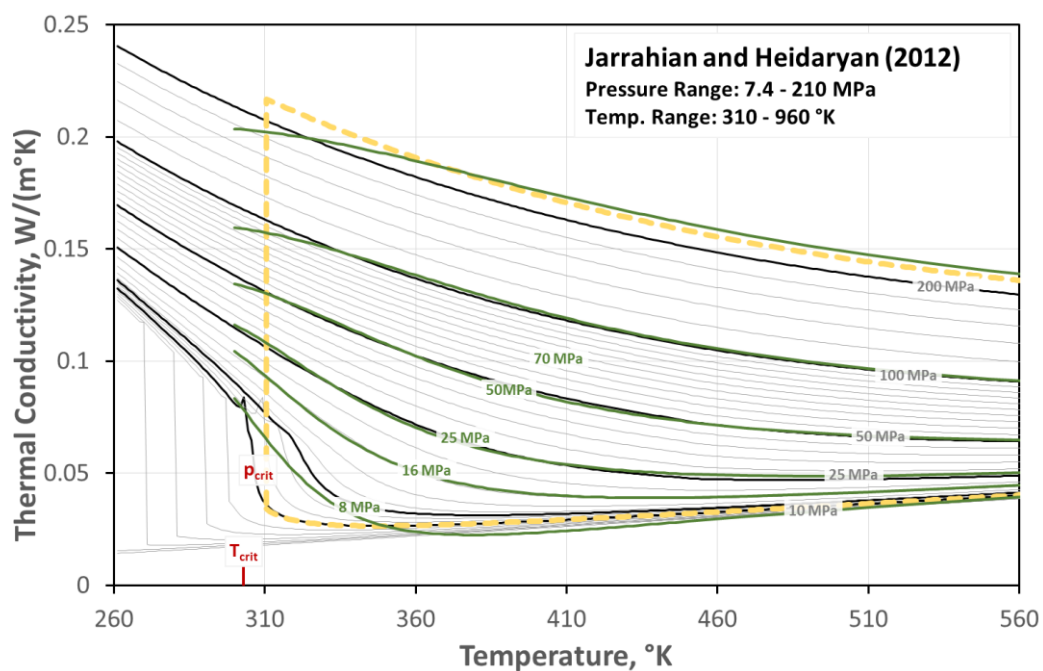


Figure 5-29: Comparison of the correlation results with NIST data. The Jarrahan and Heidaryan (2012) thermal conductivity correlation results are displayed in green for selected isobars. The yellow dotted line represents the range as recommended by the authors.

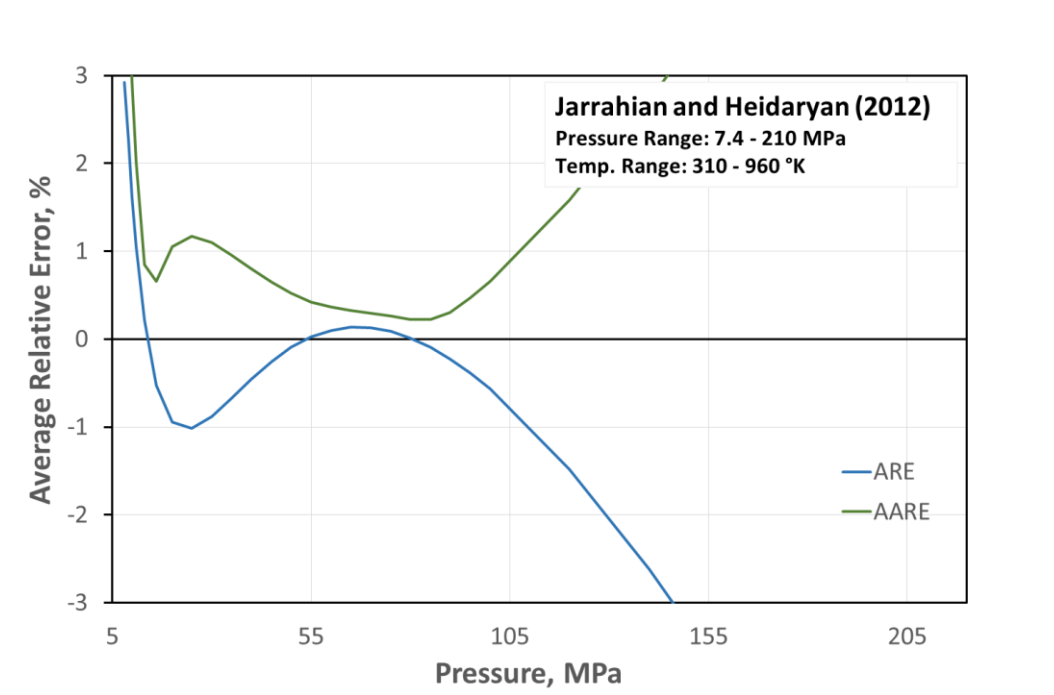


Figure 5-30 The average relative error (ARE) and absolute relative error (AARE) as a function of pressure.

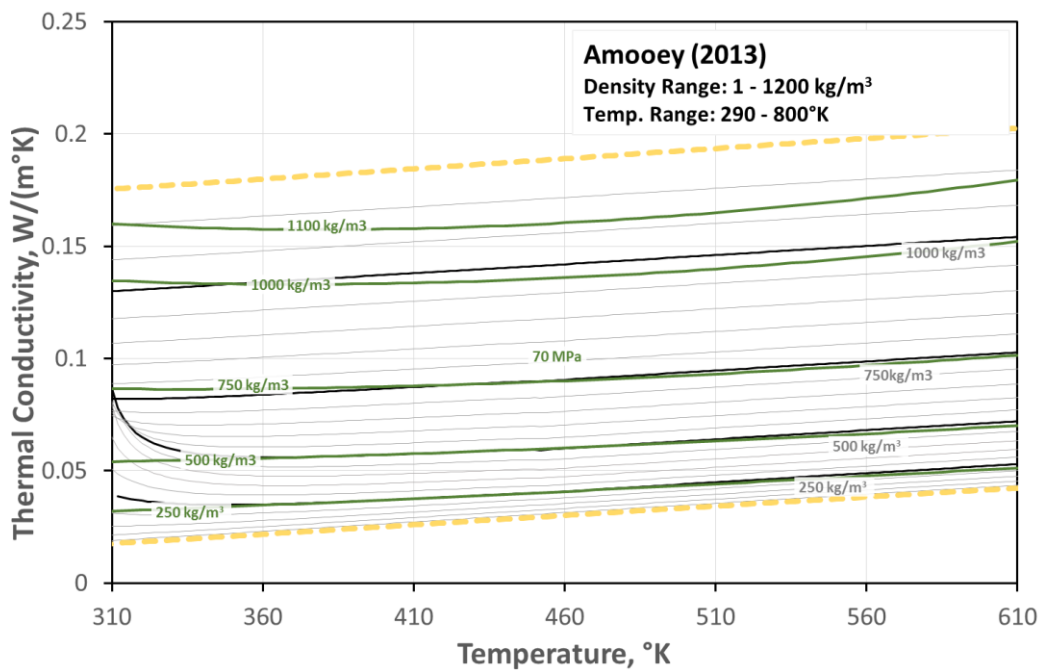


Figure 5-31: Comparison of the correlation results with NIST data. The Amooey (2013) thermal conductivity correlation results are displayed in green for selected isobars. The yellow dotted line represents the range as recommended by the authors.

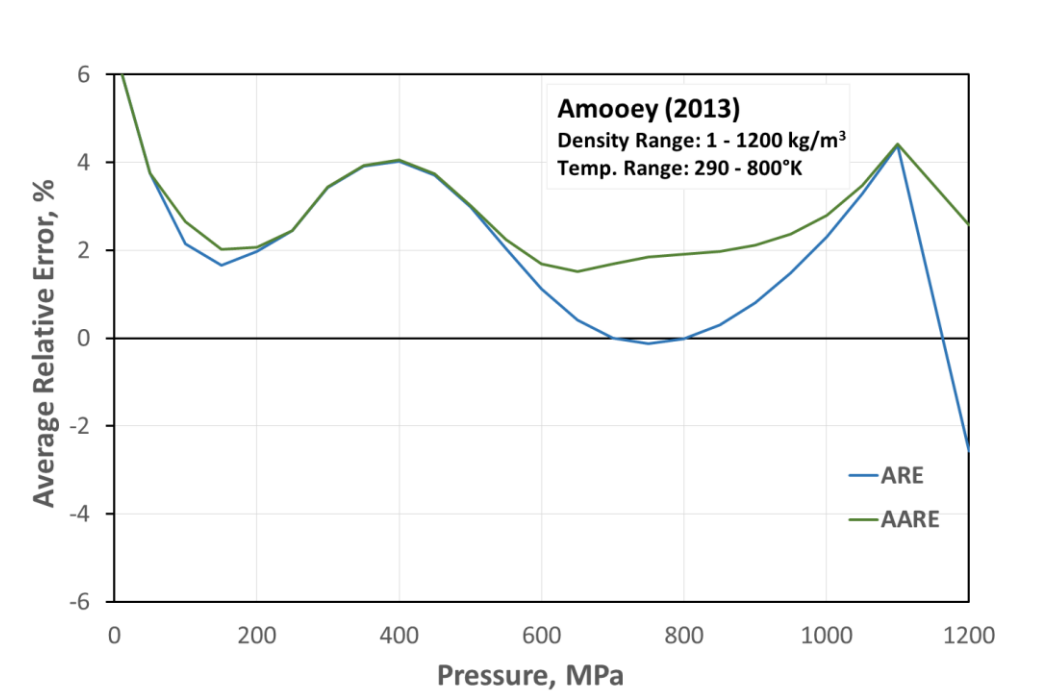


Figure 5-32: The average relative error (ARE) and absolute relative error (AARE) as a function of pressure.

5.2.3 CO₂ density correlation models

Four correlation models developed to predict the supercritical carbon dioxide density are evaluated. These are : The correlations by Bahadori et al. (2009) [79], Ouyang (2011) [84], Haghbakhsh et al.(2013) [80] and Wang et al. (2015) [83]. Again data from the NIST WebBook [25] serves as a reference. It is also validated against experimental data published by Le Neindre et al. (1973) [85] and displayed in Figure 5-33. Clearly there is a good match between the measured values and the data provided by the NIST. For pressures up to 30 MPa and temperatures up to 523 °K the NIST webpage gives estimated density uncertainty ranges from 0.03% to 0.05%.

The calculations carried out in this study do not yield any meaningful results for the correlation proposed by Haghbakhsh et al. (2013). Initially this was the same for the Wang et al model but after this problem was brought to the author's attention new coefficients for the correlation equation were provided. The results of the proposed density equation in combination with the updated coefficients are plotted in Figure 5-34. Wang et al. state that their density equation is based on their own CO₂ density measurements. However, comparing the developed correlation model with NIST data only a modest match over a limited pressure and temperature region is observed as can be seen in Figure 5-34. Correspondingly the correlation results in very high AREs and AAREs which are displayed in Figure 5-35. The overall ARE is 1.17% but this value has little significance considering an AARE of 336.4%.

The Bahadori et al. correlation, which has a recommended range for pressures from 2,5 to 70 MPa and temperatures from 293 to 433 °K has the lowest error in a pressure range of 15 to 30 MPa as displayed in Figure 5-37. The overall ARE is -0.95% and the overall AARE is 9.38%.

The Bahadori et al. correlation model does not perform so well in the areas close to the recommended temperature and pressure boundaries as showed in Figure 5-36.

Out of the four investigated density models the correlation proposed by Ouyang (2011) delivers the most accurate results in reference to the NIST data. At the same time it has smallest recommended Temperature range of only 60 °K from 313 to 373 °K. Ouyang states a pressure range from 7 to 62 MPa. It should be noted that the 7 MPa isobar representing the lower recommended pressure boundary exhibits a great deviation from the NIST data for temperatures lower than 330 °K as displayed in Figure 5-34. The Ouyang correlation has a very low ARE of -0.41% and an AARE of 0.75% in comparison to the NIST data.

Based on the above findings The Bahadori et al. and the Ouyang et al. correlation are recommended for calculating supercritical CO₂ densities. Care should be taken when applying the correlations close to the lower end of the recommended pressure and temperature range. If a temperature range of 313 to 373 °K is sufficient then the Ouyang correlation may be chosen over the Bahadori et al. model.

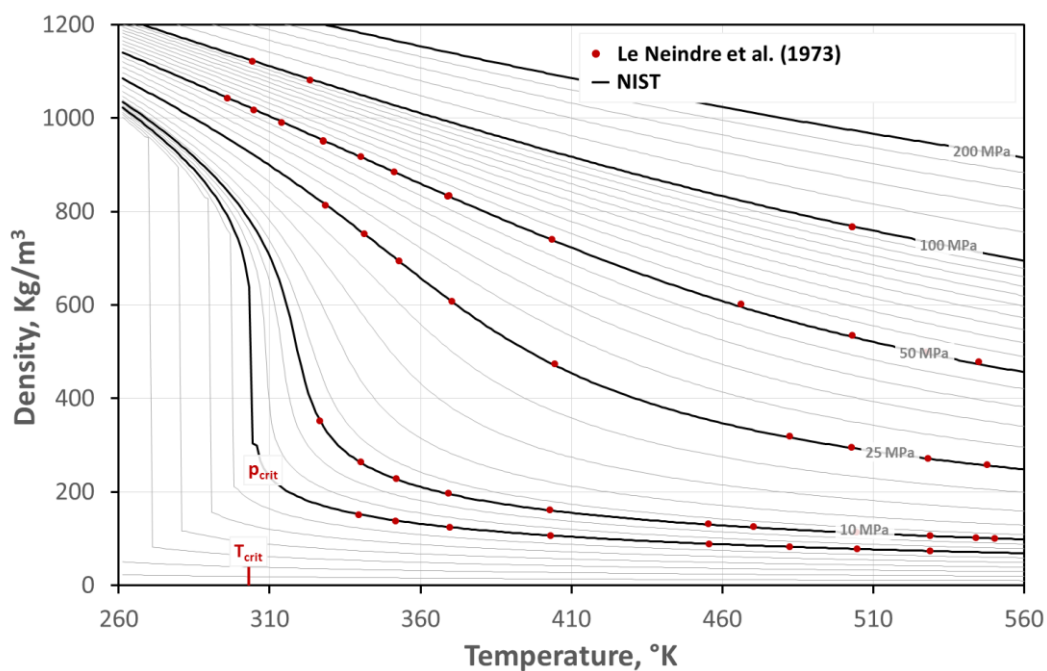


Figure 5-33: Experimental data from Le Neindre et al. (1973) plotted against the NIST reference data.

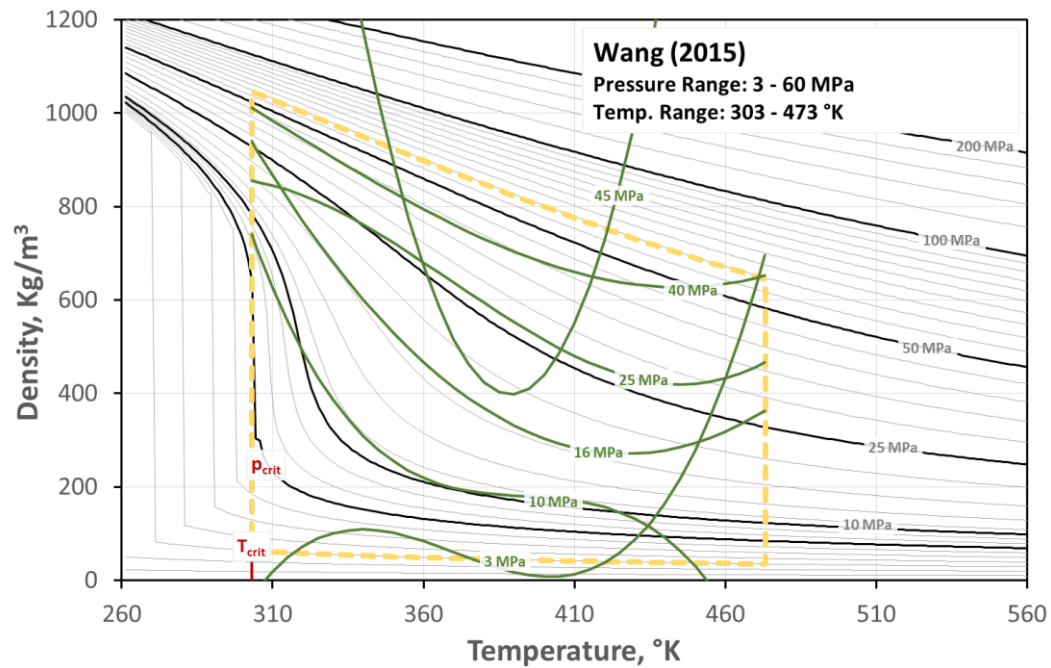


Figure 5-34: Comparison of the correlation results with NIST data. The Wang et al. (2015) density correlation results are displayed in green for selected isobars. The yellow dotted line represents the range as recommended by the authors.

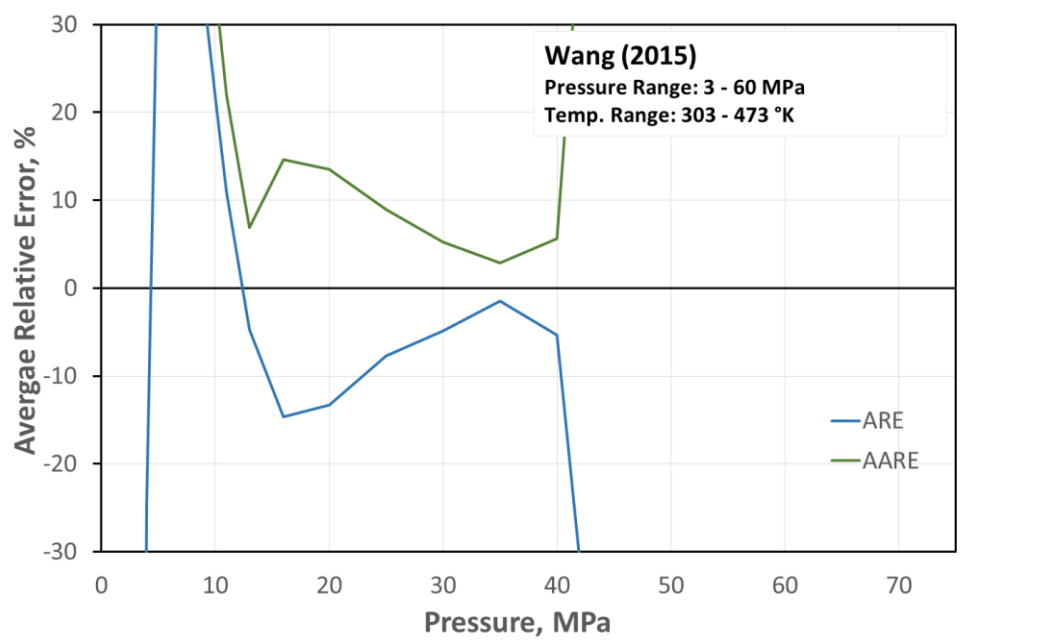


Figure 5-35: The average relative error (ARE) and absolute relative error (AARE) as a function of pressure.

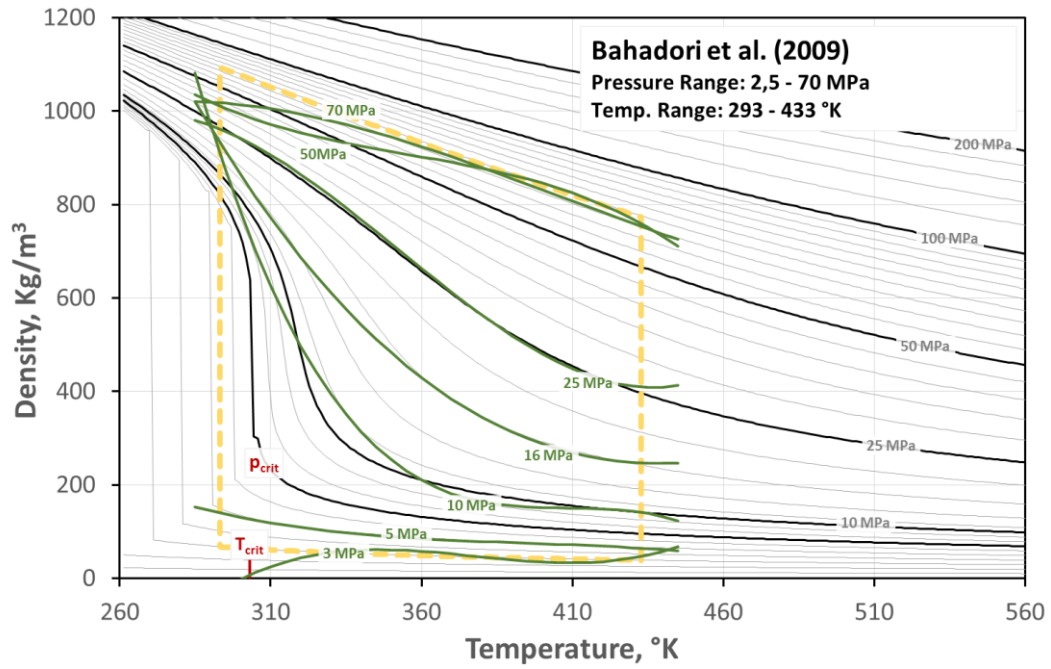


Figure 5-36: Comparison of the correlation results with NIST data. The Bahadori et al (2009) density correlation results are displayed in green for selected isobars. The yellow dotted line represents the range as recommended by the authors.

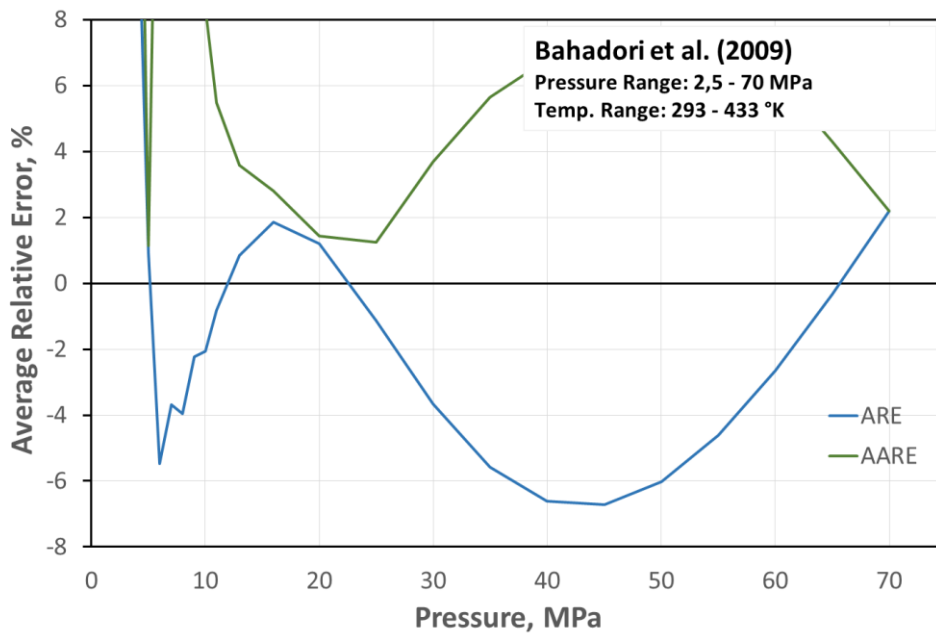


Figure 5-37: The average relative error (ARE) and absolute relative error (AARE) as a function of pressure.

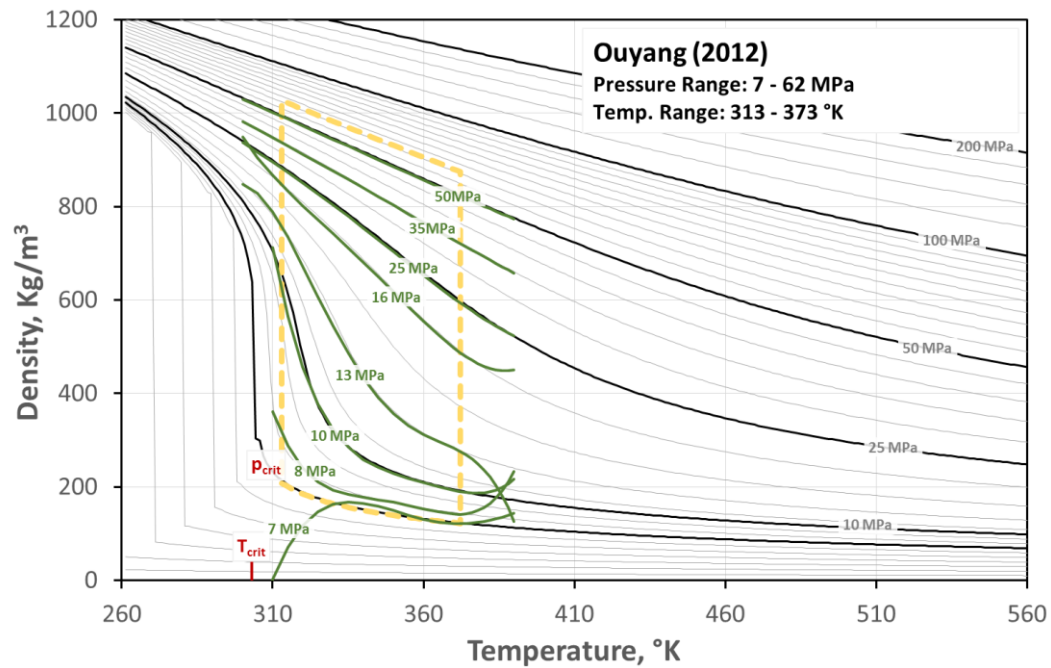


Figure 5-38: Comparison of the correlation results with NIST data. The Ouyang (2011) density correlation results are displayed in green for selected isobars. The yellow dotted line represents the range as recommended by the authors.

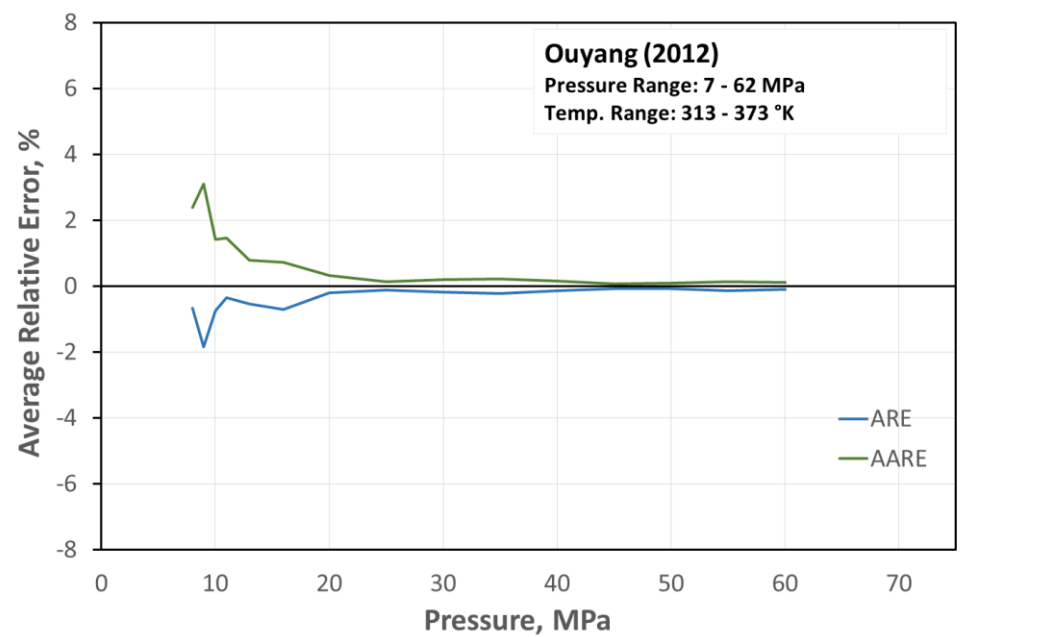


Figure 5-39: The average relative error (ARE) and absolute relative error (AARE) as a function of pressure.

5.3 Evaluation and comparison summary

Table 5-6: Pseudocritical properties correlations for unknown compositions – gas gravity correlations. AREs and AAREs according to McCain et al. [15]

	Correlation	ARE, %	AARE, %	T-Range; °K	P-Range, MPa	Comment
1	Sutton (2007)	-0.422	1.511	N/A	N/A	
2	Standing (1981)	-1.010	1.949	N/A	N/A	
3	Piper et al. (1999)	0.296	1.590	N/A	N/A	
4	Elsharkawy et al. (2000)	1.185	2.452	N/A	N/A	
5	Sutton (1985)*	1.746	2.878	N/A	N/A	
6	Londono et al. (2005)	5.157	6.432	N/A	N/A	

Table 5-7: Comparison of pseudocritical properties gas gravity correlations for mixtures with a non-hydrocarbon content greater than 5% including the Wichert and Aziz correction. AREs and AAREs according to McCain et al. [15]

	Correlation	ARE, %	AARE, %	T-Range; °K	P-Range, MPa	Comment
1	Sutton (2007)	-0.2	1.9	N/A	N/A	
2	Standing (1981)	-0.4	2.2	N/A	N/A	
3	Piper et al. (1999)	0.6	2.2	N/A	N/A	Significant deviation at higher non-hydrocarbon contents
4	Elsharkawy-Elkamel (2000)	-2.1	4.0	N/A	N/A	Significant deviation at higher non-hydrocarbon contents
5	Londono et al. (2005)	-0.1	8.4	N/A	N/A	High AARE
6	Elsharkawy et al. (2000)	4.8	7.9	N/A	N/A	High AARE
7	Sutton (1985)	11.5	12.6	N/A	N/A	High AARE

= recommended

= see comments

= no meaningful results available

Table 5-8: Comparison of pseudocritical properties for correlations based on compositional data. AREs and AAREs according to Elsharkawy and Elkamel. [33]

	Correlation	ARE, %	AARE, %	T-Range; °K	P-Range, MPa	Comment
1	Piper et. al	0.31	1.21	N/A	N/A	
2	Corredor et. al	0.25	1.36	N/A	N/A	
3	Kay- Wichert & Aziz	0.69	1.38	N/A	N/A	
4	SSVB- Wichert & Aziz	0.65	2.14	N/A	N/A	

Table 5-9: Comparison of dynamic viscosity correlations for gas mixtures. AREs and AAREs according to McCain et al. [15]. *from Chen and Ruth (1993) [41]

	Correlation	ARE, %	AARE, %	T-Range; °K	P-Range, MPa	Comment
1	Lee et al. (1966)	-1.60	2.26	N/A	N/A	
2	Gurbanov and Dadash-Zade (1986)	-	2.2*	N/A	N/A	Does not require density as input
3	Londono et al. (2005)	-2.66	3.08	N/A	N/A	
4	Sutton (2007)	2.05	3.10	N/A	N/A	
5	Poling et al. (2001)	-0.61	3.34	N/A	N/A	
6	Lee et al. (1964)	-3.23	3.70	N/A	N/A	High AARE
7	Carr et al. (1954)	-9.81	9.81	N/A	N/A	High AARE

Table 5-10: Correlation for the calculation of the natural gas mixture thermal conductivity. AREs and AAREs in reference to NIST data

	Correlation	ARE, %	AARE, %	T-Range; °K	P-Range, MPa	Comment
1	Jarrahian and Heidaryan (2014)	5.02	8.55	220 - 425	5 - 50	Modest correlation result

= recommended

= see comments

= no meaningful results available

Table 5-11: Correlation for the calculation of the natural gas mixture heat capacity. AREs and AAREs in reference to NIST data.

	Correlation	ARE, %	AARE, %	T-Range; °K	P-Range, MPa	Comment
1	Moshfeghian (2011)	0.61	2.41	293 - 473	3-15	Modest correl. result. Valid for a specific gravity range of 0,6 - 0,8
2	Lateef and Omeke (2011)	N/A	N/A	338 - 1366	N/A	No correlation results obtained

Table 5-12: Comparison of supercritical CO₂ viscosity correlations. AREs and AAREs in reference to NIST data.

	Correlation	ARE, %	AARE, %	T-Range; °K	P-Range, MPa	Comment
1	Heidaryan et al. (2010)	0.5	1.9	310 - 900	7.5 - 80	
2	The Bahadori and Vuthaluru (2009)	-1.23	1.9	260 - 450	10 - 70	

Table 5-13: Comparison of supercritical CO₂ thermal conductivity correlations. AREs and AAREs in reference to NIST data.

	Correlation	ARE, %	AARE, %	T-Range; °K	P-Range, MPa	Comment
1	Jarrahan and Heidaryan (2012)	-0.63	1.67	310 - 960	7.4 - 210	
2	Bahadori and Vuthaluru (2009)	-0.76	1.95	260 - 540	10 - 70	
3	Ouyang (2012)	-0.6	2.27	313 - 373	7.6 - 62	Recommended for 8 to 60 MPa range
4	Amooey (2013)	2.09	2.85	290 - 800	N/A	Function of density and valid within 1 and 1200 kg/m ³

= recommended


= see comments

= no meaningful results available

Table 5-14: Comparison of supercritical CO₂ density correlations. AREs and AAREs in reference to NIST data.

	Correlation	ARE, %	AARE, %	T-Range; °K	P-Range, MPa	Comment
1	Ouyang (2011)	-0.41	0.75	313 to 373	7 - 62	Recommended for 8 to 60 MPa range
2	Bahadori et al. (2009)	-0.95	9.38	293 - 433	2,5 - 7	
3	Wang et al. (2015)	1.17	336.4	303 - 473	3 - 60	Poor correlation results
4	Hagbakhsh et al.(2013)	N/A	N/A	308 - 523	7.5 – 46.8	No correlation results obtained

 = recommended

 = see comments

 = no meaningful results available

6 Conclusion

A total of 37 different correlations for the calculation of natural gas as well as supercritical carbon dioxide properties have been evaluated.

While there are numerous correlations available for the estimation of pseudocritical properties and the viscosity of natural gas mixtures, it is hard to find suitable models that offer a simple correlation approach based on temperature, pressure and specific gravity for the heat capacity, and more so for the thermal conductivity.

Most of the pseudocritical correlation models methods perform reasonably well and the accuracies are acceptable for engineering applications. It is however necessary to differentiate between condensate and associated gas correlations and include a correction method if non-hydrocarbon components (hydrogen sulphide, carbon dioxide and nitrogen) are present. Here the method proposed by Sutton (2007) in connection with the Wichert-Aziz correction offers the simplest and most accurate correlation.

Several methods for the calculation of the viscosity of a natural gas mixture are available from numerous authors. Among these, the LGE correlation is the most accurate and stands out because of simplicity and acceptability by the petroleum industry. In fact a lot of the other proposed methods are based on the LGE equations. The Gurbanov and Dadash-Zade method does not require the density and this may be seen as advantage for some applications since the density does not have to be calculated through an EOS.

Both heat capacity, and the thermal conductivity correlations show a poor or very modest performance in terms of accuracy over a considerable part of the recommended range when compared to NIST data. However depending on the given temperature and pressure conditions the methods proposed by Moshfeghian and Jarrahan - Heidaryan might still yield results acceptable for engineering applications. An individual assessment for each specific application case will be necessary.

Correlations for the estimation of the carbon dioxide supercritical density, viscosity and thermal conductivity have been proposed by several authors in recent years, yet no correlation method for the estimation of the supercritical CO₂ heat capacity was found. NIST data based on the Spann and Wagner EOS is available however and could serve as the basis for developing a correlation in the future.

Concerning the density, viscosity and thermal conductivity the correlation proposed by Ouyang (2011), Heidaryan et al. (2010) Jarrahan and Heidaryan (2012) are the best in class respectively. It has to be pointed out that all CO₂ correlation show significant deviation from the NIST data in the proximity of the critical point. Again, and individual assessment for each specific application case taking the expected temperature and pressure into account, will be necessary and helpful.

A quick assessment and performance check of each individual correlation is easily possible by selecting and applying the programmed correlation through the use of MS Excel in combination with plots that were generated as part of this thesis.

Apart from listing, comparing and evaluating correlation models for the calculation of natural gas and CO₂ properties this thesis shows that the NIST data base is a reliable source for fluid property data. It has been demonstrated that the NIST data is in very good agreement with measured experimental data.

Therefore the NIST data would lend itself as the starting point for the development of new correlation models. Especially for those properties for which currently available correlations lack in accuracy. Good correlation results could possibly achieved through the use of neural networks.

It may also be worthwhile to investigate the extended fee based NIST Reference Fluid Thermodynamic and Transport Properties Database (REFPROP) which includes additional features such as mixture models for natural gas fluids.

7 Nomenclature

a_{ij}	=	Mixture parameter
b_{ii}	=	Mixture parameter
C_p	=	Isobaric heat capacity at elevated pressure, , J/(g °K)
C_p^0	=	Ideal isobaric heat capacity, J/(g °K)
e	=	Viscosity parameter
f_0, f_1	=	Functions of reduced temperature
F_j	=	Parameter in the Stewart et al. equations
i	=	Dipole moment of Molecule i, Debye
J	=	Parameter in the Stewart et al. equations
K	=	Parameter in the Stewart et al. equations
k	=	Thermal conductivity, W/(mK)
m	=	Mass, kg
M	=	Molecular weight
M_a	=	Apparent molecular weight of the gas
M_{air}	=	Apparent molecular weight of the air = 28.96
M_{C7+}	=	Molecular weight of C7+ fraction
M_g	=	Average molecular weight of gas mixture
m_g	=	Mass of gas, kg
M_i	=	Molecular weight of the ith component in the mixture
n	=	Number of moles
N	=	Number components in a mixture
N_A	=	Avogadro number = $6.02214129 \cdot 10^{23}$, mol ⁻¹
p	=	Pressure, Pa
p_c	=	Critical pressure, Pa
p_{ci}	=	Critical pressure of component i in a gas mixture, Pa
p_{pc}	=	Pseudocritical pressure of a gas mixture, Pa
p_r	=	Reduced pressure
p_{sc}	=	Pressure at standard conditions, Pa
R	=	Universal gas constant = 8.3145, J/(g mol-K)
r	=	Intermolecular distance
S_σ	=	Slope for σ as a function of T_r
T	=	Temperature, °K
T_c	=	Critical temperature, °K
T_{ci}	=	Critical temperature of component i in a gas mixture, °K
T_{pc}	=	Pseudocritical temperature, °K
T_r	=	Reduced temperature
T_{sc}	=	Temperature at standard conditions, °K
U	=	Intermolecular potential energy, J
V	=	Volume, m ³
V_c	=	Critical volume, m ³

V_g	=	Volume, m^3
V_r	=	Reduced volume
V_{sc}	=	Volume at standard conditions, m^3
x_i	=	Mole fraction of component i in a liquid
y_i	=	Mole fraction of component i in a gas mixture
z	=	compressibility factor (gas-deviation factor)

Greek symbols:

γ_g	=	Gas specific gravity
$\Delta\mu_{CO_2}$	=	Viscosity corrections due to the presence of CO_2
$\Delta\mu_{H_2S}$	=	Viscosity corrections due to the presence of H_2S
$\Delta\mu_{N_2}$	=	Viscosity corrections due to the presence of N_2
ϵ	=	Potential depth, $J \cdot mol^{-1}$
ϵ	=	Temperature-correction factor for acid gases, $^{\circ}K$
η	=	Newtonian shear viscosity, Pas
η_0	=	Viscosity at zero density, Pas
η_{calc}	=	Calculated viscosity, Pas
η_{exp}	=	Experimental viscosity, Pas
λ	=	Thermal conductivity, $W/(mK)$
μ	=	Dynamic viscosity, Pas
μ_1	=	Corrected gas viscosity, Pas
μ_{gsc}	=	Gas viscosity at standard conditions, Pas
$\mu_{uncorr.}$	=	Uncorrected gas viscosity, Pas
ρ	=	Density, kg/m^3
ρ_{air}	=	Density of the air, kg/m^3
ρ_c	=	Critical mole density, mol per units
ρ_g	=	Density of gas, kg/m^3
ρ_r	=	Dimensionless density of gas
σ	=	Molecular diameter, m
σ	=	LJ separation distance at zero energy
σ_c	=	Critical value of σ
Φ	=	Heat flux
ψ	=	Real-gas pseudopotential
ω	=	Acentric factor
Ω_v	=	Collision integral

8 References

1. Schwaiger, G. 2016. Modelling of Critical Gas Velocities based on the Entrained Droplet Model for Gas Wells and the Effect of Heat Loss on Gas Production, Montanuniversität Leoben.
2. Ouyang, L.-B. 2012. New Correlations for Predicting the Thermodynamic Properties of Supercritical Carbon Dioxide. *The Open Petroleum Engineering Journal*, No. 5, pp. 42–52.
3. Jarrahan, A. and Heidaryan, E. 2012. A novel correlation approach to estimate thermal conductivity of pure carbon dioxide in the supercritical region. *The Journal of Supercritical Fluids*, Vol. 64, pp. 39–45.
4. *Enhanced Oil Recovery | Department of Energy*. <http://energy.gov/fe/science-innovation/oil-gas-research/enhanced-oil-recovery> (Accessed 19 May 2016).
5. Shams, R., Esmaili, S., Rashid, S. and Suleymani, M. 2015. An intelligent modeling approach for prediction of thermal conductivity of CO₂. *Journal of Natural Gas Science and Engineering*, Vol. 27, pp. 138–50.
6. Vandeginste, V. and Piessens, K. 2008. Pipeline design for a least-cost router application for CO₂ transport in the CO₂ sequestration cycle. *International Journal of Greenhouse Gas Control*, Vol. 2, No. 4, pp. 571–81.
7. Bahadori, A. and Vuthaluru, H. B. 2010. Predictive tool for an accurate estimation of carbon dioxide transport properties. *International Journal of Greenhouse Gas Control*, Vol. 4, No. 3, pp. 532–36.
8. Rozzi, N. L. and Singh, R. K. 2002. Supercritical Fluids and the Food Industry. *Comprehensive Reviews in Food Science and Food Safety*, Vol. 1.
9. Pruess, K. and Azaroual, M. (eds). 2006. *On the Feasibility of Using Supercritical CO₂ as Heat Transmission Fluid in an Engineered Hot Dry Rock Geothermal System*.
10. Poling, B. E., Prausnitz, J. M. and O'Connell, J. P. 2001. *The properties of gases and liquids*. 5th ed. New York, McGraw-Hill. (McGraw Hill professional).
11. Heidaryan, E. and Jarrahan, A. 2013. Modified Redlich–Kwong equation of state for supercritical carbon dioxide. *The Journal of Supercritical Fluids*, Vol. 81, pp. 92–98.
12. Ahmed, T. H. 2007. *Equations of state and PVT analysis. Applications for improved reservoir modeling*. Houston, Texas, Gulf Publishing Company. (In eng).
13. Rojey, A. 1997. *Natural gas. Production, processing, transport*. Paris, Editions Technip. (Institut français du pétrole publications). (In eng).
14. Sutton, R. P. 2007. Fundamental PVT Calculations for Associated and Gas/Condensate Natural-Gas Systems. *SPE Reservoir Evaluation & Engineering*, Vol. 10, No. 03, pp. 270–84.
15. McCain, W. D., Lenn, C. P. and Spivey, J. P. 2011. *Petroleum reservoir fluid property correlations*. Tulsa, Okla, PennWell Corp. (In eng).
16. Jarrahan, A. and Heidaryan, E. 2014. A simple correlation to estimate natural gas thermal conductivity. *Journal of Natural Gas Science and Engineering*, Vol. 18, pp. 446–50.

17. McCain, W. D. 1990. *The properties of petroleum fluids*. 2nd ed. Tulsa, Okla., PennWell Books. (In eng).
18. Elsharkawy, A. M. 2006. Efficient Methods for Calculations of Compressibility, Density, and Viscosity of Natural Gases. *Journal of Canadian Petroleum Technology*, Vol. 45, No. 06.
19. Standing, M. B. and Katz, D. L. 1942. Density of Natural Gases. *Transactions of the AIME*, Vol. 146, No. 01, pp. 140–49.
20. Takacs, G. 1976. Comparisons Made for Computer Z-factor Calculations. *Oil & Gas Journal*, Vol. 74, No. 51, pp. 64–66.
21. Hall, K. R. and Yarborough, L. 1973. A New Equation of State for Z-Factor Calculations. *Oil & Gas Journal*, No. 71, p. 82.
22. Dranchuk, P. M. and Abou-Kassem, H. 1975. Calculation of Z Factors For Natural Gases Using Equations of State. *Journal of Canadian Petroleum Technology*, Vol. 14, No. 03.
23. Borges, P. R. 1991. Correction improves Z-factor Values for High Gas Density. *Oil & Gas Journal*, Vol. 89, No. 9, pp. 54–55.
24. Abou-Kassem, J. H., Mattar, L. and Dranchuk, P. M. 1990. Computer Calculations Of Compressibility Of Natural Gas. *Journal of Canadian Petroleum Technology*, Vol. 29, No. 05.
25. 2016. *NIST Chemistry WebBook*. <http://webbook.nist.gov/chemistry/> (Accessed 11 March 2016).
26. Rushing, J. A., Newsham, K. E., van Fraassen, K. C., Mehta, S. A. and Moore, G. R. Natural Gas z-Factors at HP/HT Reservoir Conditions: Comparing Laboratory Measurements With Industry-Standard Correlations for a Dry Gas, *CIPC/SPE Gas Technology Symposium 2008 Joint Conference* .
27. Kay, W. 1936. Gases and Vapors At High Temperature and Pressure - Density of Hydrocarbon. *Ind. Eng. Chem.*, Vol. 28, No. 9, pp. 1014–19.
28. Sutton, R. P. 1985. Compressibility Factors for High-Molecular-Weight Reservoir Gases, *SPE Annual Technical Conference and Exhibition* .
29. Brown et al. 1948. *Natural Gasoline and the Volatile Hydrocarbons*. Tulsa, OK.
30. Standing, M. B. 1981. *Volumetric and Phase Behaviour of Oilfield Hydrocarbon Systems*. Dallas, Texas.
31. Piper, L. D., McCain, W. D. and Corredor, J. H. 1993. Compressibility Factors for Naturally Occurring Petroleum Gases (1993 version), *SPE Annual Technical Conference and Exhibition* .
32. Elsharkawy, A. M., Hashem, Y. S. K. S. and Alikhan, A. A. (eds). 2000. *Compressibility Factor for Gas Condensates*.
33. Elsharkawy, A. M. and Elkamel, A. (eds). 2000. *Compressibility Factor for Sour Gas Reservoirs*.
34. Londono, F. E., Archer, R. A. and Blasingame, T. A. 2005. Correlations for Hydrocarbon Gas Viscosity and Gas Density - Validation and Correlation of Behavior Using a Large-Scale Database. *SPE Reservoir Evaluation & Engineering*, Vol. 8, No. 06, pp. 561–72.

35. Whitson, C. H. and Brulé, M. R. 2000. *Phase behavior*. Richardson, Texas, Henry L. Doherty Memorial Fund of AIME Society of Petroleum Engineers. (SPE monograph series, 20). (In eng).
36. Stewart, W. F., Burkhardt, S. F. and Voo, D. (eds). 1959. *Prediction of Pseudo-critical Parameters for Mixtures*.
37. Whitson, C. H. and Torp, S. B. 1983. Evaluating Constant-Volume Depletion Data. *Journal of Petroleum Technology*, Vol. 35, No. 03, pp. 610–20.
38. Corredor, J. H., Piper, L. D. and McCain, W. D. Compressibility Factors for Naturally Occurring Petroleum Gases (1992 version), *SPE Annual Technical Conference and Exhibition* .
39. Carr, N. L., Kobayashi, R. and Burrows, D. B. 1954. Viscosity of Hydrocarbon Gases Under Pressure. *Journal of Petroleum Technology*, Vol. 6, No. 10, pp. 47–55.
40. Matthews, T. A., Roland, C. and Katz, D. 1942. High Pressure Gas Measurement. *Petroleum Refiner*, Vol. 21, No. 6, p. 58.
41. Chen, Z. A. and Ruth, D. W. (eds). 1993. *On Viscosity Correlations Of Natural Gas*.
42. Sanaei, A., Yousefi, S. H., Naseri, A. and Khishvand, M. 2015. A Novel Correlation for Prediction of Gas Viscosity. *Energy Sources, Part A: Recovery, Utilization, and Environmental Effects*, Vol. 37, No. 18, pp. 1943–53.
43. Carr, N. L., Kobayashi, R. and Burrows, D. B. 2013. Viscosity of Hydrocarbon Gases Under Pressure. *Journal of Petroleum Technology*, Vol. 6, No. 10, pp. 47–55.
44. Dempsey, J. R. Computer Routine Treats Gas Viscosity as a Variable. *O & G Journal*, Aug. 16, 1965, pp. 141–43.
45. Lee, A. L., Gonzalez, M. H. and Eakin, B. E. 1966. The Viscosity of Natural Gases. *Journal of Petroleum Technology*, Vol. 18, No. 08, pp. 997–1000.
46. Londono, F. E., Archer, R. A. and Blasingame, T. A. 2002. Simplified Correlations for Hydrocarbon Gas Viscosity and Gas Density - Validation and Correlation of Behavior Using a Large-Scale Database, *SPE Gas Technology Symposium* .
47. Lohrenz, J., Bray, B. G. and Clark, C. R. 1964. Calculating Viscosities of Reservoir Fluids From Their Compositions. *Journal of Petroleum Technology*, Vol. 16, No. 10, pp. 1171–76.
48. McCain, W. D. 1991. Reservoir-Fluid Property Correlations-State of the Art (includes associated papers 23583 and 23594). *SPE Reservoir Engineering*, Vol. 6, No. 02, pp. 266–72.
49. Whitson, C. H. 2013. Characterizing Hydrocarbon Plus Fractions. *Society of Petroleum Engineers Journal*, Vol. 23, No. 04, pp. 683–94.
50. Gurbanov, R. and Dadash-Zade, M. Calculations of Natural Gas Viscosity Under Pressure and Temperature. *Azerbaijanskoe Neftianoe Khoziaistvo (in Russian)*, Vol. 1986, No.2, pp. 41–44.
51. Viswanathan, A. 2007. Viscosities of Natural Gases at High Pressures and High Temperatures, Texas A&M University.
52. Galliéro, G., Boned, C., Baylaucq, A. and Montel, F. 2009. High-Pressure Acid-Gas Viscosity Correlation. *SPE Journal*, Vol. 15, No. 03, pp. 682–88.

53. Holland, P. M., Eaton, B. E. and Hanley, H. J. M. 1983. A Correlation of the Viscosity and Thermal Conductivity Data of Gaseous and Liquid Ethylene. *J. Phys. Chem. Ref. Data*, Vol. 12, No. 4, p. 917.
54. Holland, P. M., Hanley, H. J. M., Gubbins, K. E. and Haile, J. M. 1979. A correlation of the viscosity and thermal conductivity data of gaseous and liquid propane. *J. Phys. Chem. Ref. Data*, Vol. 8, No. 2, p. 559.
55. Hanley, H. J. M. and Ely, J. F. 1973. The Viscosity and Thermal Conductivity Coefficients of Dilute Nitrogen and Oxygen. *J. Phys. Chem. Ref. Data*, Vol. 2, No. 4, p. 735.
56. Pátek, J., Klomfar, J., Čapla, L. and Buryan, P. 2003. Thermal Conductivity of Nitrogen-Methane Mixtures at Temperatures Between 300 and 425 K and at Pressures up to 16 MPa. *International Journal of Thermophysics*, Vol. 24, No. 4, pp. 923–35.
57. Thermal Conductivity of Carbon Dioxide–Methane Mixtures at Temperatures Between 300 and 425 K and at Pressures up to 12 MPa. 2005. *Int J Thermophys*, Vol. 26, No. 3, pp. 577–92.
58. Chung, T. H., Ajan, M., Lee, L. L. and Starling, K. E. 1988. Generalized multiparameter correlation for nonpolar and polar fluid transport properties. *Ind. Eng. Chem. Res.*, Vol. 27, No. 4, pp. 671–79.
59. Ely, J. F. and Hanley, H. J. M. 1983. Prediction of transport properties. 2. Thermal conductivity of pure fluids and mixtures. *Ind. Eng. Chem. Fund.*, Vol. 22, No. 1, pp. 90–97.
60. Ely, J. F. and Huber, M. L. 1990. NIST standard reference database 4, Computer program SUPERTRAPP, NIST Thermophysical Properties of Hydrocarbon Mixtures, version.
61. Hanley, H. 1976. Prediction of the viscosity and thermal conductivity coefficients of mixtures. *Cryogenics*, Vol. 16, No. 11, pp. 643–51.
62. Pedersen, K. S., Fredenslund, A. and Thomassen, P. 1989. *Properties of oils and natural gases*. Houston, Gulf Publ. (Contributions in petroleum geology and engineering, 5). (In eng).
63. Guo, X.-Q., Sun, C.-Y., Rong, S.-X., Chen, G.-J. and Guo, T.-M. 2001. Equation of state analog correlations for the viscosity and thermal conductivity of hydrocarbons and reservoir fluids. *Journal of Petroleum Science and Engineering*, Vol. 30, No. 1, pp. 15–27.
64. *Gas Processors Suppliers Association Engineering Data Book. FPS Version Volumes I & II Sections 1-26*. 2004. Tulsa, Oklahoma.
65. Abou-Kassem, J. H. and Dranchuk, P. M. (eds). 1982. *Isobaric Heat Capacities of Natural Gases at Elevated Pressures and Temperatures*.
66. Dranchuk, P. M., Purvis, R. A. and Robinson, D. B. (eds). 1993. *Computer Calculation Of Natural Gas Compressibility Factors Using The Standing And Katz Correlation*.
67. Moshfeghian, M. 2011. *Correlation for natural gas heat capacity developed*. <http://www.ogj.com/articles/print/volume-109/issue-40/processing/correlation-for-natural-gas.html> (Accessed 9 April 2016).

68. US Departemen of Commerce and NIST. 2015. *NIST23*.
<http://www.nist.gov/srd/nist23.cfm> (Accessed 7 April 2016).
69. Lateef, A. K. and Omeke, J. (eds). 2011. *Specific Heat Capacity of Natural Gas; Expressed as a Function of Its Specific Gravity and Temperature*.
70. Herráez, A. and Glasser, L. 2009. *Interactive 3D phase diagrams using Jmol*. *J. Chem. Educ.* 86: 566. <http://biomodel.uah.es/Jmol/plots/phase-diagrams/> (Accessed 7 June 2016).
71. Stephan, K. and Lucas, K. 1979. *Viscosity of Dense Fluids*. Boston, MA, Springer US.
72. Reichenberg, D. 1975. New methods for the estimation of the viscosity coefficients of pure gases at moderate pressures(with particular reference to organic vapors). *AIChE J.*, Vol. 21, No. 1, pp. 181–83.
73. Zabaloy, M. S., Vasquez, V. R. and Macedo, E. A. 2005. Viscosity of pure supercritical fluids. *The Journal of Supercritical Fluids*, Vol. 36, No. 2, pp. 106–17.
74. Zabaloy, M. S., Machado, J. M. V. and Macedo, E. A. 2001. A Study of Lennardones Equivalent Analytical Relationships for Modeling Viscosities. *International Journal of Thermophysics*, Vol. 22, No. 3, pp. 829–58.
75. Vesovic, V., Wakeham, W. A., Olchowy, G. A., Sengers, J. V., Watson, J. T. R. and Millat, J. 1990. The Transport Properties of Carbon Dioxide. *J. Phys. Chem. Ref. Data*, Vol. 19, No. 3, p. 763.
76. Heidaryan, E., Hatami, T., Rahimi, M. and Moghadasi, J. 2011. Viscosity of pure carbon dioxide at supercritical region. Measurement and correlation approach. *The Journal of Supercritical Fluids*, Vol. 56, No. 2, pp. 144–51.
77. Pensado, A. S., Pádua, A. A. H., Comuñas, M. J. P. and Fernández, J. 2008. High-pressure viscosity and density of carbon dioxide + pentaerythritol ester mixtures. Measurements and modeling. *AIChE J.*, Vol. 54, No. 6, pp. 1625–36.
78. Amooey, A. A. 2014. A simple correlation to predict thermal conductivity of supercritical carbon dioxide. *The Journal of Supercritical Fluids*, Vol. 86, pp. 1–3.
79. Bahadori, A., Vuthaluru, H. B. and Mokhatab, S. 2009. New correlations predict aqueous solubility and density of carbon dioxide. *International Journal of Greenhouse Gas Control*, Vol. 3, No. 4, pp. 474–80.
80. Haghbakhsh, R., Hayer, H., Saidi, M., Keshtkari, S. and Esmailzadeh, F. 2013. Density estimation of pure carbon dioxide at supercritical region and estimation solubility of solid compounds in supercritical carbon dioxide. Correlation approach based on sensitivity analysis. *Fluid Phase Equilibria*, Vol. 342, pp. 31–41.
81. Harvey, A. H., Huber, M., Laesecke, A., Muzny, C. D. and Perkins, R. (eds). 2014. *Progress towards new refrence correlations for the transport properties of carbon dioxide*.
82. Bahadori, A. and Vuthaluru, H. B. 2010. Predictive tool for an accurate estimation of carbon dioxide transport properties. *International Journal of Greenhouse Gas Control*, Vol. 4, No. 3, pp. 532–36.
83. Wang, Z., Sun, B. and Yan, L. 2015. Improved Density Correlation for Supercritical CO₂. *Chem. Eng. Technol.*, Vol. 38, No. 1, pp. 75–84.

84. Ouyang, L.-B. 2011. New Correlations for Predicting the Density and Viscosity of Supercritical Carbon Dioxide Under Conditions Expected in Carbon Capture and Sequestration Operations. *The Open Petroleum Engineering Journal*, No. 4, pp. 13–21.
85. Le Neindre, B., Tufeu, R., Bury, P. and Sengers J.V. 1973. Thermal Conductivity of Carbon Dioxide and Steam in the Supercritical Region. *Berichte der Bunsengesellschaft für physikalische Chemie*, Volume 77, Issue 4, pp. 262–75.